

Journal of Pyrotechnics

Issue Number 6, Winter 1997

Policy Board Members:

Ettore Contestabile
Canadian Explosive Research Lab
555 Booth Street
Ottawa, Ontario K1A 0G1
Canada

Gerald Laib, Branch Manager
Explosives Components Branch
Naval Surface Warfare Center
Indian Head Div., Code 9520
101 Strauss Ave. (Bldg. 559)
Indian Head, MD 20640-5035 USA

Wesley Smith
Department of Chemistry
Ricks College
Rexburg, ID 83460-0500
USA

Roland Wharton
Health and Safety Laboratory
Harpur Hill, Buxton
Derbyshire SK17 9JN
United Kingdom

Managing Editor:

Ken Kosanke
PyroLabs, Inc.
1775 Blair Road
Whitewater, CO 81527
USA

Technical Editors (in addition to Policy Board Members that edited for this issue):

Per Alenfelt, Norabel Hansson
Billdal, Sweden

Frank Feher, Univ. of CA, Irvine
Irvine, CA, USA

Jeroen Louwers, TNO-PML
Rijswijk, The Netherlands

Scot Anderson
Conifer, CO, USA

Ian Grose, Royal Military College
Swindon, Wilts., United Kingdom

Larry Weinman, Luna Tech
Owens Cross Roads, AL, USA

Ed Brown
Rockvale, CO, USA

Mark Grubelich, Sandia Nat'l. Lab.
Albuquerque, NM, USA

Robert Winokur, Dept. of Biology
UNLV, Las Vegas, NV, USA

Joe Domanico, US Army, Edgewood
Aberdeen Proving Ground, MD, USA

Direct Editorial Concerns and Subscription Requests to:

Journal of Pyrotechnics, Inc.

Bonnie Kosanke, Publisher
1775 Blair Road
Whitewater, CO 81527 USA
(970) 245-0692 (Voice and FAX)
e-mail: bonnie@jpyro.com
web: www.jpyro.com

CAUTION

The experimentation with, and the use of, pyrotechnic materials can be dangerous; it is felt to be important for the reader to be duly cautioned. Without the required training and experience no one should ever experiment with or use pyrotechnic materials. Also, the amount of information presented in this Journal is not a substitute for necessary training and experience.

A major effort has been undertaken to review all articles for correctness. However, it is possible that errors remain. It is the responsibility of the reader to verify any information herein before applying that information in situations where death, injury, or property damage could result.

Table of Contents

Issue Number 6, Winter 1997

Thermal Hazards from the Accidental Ignition of Pyrotechnic Compositions R. K. Wharton and R. Merrifield	1
Methods for Calculation of Thrust Coefficients Ed Brown	9
Pyrotechnic Ignition and Propagation: A Review K. L. and B. J. Kosanke	17
Studies of the Thermal Stability and Sensitiveness of Sulfur/Chlorate Mixtures Part 1. Introduction D. Chapman, R. K. Wharton and G. E. Williamson	30
Hydrazinium Nitroformate: A High Performance Next Generation Oxidizer Jeroen Louwers	36
A Thermodynamic Properties Estimation Method for Isocyanates Will Meyerriecks.....	43
A Severe Human ESD Model for Safety and High Reliability System Qualification Testing R. J. Fisher	57
Correspondence:	
Consideration of Alternate Whistle Fuels by Rembert Amons	65
Frequency Stabilization of Large Diameter Strobe Flares by K. L. Kosanke	68
Estimating the Distribution of Molecular Energies by Wesley D. Smith	70
Further Comment from Fred Ryan on "Flash Powder Output Testing"	70
Comment from Terry McCreary on : "Model Rocket Motor, Theory and Design"	71
Authors' reply to Terry McCreary	71
Review by Paul E. Smith of <i>Lecture Notes for Pyrotechnic Chemistry</i>	72
Review by Tom Dimock of <i>Introductory Practical Pyrotechnics</i>	72
Errata for Issue Number 5	8
Events Calendar	35
Sponsors	74

Publication Frequency

The *Journal of Pyrotechnics* appears approximately twice annually, typically in mid-summer and mid-winter.

Subscriptions

Anyone purchasing a copy of the Journal, will be given the opportunity to receive future issues on an approval basis. Any issue not desired may be returned in good condition and nothing will be owed. So long as issues are paid for, future issues will automatically be sent. In the event that no future issues are desired, this arrangement can be terminated at any time by informing the publisher. Discounts are offered for payment in advance for issues of the *Journal of Pyrotechnics*.

Back issues of the Journal will be kept in print permanently as reference material.

Thermal Hazards from the Accidental Ignition of Pyrotechnic Compositions

R. K. Wharton* and R. Merrifield**

*Health and Safety Laboratory, Harpur Hill, Buxton, Derbyshire SK17 9JN, United Kingdom

**Chemical and Hazardous Installations Division, Explosives Inspectorate, Health and Safety Executive, Magdalen House, Stanley Precinct, Bootle, Merseyside L20 3QZ, United Kingdom

ABSTRACT

In this paper we have analysed further some of our previously published data relating to thermal effects produced on the ignition of a range of pyrotechnic compositions, and have evaluated the hazards posed to those handling and working with such materials by reference to the distances for different degrees of burn injury.

Keywords: thermal hazard, radiation, burn injury, pyrotechnics

Introduction

The thermal characteristics of fireballs from a number of fuel sources other than pyrotechnics have been reported in the literature, including liquid propellants,^[1] motor fuels^[2] and propane.^[3] Fireball effects can be described in terms of the maximum diameter D (m), the duration of the thermal effect t (s) and the heat flux radiated from the fireball surface q (kW m^{-2}). In many cases both D and t are related to the fuel mass M (kg) by a power law relationship of the approximate form $M^{1/3}$.

To investigate the applicability of this generalised equation to pyrotechnics, a series of experiments was recently done^[4] with a range of compositions in which D , t and q were quantified at various values of M , up to 25 kg. The results from these trials indicated that relationships of the form $D = aM^x$ and $t = bM^x$ applied. However, the values of x varied from 1/3, sometimes significantly, in both equations, and different compositions gave different values for

the constants a and b (within the range 0.53–26.0).

The predictive equations obtained from the study were used in a subsequent paper to examine both the fire and explosion hazards of the pyrotechnics that had been tested.^[5] Explosion hazards were evaluated since some of the compositions exploded under conditions of self confinement. The Eisenberg thermal radiation dose criterion^[6] was used to evaluate potential levels of harm (blister thresholds and degrees of burn) at different distances.

In this short paper, some of the implications of these results are examined with respect to those in the pyrotechnics industry working with relatively small quantities of loose (self confined) composition.

Discussion

Table 1 lists the compositions of the pyrotechnics examined. The potential hazards of pyrotechnic fireballs can be defined in terms of heat flux, time of exposure (or burning time, if less) and distance from the fireball surface since distance determines thermal exposure and duration influences the dose received.

The various design requirements of pyrotechnic mixes are reflected partly in their burn times and these show a significant range in duration from $t < 1$ s to > 50 s for 1–25 kg quantities of different materials.^[4]

It has been reported in the literature^[7] that it takes approximately 5 s to sense high levels of thermal radiation and start to make an escape, and it is also known that a proportion of the

Table 1. List of Pyrotechnic Compositions and Their Ingredients.

Pyrotechnic Substance	Ingredient	% by Mass
Gunpowder 3/7 Grist	Potassium nitrate	75.0
	Carbon	15.0
	Sulfur	10.0
Flare Composition 1	Magnesium	26.0
	Lithographic varnish	4.0
	Sodium nitrate	42.0
	Calcium oxalate	16.0
	PVC powder	12.0
Flare Composition 2	Magnesium	49.0
	Lithographic varnish	4.5
	Sodium nitrate	39.5
	Calcium oxalate	7.0
Star Composition 1	Magnesium	42.0
	Boiled linseed oil	6.0
	Barium nitrate	17.0
	Potassium perchlorate	27.0
	PVC powder	8.0
Star Composition 2	Gunpowder	55.6
	Potassium nitrate	18.5
	Dextrin binder	7.4
	Aluminium	18.5
Priming Composition 1	Potassium nitrate	40.0
	Silicon powder	40.0
	Gunpowder sulfurless mealed	20.0
Priming Composition 2	Gunpowder	68.0
	Potassium nitrate	14.6
	Silicon	14.6
	Dextrin binder	2.8
Flash Composition 1	Magnesium	57.0
	Potassium perchlorate	37.0
	Graphite	6.0

final burn injury can occur during the phase when the skin is cooling.^[7]

It may be possible for workers exposed to the thermal radiation from fireballs with $t > 5$ s to limit their potential thermal dose by making a rapid escape. On the other hand, certain pyrotechnic materials burn for less than 5 s and for such events an eventual escape would not be likely to limit the received thermal radiation dose.

To compare the potential of different pyrotechnics to cause burn injuries, with fireballs burning for greater than 5 s we have still used the 5 s reaction time^[7] in our calculations since, although a process operator seated directly in

front of an igniting pyrotechnic material is likely to respond in less than 5 s, the overall duration of exposure can be assumed to be approximately 5 s. The extreme conditions arising from engulfment within the fireball have been assumed to be fatal.

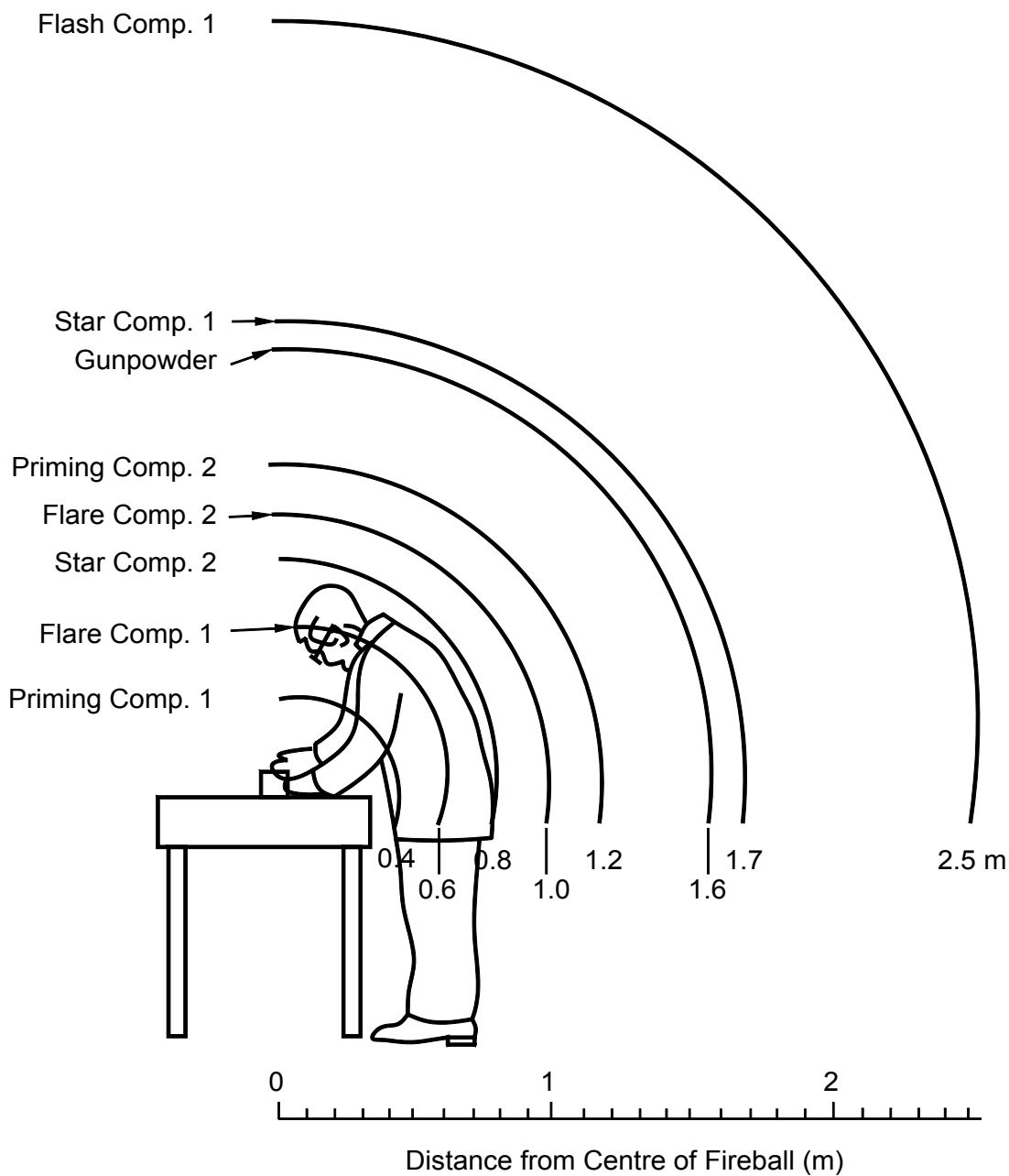


Figure 1. Flare / fire / fireball dimensions (m) for 1 kg quantities of loose pyrotechnic compositions.

From our previously published results,^[4] it is possible to compare the sizes of actual and pseudo fireballs produced by the ignition of different compositions with $M = 1$ kg, Figure 1. This diagram indicates that most of the materials examined produce fireballs that would engulf a process worker positioned at arms length from the point of initiation. Dose levels and corresponding burns injuries for process workers positioned beyond the fireball radius can be calculated using a maximum exposure time of 5 s.

A dosage of $1200 \text{ (kW m}^{-2}\text{)}^{4/3}\text{s}$ has been used in the literature^[7] as the mean value to produce second degree burns with depths >0.1 mm on unprotected skin and this value was employed in our work. Clearly, appropriate fire protective clothing can offer some mitigation, but nevertheless, this dose has been reported to result in 1% lethality to averagely dressed exposees.^[7] The distances to second degree burns for every composition with $M = 1$ kg, Figure 2, show that other process workers in the same room could

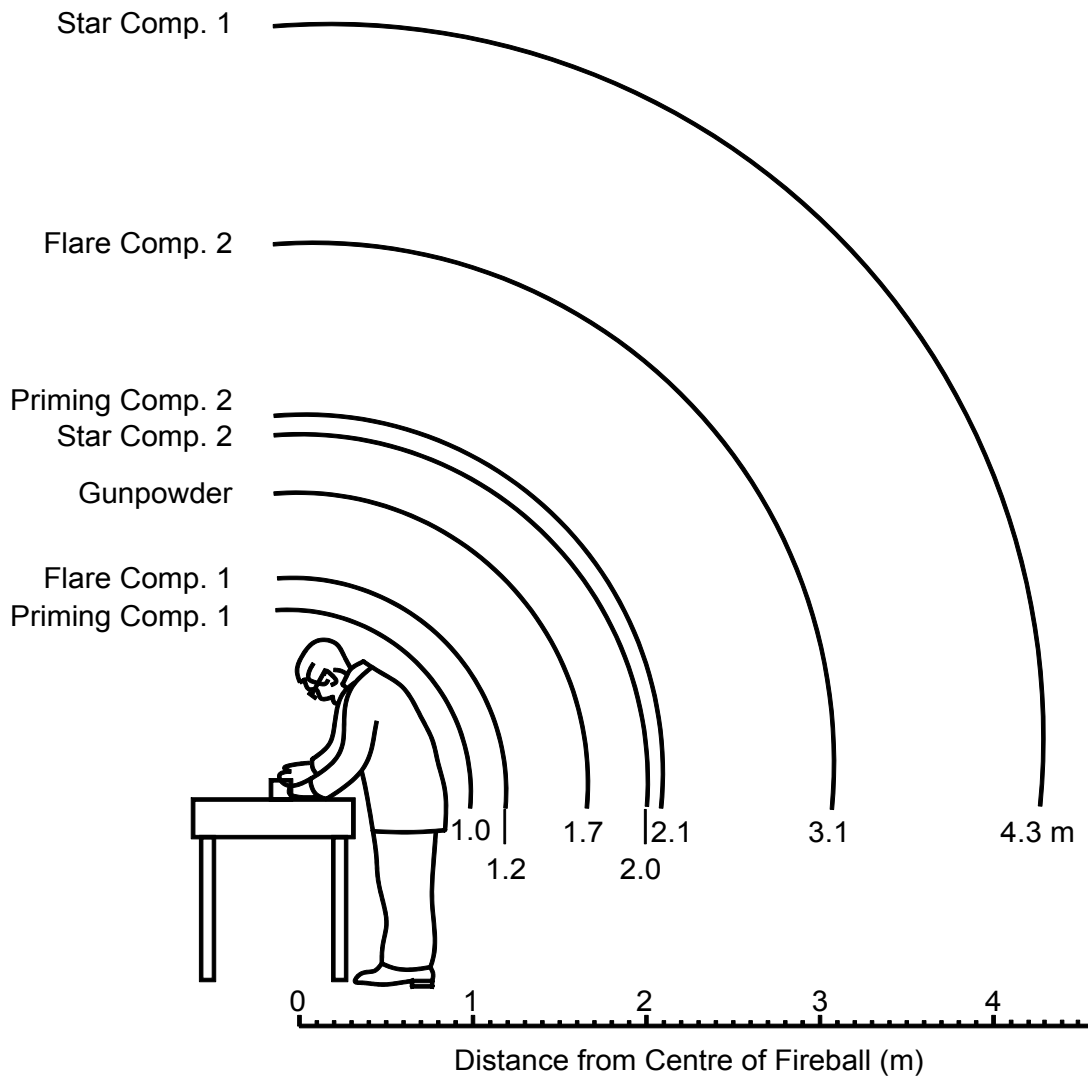


Figure 2. Distances (m) to second degree burns from 1 kg quantities of loose pyrotechnic compositions.

well be within the minimum distances to be affected. The information summarised in Figure 2 should, however, be taken as a first approximation since the hazards posed by the slowest burning materials may be overestimated because the flames can take time to build up to peak irradiance (i.e., the calculations assume 5 s of exposure to the peak surface emissive power from fireballs).

Since the blister threshold dosage^[7] is only $210 \text{ (kW m}^{-2}\text{)}^{4/3}\text{s}$, such injuries can be sustained at greater distances from the point of initiation of a range of substances with $M = 1 \text{ kg}$, Figure 3. Again, other workers in the same process

room and at considerable distances from the source could receive blister injuries.

The importance of taking account of exposure time in determining dosage is illustrated by the different rankings obtained for the potential hazards posed by the fireballs from 1 kg quantities of materials when using either distance to second degree burns (dosage) or fireball dimensions as the ranking criterion, Table 2. This Table shows that a simplistic ranking based on fireball dimensions alone may not accurately represent the hazard posed to workers outside the fireball diameter by the ignition of certain

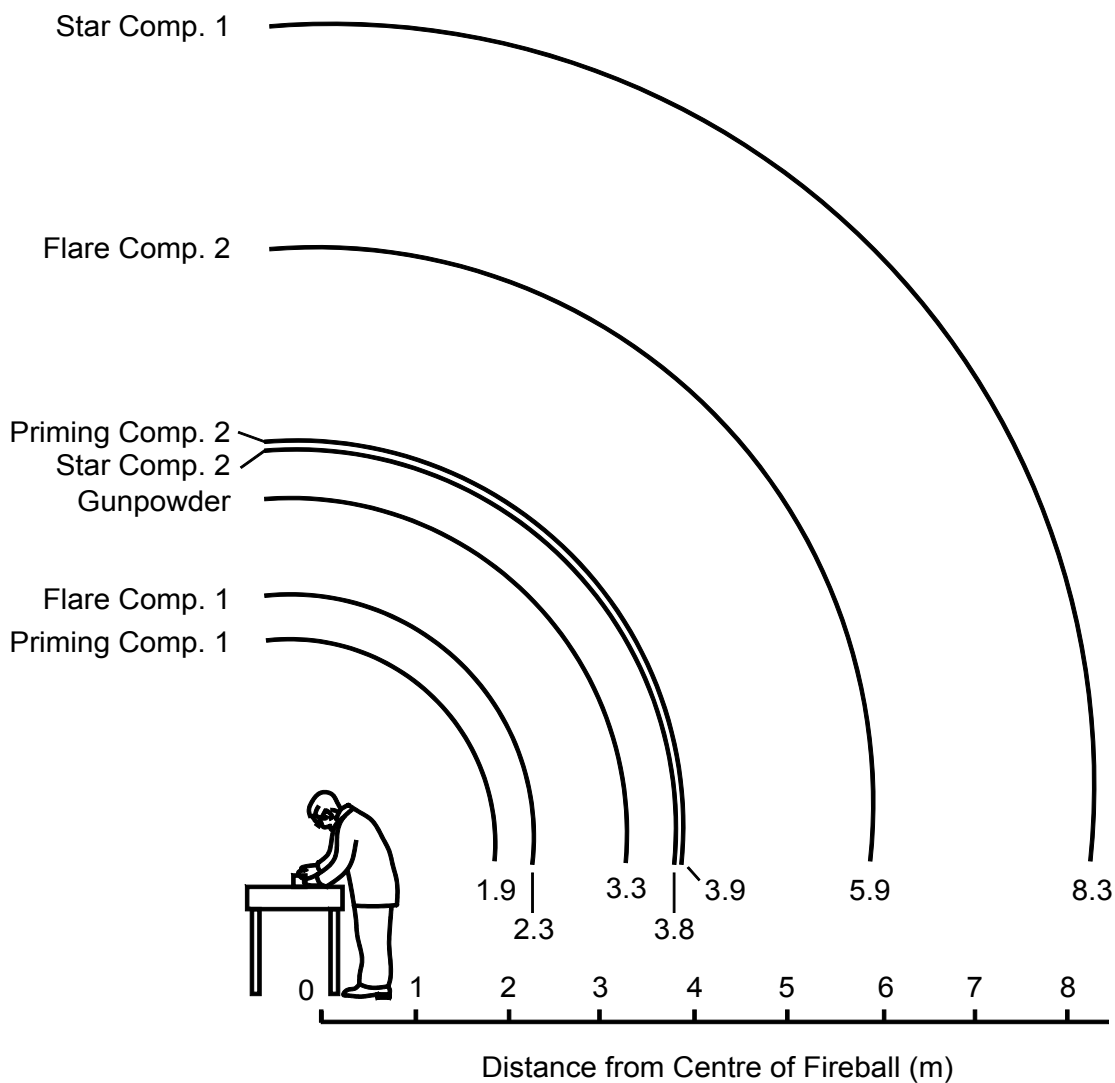


Figure 3. Distances (m) to blister threshold for 1 kg quantities of loose pyrotechnic compositions.

pyrotechnic compositions (e.g., gunpowder and flare composition 2).

By assuming that our fireball data for gunpowder with $M = 1$ to 25 kg can be extrapolated to lower values of M , it is possible to use the relationship^[4] $D = 3.1 M^{0.279}$ to estimate fireball sizes and hence the hazards posed by the ignition of small quantities of gunpowder, as indicated in Figure 4. This diagram shows that a fireball produced by burning quantities as low as 100 g can engulf a process worker.

In terms of reducing potential hazards in the working environment posed by the accidental ignition of pyrotechnics, the first step is to

minimise the quantities being handled. This is often supplemented by the introduction of engineering controls to ensure that a suitable physical separation exists between the worker and the potential heat source. Techniques employed include remote handling, the use of robotics, and the use of protective screens. Some fire protection can also be gained by using quenching systems.^[8,9,10]

As a last resort, personal protective equipment can be employed and a recently published guide gives an indication of the current position with regard to the selection and use of fire protective clothing for explosives workers in the UK.^[11] The ICARUS code^[12] is also able to

Table 2. Relative Rankings of the Hazards Posed by Fireballs from 1 kg Quantities of Pyrotechnic Compositions.

Pyrotechnic	Fireball Radius (m)	Ranking Based on Fireball Dimensions	Distance to Second Degree Burns (m)	Ranking Based on Level of Harm (Second Degree Burns)
Star comp. 1	1.7	1	4.3	1
Gunpowder	1.6	2	1.7	5
Priming comp. 2	1.2	3	2.1	3
Flare comp. 2	1.0	4	3.1	2
Star comp. 2	0.8	5	2.0	4
Flare comp. 1	0.6	6	1.2	6
Priming comp. 1	0.4	7	1.0	7

predict burn injuries for workers exposed to thermal radiation when wearing appropriate protective clothing.

Research sponsored by the Health and Safety Executive is currently underway to develop a full torso portable manikin to enable the evaluation of complete garments against the thermal threat posed by burning pyrotechnics and propellants, and this may provide a useful means of ranking the performance of protective clothing, thus aiding selection.

Conclusions

In this paper the potential thermal hazards posed to workers in the pyrotechnics industry by the ignition of different types of compositions have been examined. Relatively small quantities of material can produce a significant fireball and, because thermal emissive powers are relatively large, even short duration exposure can result in burn injuries at considerable distances from the source.

The main factors affecting hazard are the close proximity of the pyrotechnic worker to the composition and the quantity present in the process room. Means of minimising the role of these factors (i.e., reducing quantity, increasing distance) are desirable in terms of improving safety in the workplace.

References

- 1) R. W. High, "The Saturn Fireball", *Annals New York Academy of Sciences*, Vol. 152, 1968, pp 441–451.
- 2) S. B. Dorofeev et al., "Fireballs from Deflagration and Detonation of Heterogeneous Fuel-rich Clouds", *Fire Safety Journal*, Vol. 25, 1995, pp 323–336.
- 3) A. F. Roberts, "Thermal Radiation Hazards from Releases of LPG from Pressurised Storage", *Fire Safety Journal*, Vol. 4, 1981, pp 197–212.
- 4) R. K. Wharton, J. A. Harding, A. J. Barratt and R. Merrifield, "Measurement of the Size, Duration and Thermal Output of Fireballs Produced by a Range of Pyrotechnics", *Proceedings of the 21st International Pyrotechnics Seminar*, Moscow, Russia, 1995, pp 916–931.
- 5) R. Merrifield, R. K. Wharton and S. A. Formby, "Potential Fire and Explosion Hazards of a Range of Loose Pyrotechnic Compositions", *US Dept. of Defense, Explosives Safety Board, 27th Explosives Safety Seminar*, 20–22 Aug. 1996, Sahara Hotel, Las Vegas, Nevada, USA.

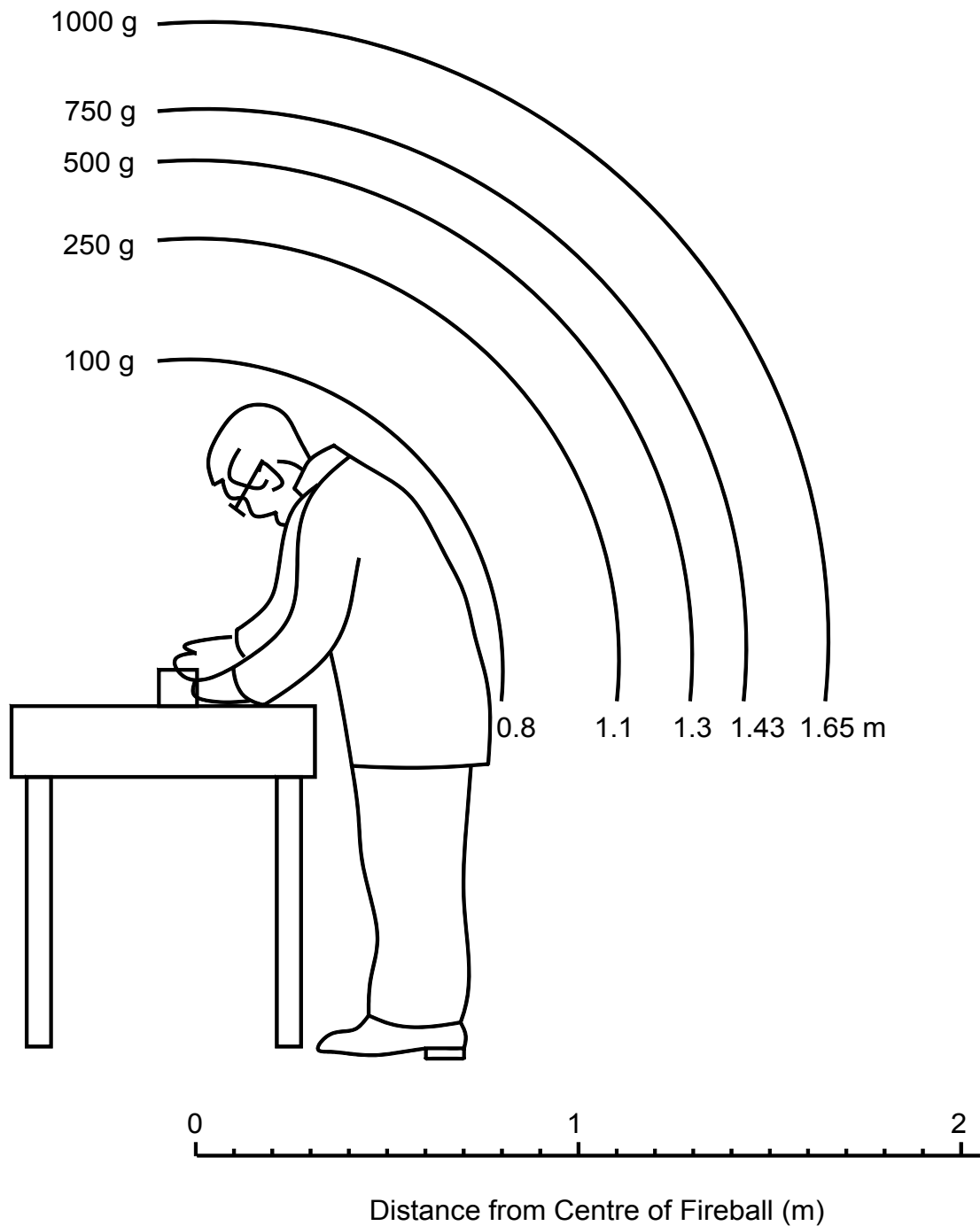


Figure 4. Fireball dimensions for small quantities of loose gunpowder.

6) N. A. Eisenberg et al., "Vulnerability Model. A Simulation System for Assessing Damage Resulting from Marine Spills", *Final Report AD/A - 015 245*, US Department of Transport, US Coast Guard, 1975.

7) I. Hymes, W. Boydell and B. Prescott, "Thermal Radiation: Physiological and Pathological Effects", *Major Hazards Monograph*, Institute of Chemical Engineers, 1996 [ISBN 0 85295 328 3].

- 8) P. Goffart and G. Hendrickx, “Automatic Fire Quenching System for Pyrotechnical Plants”, *Proceedings of the Joint 16th International Annual Conference of ICT, Jahrestagung and 10th International Pyrotechnic Seminar*, Fraunhofer Institut für Treib – und Explosivstoffe, 1985, paper 51-1.
- 9) P. Goffart and G. Hendrickx, “Automatic Fire Quenching System for Pyrotechnical Plants, Part II”, *Proceedings of the 14th International Pyrotechnics Seminar*, Jersey, Channel Islands, UK, 1980, pp 365–370.
- 10) G. Fadorsen, “Methods and Effectiveness of Fire Protection Systems in Fireworks Manufacturing Facilities”, *Proceedings 1st International Symposium on Fireworks*, Montreal, 1992, pp 120–131.
- 11) “Fire Protective Clothing”, CBI Explosives Industry Group, Confederation of British Industry, November 1995 [ISBN 0 85201 513 5].
- 12) G. J. Bamford and W. Boydell, “ICARUS: A Code for Evaluating Burn Injuries”, *Fire Technology*, 4th Quarter, 1995, pp 307–335.

© British Crown copyright, 1997

Errata — Number 5

Page 3, Figure 3 Incorrect subscript for “h”. It should have been “con”.

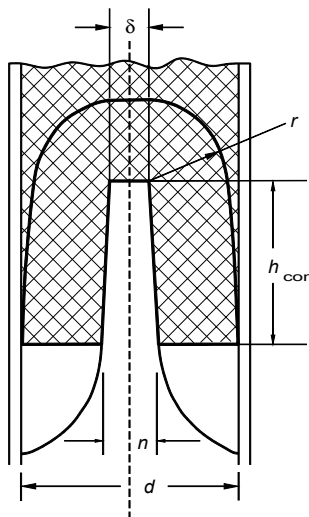


Figure 3. Cross section of a rocket motor with a conical combustion cavity.

Methods for Calculation of Thrust Coefficients

Ed Brown

PO Box 177, Rockvale, CO 81244, USA

ABSTRACT

When one wishes to predict or analyze rocket motor/engine performance accurately, a method for determining the nozzle thrust coefficient at each point in time is essential. If the vacuum thrust coefficient for the nozzle is known, the thrust coefficient for other conditions can easily be determined. This paper outlines several methods for determining the vacuum thrust coefficient in the hope that it will encourage this type of calculation and lead to new and better methods for simulation and analysis in the future.

Key Words: vacuum thrust coefficient, thrust coefficient, expansion ratio, specific heat ratio, chamber pressure, thrust, rocket propulsion theory

Introduction

This paper will neither present nor attempt to explain any of the theory involved, as references^[1,2,3] exist that do this more than adequately and far better than this writer could. It will attempt to outline and present methods that may be used to simplify basic design and analysis calculations. While graphs^[1] and tables^[4] exist for thrust coefficients etc., determining more accurate values than can be obtained from a graph or table is often desirable. Also, incorporating their real time calculation in a simulation or analysis program or procedure is often beneficial, and graphs and tables are not always available or convenient to use. One equation^[5] used to calculate values for the thrust coefficient (C_F) is:

$$C_F = \Gamma \sqrt{\frac{2\gamma}{\gamma-1}} \sqrt{1 - \left[\frac{P_e}{P_c}\right]^{\left(\frac{\gamma-1}{\gamma}\right)}} + \frac{A_e}{A_t} \left(\frac{P_e - P_a}{P_c}\right) \quad (1)$$

where capital gamma (Γ), also known as the Vandekerckhove function,^[6] is defined by:

$$\Gamma = \sqrt{\gamma} \left[\frac{2}{\gamma+1} \right]^{\left(\frac{\gamma+1}{2(\gamma-1)}\right)} \quad (2)$$

in addition, gamma (γ) is the ratio of specific heats (or specific heat ratio) for the exhaust gases. The pressure at the nozzle exit plane (P_e), the chamber pressure (P_c), and the ambient pressure (P_a) need to be in absolute pressure units. Nozzle exit area (A_e) and nozzle throat area (A_t) should be given using the same units for each. Nozzle expansion ratio^[5] (ϵ) can be defined as:

$$\epsilon = \frac{A_e}{A_t} \quad (3)$$

or by:

$$\epsilon = \Gamma \sqrt{\frac{\gamma-1}{2\gamma}} \left[\frac{\left[\frac{P_c}{P_e}\right]^{\left(\frac{1}{\gamma}\right)}}{\sqrt{1 - \left[\frac{P_e}{P_c}\right]^{\left(\frac{\gamma-1}{\gamma}\right)}}} \right] \quad (4)$$

Equation 4 can be shortened by defining alpha (α) as:

$$\alpha = \sqrt{\frac{\gamma-1}{2\gamma}} \quad (5)$$

beta (β) as:

$$\beta = \frac{\gamma-1}{\gamma} \quad (6)$$

and delta (Δ) as:

$$\Delta = \frac{1}{\gamma} \quad (7)$$

This allows equation 4 to be rewritten as:

$$\varepsilon = \Gamma \alpha \frac{\left[\frac{P_c}{P_e} \right]^\Delta}{\sqrt{1 - \left[\frac{P_e}{P_c} \right]^\beta}} \quad (8)$$

Except for pressure terms, all variables in equation 8 are defined in terms of the specific heat ratio (γ). The specific heat ratio is usually known or can be calculated using one of the many PEP programs (PROPEP, CETPC, ISP, SP-273 etc.). However, if it is not known, a value of 1.25 can be used (not a bad assumption for most solid propellants used in high power rocketry).

If atmospheric pressure is reduced to zero in equation 1, then the thrust coefficient becomes the vacuum thrust coefficient ($C_{F_{vac}}$):

$$C_{F_{vac}} = \Gamma \sqrt{\frac{2\gamma}{\gamma-1}} \sqrt{1 - \left(\frac{P_e}{P_c} \right)^\beta} + \varepsilon \left(\frac{P_e}{P_c} \right) \quad (9)$$

This allows equation 1 to be rewritten in a simpler form:

$$C_F = C_{F_{vac}} - \varepsilon \left(\frac{P_a}{P_c} \right) \quad (10)$$

Tools are now in place for further calculations.

Short BASIC program listings are included in the appendices to illustrate each calculation method described. The simplest, a method for calculating the optimum expansion ratio and thrust coefficient for a fixed pressure ratio is outlined first. A method for calculating thrust coefficients using a fixed expansion ratio is then presented. Following this is an approximate method for calculation of thrust coefficients (again using a fixed expansion ratio). The final method is for converting thrust levels to chamber pressures. This method can be reversed to predict thrust versus time in simulation programs (after using Kn values to determine pressures). For all methods, it is assumed that a specific heat ratio has been provided for use.

A Method for Calculation of Optimum Thrust Coefficient Using a Fixed Pressure Ratio^[Appendix A]

The easiest thrust coefficient calculation is determination of the optimum expansion ratio and thrust coefficients for a fixed pressure ratio. Ambient pressure at the operation or simulation location of the motor must be known or selected. Motor operating pressure is then selected. A nozzle's optimum thrust coefficient is obtained when its exit pressure is equal to ambient pressure. The pressure ratio is calculated using:

$$PR = \frac{P_c}{P_e} = \frac{P_c}{P_a} \quad (11)$$

Values for equations 5, 6, and 7 are determined and the results, to this point, are inserted into equations 2 and 8 to produce values for capital gamma and the expansion ratio. Final steps are the calculation of the vacuum thrust coefficient and thrust coefficient using equations 9 and 10.

A Method for Calculation of Thrust Coefficient Using a Specific Expansion Ratio^[Appendix B]

In the real world, the expansion ratio is usually a fixed value for initial design and testing, with possible optimization occurring during final development. One very accurate method of calculating vacuum thrust coefficients is to select an expansion ratio and then calculate a temporary expansion ratio using an arbitrarily chosen pressure ratio. This result is then compared with the selected expansion ratio. If they do not match, a new temporary expansion ratio is calculated using a new pressure ratio (selected to ensure convergence of expansion ratio values). This process is repeated until the temporary expansion ratio matches the selected expansion ratio. This pressure ratio is then used to calculate the vacuum thrust coefficient using equation 9. The thrust coefficient for any chamber operating pressure can now be calculated using equation 10, if ambient pressure is known for motor operation location. This method gives results for vacuum thrust coefficients and pres-

sure ratios that have very good agreement with tables.^[4]

A Brute Force Method for Calculation of Thrust Coefficients Using Specified Expansion Ratios^[Appendix C]

The writer believes that calculating the pressure ratio directly from the specific heat ratio and expansion ratio may be advantageous. While this may not be true, he has been unable to accomplish this to date. An attempt to “force” a solution to the problem has been made. Using the method outlined in Appendix B, vacuum thrust coefficients and pressure ratios were calculated for expansion ratios ranging from one to eight (by increments of 0.5) for specific heat ratios ranging from 1.1 to 1.4 (by increments of 0.5). A shareware program, *CurveFit*^[7] was then used for each ratio of specific heat to relate pressure ratio and expansion ratio. An equation having the form:

$$PR = a + b\varepsilon + c\varepsilon^2 \quad (12)$$

seemed to fit each group of data. A new problem was that a , b , and c had differing values for each specific heat ratio. In an attempt to make the results more universal, another round of

curve fitting was attempted to relate each coefficient to specific heat ratios. This resulted in the following results:

$$a = \frac{38.7019}{\gamma} - \frac{15.5227}{\gamma^2} - 25.6441 \quad (13)$$

$$b = \frac{1}{0.3283(\gamma - 1.5242)^2 + 0.1423} \quad (14)$$

$$c = (52.4092)\gamma^{15.0965} (0.0013)^\gamma \quad (15)$$

The equations for coefficients a and b were the first listed by the program while the equation for c was the third listed (but appeared to fit the data almost as well and was much easier to calculate).

Next, a short program was written using these equations to see if results were comparable to table values or those produced using the method in Appendix B. The program produced very good agreement for vacuum thrust coefficients, but only good agreement for pressure ratios. Since these pressure ratios are only being used for calculating vacuum thrust coefficients, this method may be an acceptable substitute for other calculation methods. Table 1 compares results from programs in Appendix B and Appendix C using a specific heat ratio of 1.25.

Table 1. Comparison of Results Using Appendix B and Appendix C Methods.

ε	Appendix B ($C_{F_{vac}}$)	Appendix B (PR)	Appendix C ($C_{F_{vac}}$)	Appendix C (PR)
1.0	1.248592	1.845	1.248586	1.747
1.5	1.391232	5.405	1.391338	5.211
2.0	1.463144	8.827	1.463145	8.863
2.5	1.510494	12.557	1.510502	12.703
3.0	1.545099	16.569	1.545105	16.73
3.5	1.571987	20.829	1.571989	20.945
4.0	1.593750	25.305	1.593750	25.349
4.5	1.611888	29.989	1.611888	29.94
5.0	1.627345	34.861	1.627346	34.718
5.5	1.640747	39.901	1.640749	39.685
6.0	1.652532	45.101	1.652533	44.84
6.5	1.663012	50.445	1.663013	50.182
7.0	1.672423	55.935	1.672424	55.712
7.5	1.680943	61.553	1.680943	61.431
8.0	1.688710	67.297	1.688710	67.337

Determining Operating Pressures from Thrust Levels Using Vacuum Thrust Coefficients ^[8, Appendix D]

Thrust levels used to calculate chamber pressures may come from thrust curve data, manufacturer supplied information or any other reasonable source. Nozzle throat and exit areas are needed (easily calculated if we measure or are given throat and exit diameters). A simple equation^[5] for thrust (F) is:

$$F = C_F P_c A_t \quad (16)$$

Rearranging to solve for chamber pressure gives:

$$P_c = \frac{F}{C_F A_t} \quad (17)$$

Multiplying both sides of equation 10 by P_c gives:

$$C_F P_c = C_{F_{vac}} P_c - \epsilon P_a \quad (18)$$

Rearranging this to solve for chamber pressure (P_c):

$$P_c = \frac{C_F P_c + \epsilon P_a}{C_{F_{vac}}} \quad (19)$$

Reexamining equation 17 and multiplying both sides by C_F produces:

$$C_F P_c = \frac{F}{A_t} \quad (20)$$

which can easily be solved using throat areas and thrust levels. Inserting this and earlier results into equation 19 produces a value for chamber pressure. While many other factors can (and perhaps should) be considered,^[1,2,3] chamber pressure values calculated using this method give surprisingly good agreement with measured pressures. In this writer's opinion, thrust levels are much easier to obtain than pressure measurements.

Summary

Several methods of calculating vacuum thrust coefficients and a method for calculating chamber pressure have been presented. Once the vacuum thrust coefficient has been calculated, it is

an easy matter to calculate the thrust coefficient for any chamber pressure using equation 10. A value for the thrust coefficient is essential for simulating or analyzing motor performance. A word of warning, if the nozzle is severely over-expanded, separation of flow will occur in the nozzle with an effective reduction in expansion ratio. Although most of the discussion has implied usage with solid motors, these methods apply to hybrid motors or liquid rocket engines as well. The programs in the appendices include a calculation for approximate characteristic exhaust velocity (c^*) if the chamber temperature and molecular weight of the exhaust gases are known. If not, enter any positive number when prompted for them. They do not affect the calculation of the other values. The programs are written anticipating the use of English units. It is hoped that encouragement of development of more and better methods for simulating and analyzing motor performance has been accomplished.

References

- 1) M. Summerfield, "Performance Analysis of the Ideal Rocket Motor", *High Power Rocketry*, January 1997. [A partial reprint with a foreword by C. Rogers.]
- 2) G. Sutton, *Rocket Propulsion Elements*, 6th ed., John Wiley and Sons (1992).
- 3) R. Humble, G. Henry, and W. Larson, *Space Propulsion Analysis and Design*, McGraw-Hill (1995).
- 4) H. Siefert and J. Crum, *Thrust Coefficient and Expansion Ratio Tables*, Ramo-Wooldridge Corp. (1956).
- 5) G. Mandell, "The Wayward Wind", *Model Rocketry*, January and February (1970).
- 6) J. Louwers, TNO Prins Maurits Laboratory, personal communication 1997.
- 7) T. Cox, *CurveFit 2.11B*, July 1988. [A shareware program.]
- 8) E. Brown, "Model Rocket Engine Performance / A Method for Calculating Chamber Pressures for Estes Model Rocket Engines", Estes Industries, 1971/1978.

Appendix A

```
10 CLS          ' PROGRAM NAME IS APPENDXA.BAS
20 PRINT "PLEASE ENTER RATIO OF SPECIFIC HEATS."
30 INPUT "ENTER NUMBER BETWEEN 1.05 AND 1.71"; GAMMA
40 IF GAMMA >= 1.05 AND GAMMA <= 1.71 THEN GOTO 50 ELSE BEEP: GOTO 20
50 '          ***          CALCULATE VALUE FOR CAPITAL GAMMA          ***
60 CAPITAL.GAMMA = SQR(GAMMA) * (2 / (GAMMA + 1)) ^ ((GAMMA + 1) / (2 *
   (GAMMA - 1)))
70 ALPHA = SQR((GAMMA - 1) / (2 * GAMMA)); BETA = (GAMMA - 1) / GAMMA:
   DELTA = 1 / GAMMA
80 INPUT "ENTER ATMOSPHERIC PRESSURE (PSIA)"; ATMOS.PRESS
90 INPUT "ENTER CHAMBER PRESSURE (PSIA)"; CHAMBER.PRESS
100 PRESS.RATIO = CHAMBER.PRESS / ATMOS.PRESS
110 PRESS.RATIO = INT(PRESS.RATIO * 1000 + .5) / 1000
120 NUMERATOR = CAPITAL.GAMMA * ALPHA * (PRESS.RATIO) ^ DELTA
130 DENOMINATOR = SQR(1 - (1 / PRESS.RATIO) ^ BETA)
140 '          ***          CALCULATE EXPANSION RATIO          ***
150 EXPANSION.RATIO = NUMERATOR / DENOMINATOR
160 EXPANSION.RATIO = INT(EXPANSION.RATIO * 1000 + .5) / 1000
170 PRINT "OPTIMUM EXPANSION RATIO IS"; EXPANSION.RATIO
180 INPUT "ENTER ADIABATIC FLAME TEMPERATURE IN DEGREES RANKINE";
   FLAME.TEMP
190 INPUT "ENTER MOLECULAR WEIGHT OF COMBUSTION PRODUCTS"; MOL.WEIGHT:
   PRINT
200 '          ***          CALCULATE VACUUM THRUST COEFFICIENT          ***
210 DENOMINATOR = SQR(1 - (1 / PRESS.RATIO) ^ ((GAMMA - 1) / GAMMA))
220 VACTHRUST.COEFF = CAPITAL.GAMMA * SQR(2 * GAMMA / (GAMMA - 1)) * DE-
   NOMINATOR + EXPANSION.RATIO *
   (1 / PRESS.RATIO)
230 PRINT "VACUUM THRUST COEFFICIENT IS"; VACTHRUST.COEFF
240 '          ***          CALCULATE CHARACTERISTIC EXHAUST VELOCITY          ***
250 C.STAR = SQR(49800! * FLAME.TEMP / MOL.WEIGHT) / CAPITAL.GAMMA
260 PRINT "CHARACTERISTIC EXHAUST VELOCITY IS"; C.STAR; "FEET PER SECOND."
270 PRINT "PRESSURE RATIO IS"; PRESS.RATIO: PRINT
280 THRUST.COEFF = VACTHRUST.COEFF - EXPANSION.RATIO * (1 / PRESS.RATIO)
290 PRINT "THRUST COEFFICIENT AT"; CHAMBER.PRESS; "PSIA IS"; THRUST.COEFF
300 INPUT "DO YOU WISH TO CONTINUE (Y/N)"; ANSWER$
310 IF ANSWER$ = "y" OR ANSWER$ = "Y" THEN GOTO 10 ELSE END
```

Appendix B

```
10 CLS ' PROGRAM NAME IS APPENDXB.BAS
20 PRINT "PLEASE ENTER RATIO OF SPECIFIC HEATS."
30 INPUT "ENTER NUMBER BETWEEN 1.05 AND 1.71"; GAMMA
40 IF GAMMA >= 1.05 AND GAMMA <= 1.71 THEN GOTO 50 ELSE BEEP: GOTO 20
50 ' *** CALCULATE VALUE FOR CAPITAL GAMMA ***
60 CAPITAL.GAMMA = SQR(GAMMA) * (2 / (GAMMA + 1)) ^ ((GAMMA + 1) / (2 *
(GAMMA - 1))) '
70 ALPHA = SQR((GAMMA - 1) / (2 * GAMMA)); BETA = (GAMMA - 1) / GAMMA:
DELTA = 1 / GAMMA
80 ' *** INITIALIZE CHAMBER PRESSURE/EXIT PRESSURE ***
90 LET PRESS.RATIO = 1.72
100 PRINT "ENTER SELECTED EXPANSION RATIO."
110 INPUT "VALUE MUST BE BETWEEN 1.00 AND 50.00"; EXPANSION.RATIO: PRINT
: PRINT
120 EXPANSION.RATIO = INT(EXPANSION.RATIO * 1000 + .5) / 1000
130 IF EXPANSION.RATIO >= 1 AND EXPANSION.RATIO <= 50 THEN GOTO 140 ELSE
BEEP: GOTO 100
140 LET TEMP.EXP.RATIO = 0: COUNT = 0
150 ' *** LOOP TO MATCH SELECTED EXPANSION RATIO ***
160 WHILE TEMP.EXP.RATIO <> EXPANSION.RATIO
170 IF TEMP.EXP.RATIO < EXPANSION.RATIO THEN PRESS.RATIO = PRESS.RATIO
+ (EXPANSION.RATIO - TEMP.EXP.RATIO) * 4! + .001 ELSE GOTO 180
180 PRESS.RATIO = PRESS.RATIO - (TEMP.EXP.RATIO - EXPANSION.RATIO) *
4! - .002
190 PRESS.RATIO = INT(PRESS.RATIO * 1000 + .5) / 1000
200 NUMERATOR = CAPITAL.GAMMA * (PRESS.RATIO) ^ DELTA * ALPHA
220 DENOMINATOR = SQR(1 - (1 / PRESS.RATIO) ^ BETA)
230 TEMP.EXP.RATIO = NUMERATOR / DENOMINATOR
240 TEMP.EXP.RATIO = INT(TEMP.EXP.RATIO * 1000 + .5) / 1000
250 COUNT = COUNT + 1
260 WEND
270 ' *** CONTINUE WITH FURTHER CALCULATIONS ***
280 INPUT "ENTER LOCAL ATMOSPHERIC PRESSURE (14.7 IF UNSURE)"; ATMOS.PRESS
290 INPUT "ENTER ADIABATIC FLAME TEMPERATURE IN DEGREES RANKINE";
FLAME.TEMP
300 INPUT "ENTER MOLECULAR WEIGHT OF COMBUSTION PRODUCTS"; MOL.WEIGHT:
PRINT
310 ' *** CALCULATE VACUUM THRUST COEFFICIENT ***
320 VACTHRUST.COEFF = CAPITAL.GAMMA * SQR(2 / BETA) * DENOMINATOR + EXPAN-
SION.RATIO * (1 / PRESS.RATIO)
330 PRINT "VACUUM THRUST COEFFICIENT IS"; VACTHRUST.COEFF
340 ' *** CALCULATE CHARACTERISTIC EXHAUST VELOCITY ***
350 C.STAR = SQR(49800! * FLAME.TEMP / MOL.WEIGHT) / CAPITAL.GAMMA
360 PRINT "CHARACTERISTIC EXHAUST VELOCITY IS"; C.STAR; "FEET PER SECOND."
370 PRINT "PRESSURE RATIO IS"; PRESS.RATIO: PRINT
380 INPUT "WHAT IS THE DESIRED CHAMBER PRESSURE"; CHAMBER.PRESS
390 THRUST.COEFF = VACTHRUST.COEFF - EXPANSION.RATIO * (1 / PRESS.RATIO)
400 PRINT "THE THRUST COEFFICIENT AT"; CHAMBER.PRESS; "PSIA IS";
THRUST.COEFF
410 INPUT "DO YOU WISH TO CONTINUE (Y/N)"; ANSWER$
420 IF ANSWER$ = "Y" OR ANSWER$ = "y" THEN GOTO 10 ELSE END
```

Appendix C

```

10  CLS          ' PROGRAM NAME IS APPENDXC.BAS
20  PRINT "PLEASE ENTER RATIO OF SPECIFIC HEATS."
30  INPUT "ENTER NUMBER BETWEEN 1.05 AND 1.71"; GAMMA
40  IF GAMMA >= 1.05 AND GAMMA <= 1.71 THEN GOTO 50 ELSE BEEP: GOTO 20
50  '          ***          CALCULATE VALUE FOR CAPITAL GAMMA          ***
60  CAPITAL.GAMMA = SQR(GAMMA) * (2 / (GAMMA + 1)) ^ ((GAMMA + 1) / (2 *
    (GAMMA - 1))) '
70  BETA = (GAMMA - 1) / GAMMA
80  '          ***          INITIALIZE CHAMBER PRESSURE/EXIT PRESSURE          ***
90  PRINT "ENTER SELECTED EXPANSION RATIO."
100 INPUT "VALUE MUST BE BETWEEN 1.00 AND 50.00"; EXPANSION.RATIO: PRINT
    :          PRINT
110 IF EXPANSION.RATIO >= 1 AND EXPANSION.RATIO <= 50 THEN GOTO 120 ELSE
    BEEP: GOTO 90
120 '          ***          CALCULATE COEFFICIENTS A, B, AND C          ***
130 A = 38.7019 / GAMMA - 15.5227 / GAMMA ^ 2 - 25.6441
140 B = 1 / (.3283 * (GAMMA - 1.5242) ^ 2 + .1423)
150 C = 52.4092 * GAMMA ^ 15.0965 * .0013 ^ GAMMA
160 '          ***          CALCULATE PRESSURE RATIO          ***
170 PRESS.RATIO = A + B * EXPANSION.RATIO + C * EXPANSION.RATIO ^ 2:
    PRESS.RATIO = INT(PRESS.RATIO * 1000 + .5) / 1000
180 DENOMINATOR = SQR(1 - (1 / PRESS.RATIO) ^ BETA)
190 '          ***          CONTINUE WITH FURTHER CALCULATIONS          ***
200 INPUT "ENTER LOCAL ATMOSPHERIC PRESSURE (14.7 IF UNSURE)"; ATMOS.PRESS
210 INPUT "ENTER ADIABATIC FLAME TEMPERATURE IN DEGREES RANKINE";
    FLAME.TEMP
220 INPUT "ENTER MOLECULAR WEIGHT OF COMBUSTION PRODUCTS"; MOL.WEIGHT:
    PRINT
230 '          ***          CALCULATE VACUUM THRUST COEFFICIENT          ***
240 VACTHRUST.COEFF = CAPITAL.GAMMA * SQR(2 / BETA) * DENOMINATOR + EXPAN-
    SION.RATIO * (1 / PRESS.RATIO)
250 PRINT "VACUUM THRUST COEFFICIENT IS"; VACTHRUST.COEFF
260 '          ***          CALCULATE CHARACTERISTIC EXHAUST VELOCITY          ***
270 C.STAR = SQR(49800! * FLAME.TEMP / MOL.WEIGHT) / CAPITAL.GAMMA
280 PRINT "CHARACTERISTIC EXHAUST VELOCITY IS"; C.STAR; "FEET PER SECOND."
290 PRINT "PRESSURE RATIO IS"; PRESS.RATIO: PRINT
300 INPUT "ENTER DESIRED CHAMBER PRESSURE"; CHAMBER.PRESS
310 THRUST.COEFF = VACTHRUST.COEFF - EXPANSION.RATIO * (AT-
    MOS.PRESS/CHAMBER.PRESS)
320 PRINT "THE THRUST COEFFICIENT AT"; CHAMBER.PRESS; "PSIA IS";
    THRUST.COEFF
340 INPUT "DO YOU WISH TO CONTINUE? (Y/N)"; ANSWER$
350 IF ANSWER$ = "y" OR ANSWER$ = "Y" GOTO 10 ELSE END

```

Appendix D

```
10 CLS ' PROGRAM NAME IS APPENDXD.BAS
20 PRINT "PLEASE ENTER RATIO OF SPECIFIC HEATS."
30 INPUT "ENTER NUMBER BETWEEN 1.05 AND 1.71"; GAMMA
40 IF GAMMA >= 1.05 AND GAMMA <= 1.71 THEN GOTO 50 ELSE BEEP: GOTO 20
50 ' *** CALCULATE VALUE FOR CAPITAL GAMMA ***
60 CAPITAL.GAMMA = SQR(GAMMA) * (2 / (GAMMA + 1)) ^ ((GAMMA + 1) / (2 *
(GAMMA - 1))) '
70 ALPHA = SQR((GAMMA - 1) / (2 * GAMMA)): BETA = (GAMMA - 1) / GAMMA:
DELTA = 1 / GAMMA
80 ' *** INITIALIZE CHAMBER PRESSURE/EXIT PRESSURE ***
90 LET PRESS.RATIO = 1.72
100 PRINT "ENTER SELECTED EXPANSION RATIO."
110 INPUT "VALUE MUST BE BETWEEN 1.00 AND 50.00"; EXPANSION.RATIO: PRINT
: PRINT
120 EXPANSION.RATIO = INT(EXPANSION.RATIO * 1000 + .5) / 1000
130 IF EXPANSION.RATIO >= 1 AND EXPANSION.RATIO <= 50 THEN GOTO 140 ELSE
BEEP: GOTO 100
140 LET TEMP.EXP.RATIO = 0: COUNT = 0
150 ' *** LOOP TO MATCH SELECTED EXPANSION RATIO ***
160 WHILE TEMP.EXP.RATIO <> EXPANSION.RATIO
170 IF TEMP.EXP.RATIO < EXPANSION.RATIO THEN PRESS.RATIO = PRESS.RATIO
+ (EXPANSION.RATIO - TEMP.EXP.RATIO) * 4! + .001 ELSE GOTO 180
180 PRESS.RATIO = PRESS.RATIO - (TEMP.EXP.RATIO - EXPANSION.RATIO) *
4! - .002
190 PRESS.RATIO = INT(PRESS.RATIO * 1000 + .5) / 1000
200 NUMERATOR = CAPITAL.GAMMA * (PRESS.RATIO) ^ DELTA * ALPHA
220 DENOMINATOR = SQR(1 - (1 / PRESS.RATIO) ^ BETA)
230 TEMP.EXP.RATIO = NUMERATOR / DENOMINATOR
240 TEMP.EXP.RATIO = INT(TEMP.EXP.RATIO * 1000 + .5) / 1000
250 COUNT = COUNT + 1
260 WEND
270 ' *** CONTINUE WITH FURTHER CALCULATIONS ***
280 INPUT "ENTER LOCAL ATMOSPHERIC PRESSURE (14.7 IF UNSURE)"; ATMOS.PRESS
290 INPUT "ENTER ADIABATIC FLAME TEMPERATURE IN DEGREES RANKINE";
FLAME.TEMP
300 INPUT "ENTER MOLECULAR WEIGHT OF COMBUSTION PRODUCTS"; MOL.WEIGHT:
PRINT
310 ' *** CALCULATE VACUUM THRUST COEFFICIENT ***
320 VACTHRUST.COEFF = CAPITAL.GAMMA * SQR(2 / BETA) * DENOMINATOR + EXPAN-
SION.RATIO * (1 / PRESS.RATIO)
330 PRINT "VACUUM THRUST COEFFICIENT IS"; VACTHRUST.COEFF
340 ' *** CALCULATE CHARACTERISTIC EXHAUST VELOCITY ***
350 C.STAR = SQR(49800! * FLAME.TEMP / MOL.WEIGHT) / CAPITAL.GAMMA
360 PRINT "CHARACTERISTIC EXHAUST VELOCITY IS"; C.STAR; "FEET PER SECOND."
370 PRINT "PRESSURE RATIO IS"; PRESS.RATIO: PRINT
380 INPUT "ENTER NOZZLE THROAT DIAMETER (IN INCHES)"; THROAT.DIA
390 THROAT.AREA = 3.14159 * (THROAT.DIA / 2) ^ 2
400 INPUT "ENTER THRUST LEVEL (POUNDS)"; THRUST
410 CFPC = THRUST / THROAT.AREA
420 CHAMBER.PRESS = (CFPC + EXPANSION.RATIO * ATMOS.PRESS) / VAC-
THRUST.COEFF
430 PRINT "CHAMBER PRESSURE WHEN THRUST IS"; THRUST; "POUNDS IS"; CHAM-
BER.PRESS; "PSIA."
1000 INPUT "DO YOU WISH TO CONTINUE (Y/N)"; ANSWER$
1010 IF ANSWER$ = "Y" OR ANSWER$ = "y" THEN GOTO 10 ELSE END
```

Pyrotechnic Ignition and Propagation: A Review

K. L. and B. J. Kosanke

PyroLabs, Inc., 1775 Blair Road, Whitewater, CO 81527, USA

ABSTRACT

The ideal pyrotechnic is completely stable in storage and handling, yet performs its mission completely with absolute reliability upon demand. Many accidents in pyrotechnics are the result of unintentional ignitions during handling and storage. There can also be serious safety ramifications of ignition and propagation failures of pyrotechnic devices. This review article presents a fairly rigorous, but mostly non-mathematical discussion of the ignition and propagation processes.

Keywords: ignition, propagation, heat of reaction, activation energy, spontaneous ignition, thermal run-away, cook-off

Introduction

An understanding of the mechanism of pyrotechnic ignition and propagation will improve one's ability to identify and solve problems with ignition failures (duds) and unintended ignitions (accidents). In addition, many of these same principles play an important role in understanding the control of pyrotechnic burn rates. This article will examine these important topics thoroughly, however, not at a mathematically rigorous level. For more detailed and rigorous discussions, readers are referred to the writings of Merzhanov and Abramov.^[1,2]

Pyrotechnic Reaction Energy Considerations

Pyrotechnic compositions are mixtures of fuel(s) and oxidizer(s) and possibly other materials. They are used to produce energy on demand in the form of heat, light, sound, etc. Pyrotechnic compositions are said to be in a "meta-

stable" state. That is to say under typical conditions they are stable and do not react to release their internal chemical energy unless externally stimulated in some way. Probably the most common stimulus is the addition of heat, such as provided by a burning match or fuse. Ignition is the process of stimulating a pyrotechnic composition to release its internal energy and can be defined as "the initiation of self-sustained burning or explosion of a pyrotechnic material".^[3]

Figure 1 illustrates the process of ignition by graphing the internal energy of a tiny portion of pyrotechnic composition during the progress of its chemical reactions and is typical of non-spontaneous exothermic chemical reactions.^[4] At the left of the graph, where the process begins, the pyrotechnic composition has a certain amount of internal energy. To accomplish ignition, external energy is supplied, such as from a burning match. This addition of energy increases the internal energy of the composition and is seen as a rise in the curve of Figure 1. This is indicated as the "Energy In" part of the reaction. As the process continues, eventually the pyrotechnic composition ignites to release its stored chemical energy to the surroundings.

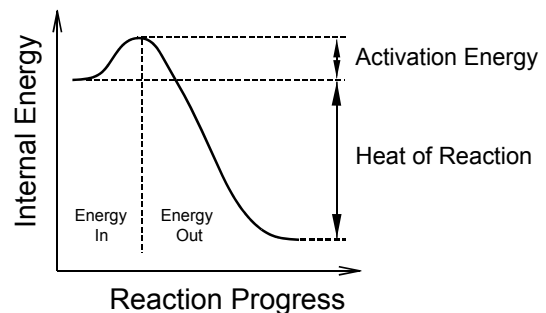


Figure 1. A graph illustrating the flow of energy into and out of a tiny portion of pyrotechnic composition.

Table 1. Heats of Reaction of Binary Pyrotechnic Compositions.^[5a]

Fuel (%)	Oxidizer (%)	ΔH_r (kcal/g)
Magnesium (37)	Potassium chlorate (63)	2.29
Magnesium (40)	Potassium perchlorate (60)	2.24
Magnesium (32)	Barium nitrate (68)	1.65
Aluminum (34)	Potassium perchlorate (66)	2.45
Aluminum (40)	Sodium nitrate (60)	2.00
Aluminum (25)	Iron(II) oxide (75)	0.96

This loss of internal energy is seen as a drop in the curve of Figure 1 and is indicated as the “Energy Out” part of the reaction. The energy that was required to stimulate this release is commonly referred to as the “Activation Energy” (E_a). The net amount of energy produced by the pyrotechnic reaction is referred to as the “Heat of Reaction” (ΔH_r).^[a]

Even the smallest particles of fuel and oxidizer in the pyrotechnic composition, are clusters of many billions of atoms bound together to form the particle. It is possible to think of the two-step process, energy in and energy out, as first when old chemical bonds are being broken in the fuel and oxidizer, and second, when new chemical bonds are being formed to make the reaction products. This also helps to make it clear why the activation energy^[b] requirement acts as a barrier that must be surmounted to initiate the chemical reaction. Until the necessary energy is supplied to break the original chemical bonds, thus freeing individual fuel and oxidizer atoms, they are not available to react with each other to form new chemical bonds.

In a pyrotechnic chemical reaction, a net amount of energy will be produced, providing the new chemical bonds being formed in the reaction products are stronger than the old bonds that must first be broken in the fuel and oxidizer. Table 1 is a listing of the heats of reaction for some two-component pyrotechnic reactions. The reason that varying amounts of energy are produced is that in each case different numbers and strengths of chemical bonds are broken and formed.

A collection of atoms, such as those bound together in a particle of fuel or oxidizer, are not held in absolutely rigid positions. The individual atoms jostle about (vibrate), back and forth,

and up and down. Because of these internal motions, the individual atoms possess energy, often referred to as thermal energy. In the process of jostling with one another, the atoms transfer some of their thermal energy from one to another. The net result of this jostling and energy sharing is that some atoms have much energy while others have little, and an atom that has much energy now may have little energy later.

Figure 2 is a graph illustrating the distribution of thermal energies^[4] of individual atoms in fuel and oxidizer particles in a pyrotechnic composition at some temperature T_1 . The curve goes through the origin of the graph, meaning that zero atoms have zero energy. Thereafter an increasing number of atoms have increasing energy, until a peak is reached, followed by continuously decreasing numbers of atoms possessing higher and higher energies. Also shown in Figure 2 is the activation energy E_a , which is

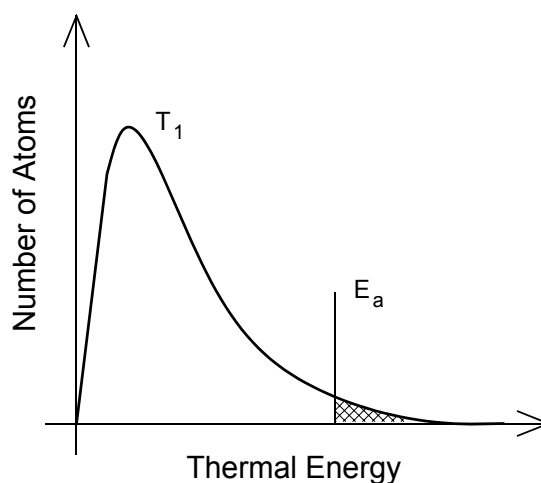


Figure 2. A graph illustrating the distribution of thermal energies of atoms in a pyrotechnic composition.

required to initiate the pyrotechnic reaction. Note that the composition contains some atoms with energies exceeding the activation energy barrier. (In Figure 2 the number of atoms with energies greater than E_a has been exaggerated for clarity.)

Since some atoms in the pyrotechnic composition have sufficient energy to react, the question should be, “Why isn’t the pyrotechnic composition reacting?” The answer is, “It is reacting, but very, very slowly.” To see why this is the case, consider the following: At room temperature, only 1 atom in roughly every million billion (10^{15}) has the needed activation energy.^[6] Additionally, it is only the fuel atoms that are in direct contact with oxidizer atoms that can react. When considering the fraction of atoms in a tiny particle that are on its surface, and the fraction of surface atoms that are likely to be in direct contact with the right atoms on the surface of other particles, only 1 atom in roughly every thousand billion billion (10^{21}) is capable of reacting at any given time.

Thermal Run-Away and Spontaneous Ignition

If the temperature of the pyrotechnic composition is raised, from T_1 to a higher temperature T_2 , as illustrated in Figure 3, on average the atoms jostle around with more energy. More significantly, however, the number of atoms with energies exceeding the activation energy barrier increases greatly.^[4] As a consequence, there are now many more atoms capable of reacting, and there is a corresponding increase in the rate at which the reactions occur. Recall, however, that these chemical reactions produce thermal energy; thus an increase in the reaction rate causes an increase in the rate of production of heat; which would seem to produce a further increase in temperature; which causes still more atoms to have energies exceeding the activation energy barrier; which causes a still greater increase in reaction rate and the rate of heat production; which causes a further increase in temperature; etc. This accelerating cyclic process is outlined in Figure 4 and leads to what can be called “thermal run-away” and ignition.

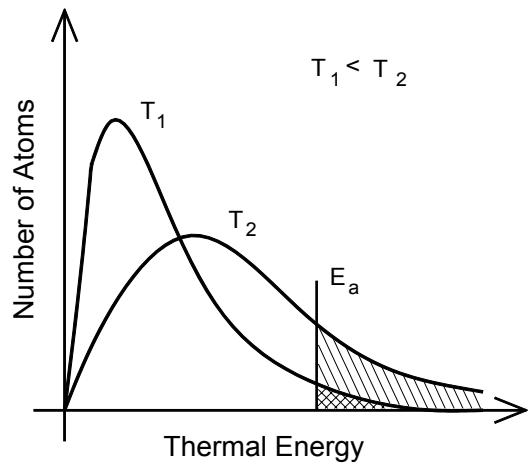


Figure 3. An illustration of the effect of increasing temperature on the distribution of the thermal energy of atoms.

Taken literally, the process outlined in Figure 4, suggests that the slightest temperature rise of a pyrotechnic composition will eventually lead to thermal run-away and ignition. Obviously, this is not correct. The reason is that, thus far, only the rate of thermal energy production has been considered, which is only half of the total picture. The rate of thermal energy

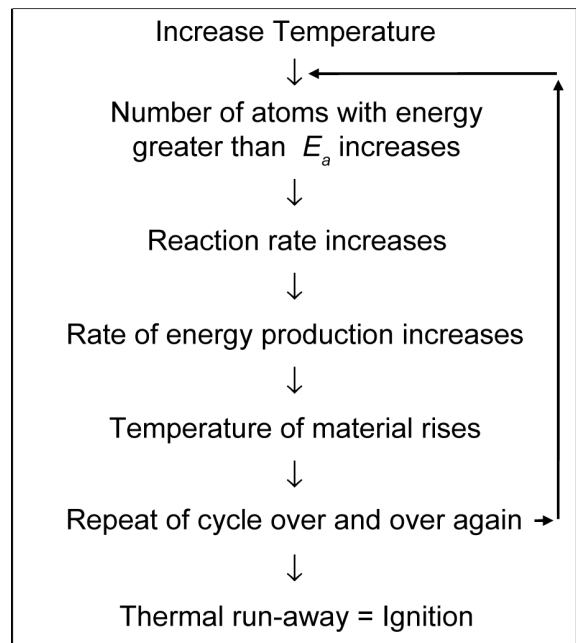


Figure 4. Outline of the accelerating cyclic process leading to thermal run-away and ignition.

loss from the pyrotechnic composition to the surroundings must also be considered. This more complete energy picture is presented in Figure 5, with both heat-gain and heat-loss rates plotted as a function of temperature.

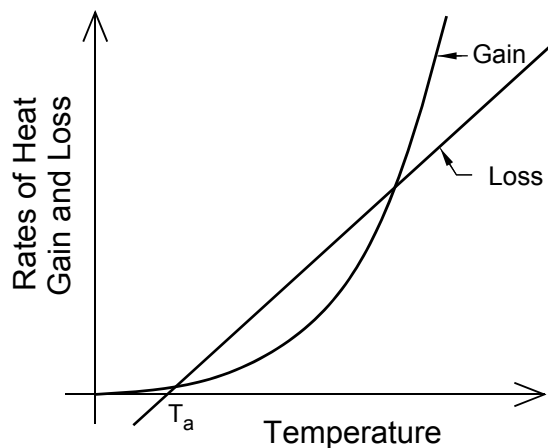


Figure 5. Graph illustrating the rates of heat gain and loss for a pyrotechnic composition as a function of temperature.

The rate of the pyrotechnic chemical reaction k follows an exponential relationship,^[4] sometimes referred to as the Arrhenius equation:

$$k = Ae^{-E_a/RT} \quad (1)$$

where A and R are constants, and T is absolute temperature. The rate of heat gain Q_g is just the reaction rate multiplied by the heat of reaction:

$$Q_g = k \cdot \Delta H_r \quad (2)$$

Thus, in Figure 5, the rate of heat gain curve passes through the origin and rises ever more steeply with increasing temperature.

For a mass of pyrotechnic composition, heat loss from the surface will primarily be from convection through contact with the air. However, any heat generated internally, will first need to be conducted to the surface. Accordingly, for spontaneous heat generation, temperatures at the center of the mass would normally be highest.^[c] The rate of heat loss Q_l from the center of the pyrotechnic composition depends on the thermal conductivity of the composition and any packaging, the convective heat loss coefficient, the geometry of the sample (or

item), and the difference in temperature between the center of the composition T and ambient temperature T_a . This may be expressed as:^[6]

$$Q_l = C(T - T_a) \quad (3)$$

where C is a constant derived from the geometry and thermal properties of the pyrotechnic sample (or item). Accordingly, in Figure 5, the rate of heat loss curve is a straight line crossing the temperature axis at ambient temperature and with a slope equal to C .

To illustrate why, under typical storage conditions, pyrotechnic compositions are meta-stable and do not spontaneously ignite, as suggested by the process outlined in Figure 4, consider Figures 6 and 7. Figure 6 is an enlarged view of the low temperature region from Figure 5. If a pyrotechnic composition is formulated from materials at ambient temperature, the composition will be at the same temperature, at least initially. In Figure 6, note that at ambient temperature, the rate of heat loss is zero, while the rate of heat gain is greater than zero. Accordingly, the temperature of the sample will begin to increase. The temperature of the sample will continue to rise until the rates of gain and loss are equal. This occurs at the crossing point of the “gain” and “loss” curves, where the temperature of the sample T_s has risen to slightly above ambient temperature. (Note that in Figure 6, the temperature difference between T_a and T_s has been exaggerated for clarity.)^[d]

Now imagine that for some reason the pyrotechnic composition were momentarily raised from temperature T_s to T_1 , somewhat further

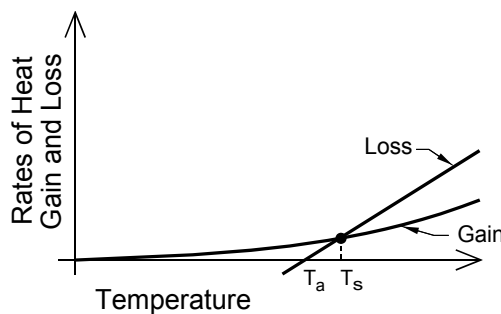


Figure 6. Enlarged view of the low temperature region of Figure 5.

above ambient, see Figure 7. In this case, both the rate of heat gain of the pyrotechnic composition and the rate of heat loss from the composition, increase. However, the rate of loss is greater than the rate of gain. Accordingly, the net effect will be a loss of thermal energy with time. Thus, the temperature of the composition will decrease and must continue to fall to the temperature where the rates of loss and gain are equal (at temperature T_s). From the above discussion, it can be seen that pyrotechnic compositions are at least meta-stable, in that any small addition of energy will not ultimately cause thermal run-away and ignition.

Figure 7 shows that if the temperature of the pyrotechnic composition were to be raised momentarily to a still higher temperature T_2 , that the results would be quite different. In this case, again both the rate of heat gain and the rate of heat loss increase. However, this time the rate of gain has overtaken the rate of loss. At this temperature, there is a net accumulation of heat, producing a further increase in temperature. In fact, this is an ever accelerating process, because as the temperature increases, the rate of gain increases much faster than the rate of loss. In this case, the process outlined in Figure 4 does apply and leads to thermal run-away and spontaneous ignition.

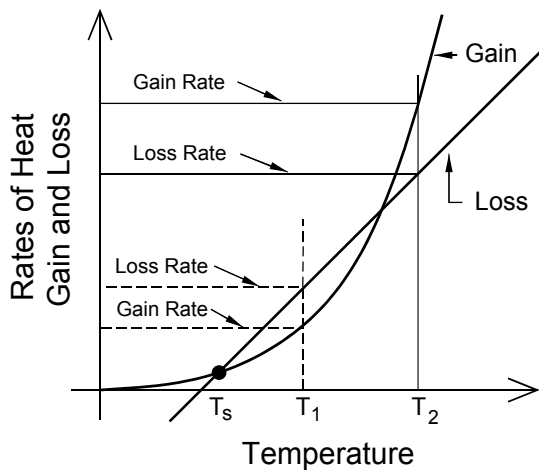


Figure 7. Illustration of the effect of raising the temperature of a pyrotechnic composition.

Thermal Run-Away Temperature^[e]

Obviously the temperature at which thermal run-away can occur for each pyrotechnic composition is of great importance from a safety standpoint. Whenever a pyrotechnic composition is raised above this temperature, it will begin to undergo thermal run-away and will eventually ignite spontaneously. In Figure 8, the run-away temperature is designated as T_r and is the temperature corresponding to where the gain and loss curves cross for the second time. For any composition, this temperature could be established experimentally (with some effort and much time) or mathematically (providing the gain and loss relationships are known).

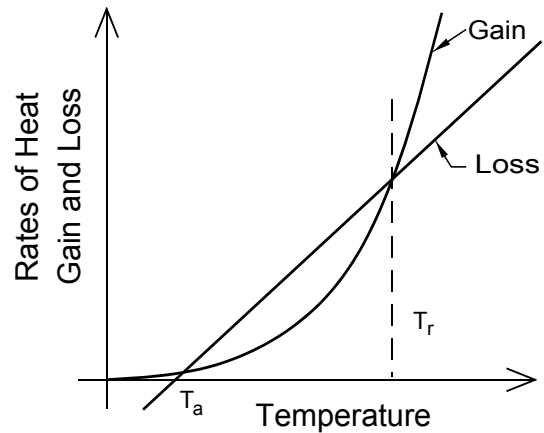


Figure 8. Illustration of the thermal run-away temperature of a pyrotechnic composition, under one set of conditions.

From equations 1 and 2 it can be seen that the rate of heat gain depends on the activation energy and the heat of reaction, which are determined by the formulation of the pyrotechnic composition. The heat of reaction is easy to calculate, providing one knows the equation for the chemical reaction,^[5b] or it can be determined experimentally.^[5c] Determination of activation energy must be established through experimentation.^[9,10] From equation 3, as expressed by the constant C , it can be seen that the rate of heat loss depends on the thermal conductivity, the convection coefficient and geometry of the composition, and on ambient temperature. All of these parameters can be determined with only modest effort. However, the

rate of heat loss depends on many things other than the pyrotechnic formulation. For example, the degree of compaction of the composition, the size (mass) of the item or sample, and the packaging of the composition all affect the thermal conductivity of the composition or item. Also, the rate of heat loss is a function of ambient temperature. Thus, for each pyrotechnic formulation there is not just one thermal run-away temperature, rather there is one for each of an infinite number of different conditions. This illustrates the problem in trying to use thermal run-away temperatures to characterize a pyrotechnic formulation (and why many pyrotechnists have never heard of it).

Spontaneous Ignition Due to Thermal Run-Away

Even though the use of thermal run-away temperature as a way of characterizing pyrotechnic compositions is of limited value, the concept is important because it helps to identify some potentially dangerous conditions where there will be delayed spontaneous ignitions. For example, Figure 9 illustrates the effect of varying sample size. Note that the rate of heat gain (per gram of composition) is unaffected by sample size, but the rate of heat loss is sample-size dependent. Small samples generally lose heat easily and have a rate of heat-loss curve that is steep, with two crossing points, the higher of which is the thermal run-away temperature. As the sample size increases (medium sample size in Figure 9), the slope of the curve decreases, lowering the run-away temperature more and more with increasing sample size. At some point, for a large sample, there will only be a single point of contact between the curves. This represents the largest sample, under a specific set of conditions, that theoretically will not spontaneously run-away and ignite. For samples larger than this, the rate of heat gain is always more than the rate of loss, and the sample will always run-away thermally. It may take a very long time, but for large enough samples, eventually, there will always be a spontaneous ignition.

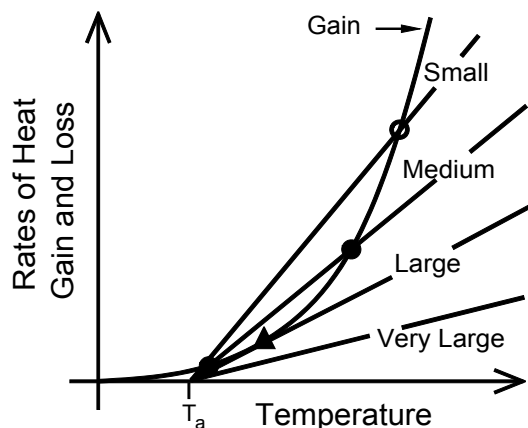


Figure 9. An illustration of the effect of increasing sample size on the rate of heat loss and therefore on thermal run-away temperature.

The rate of heat loss is sample-size dependent because sample size is one factor that affects the constant C in equation 3. Another factor is the thermal conductivity of the pyrotechnic composition and its packaging. In Figure 9, poorly conducting compositions and insulating packaging, produce effects equivalent to a large sample size.

A somewhat similar situation arises for increasing ambient temperature, see Figure 10. When the ambient temperature is low, samples lose heat to the surroundings fairly easily. This places the heat-loss rate curve fairly high on the heat-gain curve, producing two crossing points, the higher of which is the thermal run-away temperature. As the ambient temperature increases, it becomes more difficult for the sample to lose heat. The slope of the heat-loss curve is unchanged, but its position relative to the heat-gain curve is lower. This lowers the run-away temperature more and more with increasing ambient temperature. At some point, for high enough ambient temperature, there will only be a single point of contact between the curves. This represents the highest ambient temperature, for this type and size of sample, that will not spontaneously run-away thermally (ignite). For ambient temperatures greater than this, the rate of heat gain is always more than the rate of heat loss, and the sample will always run-away thermally. It may take a long time,

but for such hot ambient conditions there will eventually be a spontaneous ignition.

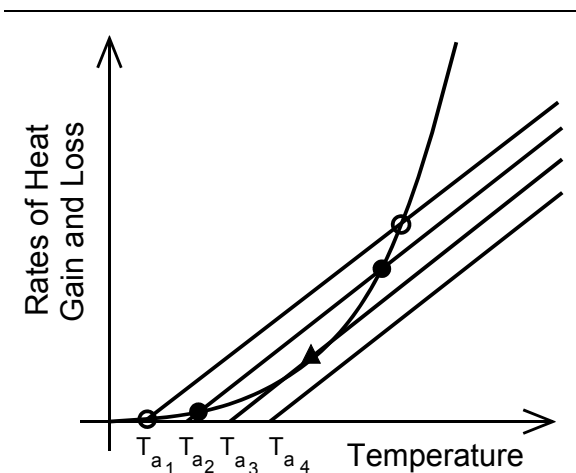


Figure 10. An illustration of the effect of increasing ambient temperature on the rate of heat loss and therefore on thermal run-away temperature.

Just how large a sample and just how high an ambient temperature are required for thermal run-away and spontaneous ignition depends on the chemical formulation and the conditions of its packaging and storage. For some compositions under favorable conditions, it may require millions of tons of material and take years to run-away and spontaneously ignite. However, under more extreme conditions, or for other compositions, tiny samples of composition may ignite very quickly.

Time to Ignition, Cook-Off Tests

The time for any given pyrotechnic composition to ignite is a function of the temperature to which it is exposed, as illustrated in Figure 11. If a sample is placed in an oven, its temperature will begin to rise from ambient temperature T_a , eventually reaching the temperature of the oven. If the temperature of the oven T_1 is less than the run-away temperature T_r for the pyrotechnic composition, the sample will never ignite (i.e., the time to ignition is infinite).

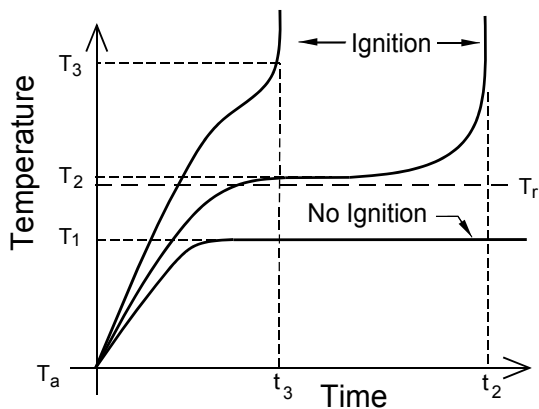


Figure 11. An illustration of the dependence of time to ignition on the temperature to which a pyrotechnic composition is heated.

If the temperature of the oven T_2 is slightly higher than the run-away temperature, upon placement in the oven, the sample will start to heat up and will eventually rise to the temperature of the oven. For a while, it may appear that nothing is happening with the sample. However, inside the sample, heat is slowly accumulating, raising the temperature, at first perhaps imperceptibly. As the internal temperature rises, the rate of reaction increases, increasing the rate of heat gain, and further increasing the temperature (i.e., thermal run-away has begun). As a result of this ever accelerating process, the internal temperature rises ever more rapidly, until eventually there is an ignition, at time t_2 in Figure 11.

If the temperature of the oven (T_3) is significantly higher than the run-away temperature, upon placement in the oven, the sample again will heat up, approaching the oven temperature. However, under these conditions, the sample's temperature rise may not slow significantly as it reaches the oven temperature, before thermal run-away is at an advanced state with ignition occurring more quickly at time t_3 .

Determining the time to ignition as a function of temperature, has important ramifications for the storage of pyrotechnics (and explosives). If one were to guess wrong, the consequences of an accidental spontaneous ignition could be disastrous. Tests performed to discover the time-to-ignition and temperature relationship are sometimes called "cook-off" tests.^[11] In these

tests, samples or items are typically placed in a heated bath, after having thermocouples installed internally. Bath and sample temperatures are monitored as a function of time from the start of the test, and the time to ignition or explosion (if either occurs) is recorded.

Ignition and Ignition Temperature

Ignition is one of the more difficult terms to define in pyrotechnics. Obviously it cannot be defined as when chemical reactions start. As was discussed earlier, some pyrotechnic reactions are occurring all the time, although at a very, very low rate. Even after the thermal runaway temperature has been reached, there may be no obvious sign anything is happening. For most observers, the appearance of a flame (high temperature radiant gases) or at least obvious incandescence of the solid phase is taken as the indication that ignition has occurred. As suggested in Figure 11, at the time of ignition very rapidly accelerating reaction rates produce a near instantaneous rise in temperature, typically from several hundred to two thousand degrees Celsius or higher. Thus the physical manifestations of ignition develop very rapidly as ignition is occurring.

Ignition temperature can be defined as “the minimum temperature required for the initiation of a self-propagating reaction”.^[12a] However, from the above discussion, that temperature can vary widely depending on sample conditions and on how long one is willing to wait for the ignition to occur. These problems are mostly eliminated for ignition temperature measurements, because the conditions and delay time are usually specified in the procedure to be used. Unfortunately, there are many different procedures that are used; the *Encyclopedia of Explosives*^[13] alone lists 14 different methods. This means there can be more than one ignition temperature reported for the same pyrotechnic composition, depending on which method was used. Fortunately, the various ignition temperatures of the most commonly used methods all tend to be in the same general range, primarily because the measurement conditions of the various methods tend to be somewhat similar.

Obviously, however, the most consistent results will be achieved if all measurements are made using the same method. Also, when evaluating reported ignition temperature data, it is useful to know which method has been used. Three hot bath methods and one differential thermal analysis method are described in the following paragraphs.

Hot Bath Method One: Ignition temperature is the lowest temperature of a bath of Wood’s metal,^[1] to within 5 °C, that results in ignition within 5 minutes for a 0.1 g sample in a pre-heated small glass test tube inserted 1/3 its length into the bath.^[5a]

Hot Bath Method Two: Ignition temperature is the temperature of a bath of Wood’s metal that results in ignition in 5 seconds (determined graphically using time to ignition data) for a 1.0 g sample in a thin-walled brass or copper tube (typically a No. 6 detonator shell).^[10]

Hot Bath Method Three: Ignition temperature is the temperature of a bath of Wood’s metal, heated at a rate of 5 °C per minute, at which ignition occurs for a 0.5 g sample in a tightly corked glass test tube (125 mm long by 15 mm inside diameter with a 0.5 mm wall thickness).^[13]

Differential Thermal Analysis Method: Ignition temperature is the temperature of onset of the ignition exotherm for a 10 to 100 mg sample heated at a rate of 50 °C per minute.^[14]

A collection of ignition temperatures for a series of two-component, stoichiometric pyrotechnic compositions is presented in Table 2. Shidlovskiy reports the method as one using an electric furnace instead of a bath of Wood’s metal. Unfortunately, he provides no information on the method, other than an estimate of the accuracy of the results to be within 10 °C. (This data was chosen for inclusion because it is the most systematically complete set of data known to the authors.)

It might be of interest to note that a typical pyrotechnic composition raised to its ignition temperature will have about 30 million times more atoms with energies exceeding E_a than at room temperature.^[6]

Table 2. Ignition Temperatures for Binary Pyrotechnic Compositions.^[5c]

Oxidizer	Ignition Temperature (°C)				
	Sulfur	Lactose	Charcoal	Mg powder	Al dust
Potassium chlorate	220	195	335	540	785
Potassium perchlorate	560	315	460	460	765
Potassium nitrate	440	390	415	565	890

The Effect of Melting and Tammann Temperature

For a pyrotechnic reaction to occur, the atoms (or molecules) must have the required activation energy, and they must be in direct contact with another atom of the correct type. Even for well-mixed solid particles, there are relatively few points of contact between individual particles; see the top illustration of Figure 12. Thus the number of fuel and oxidizer atoms that are in contact with one another is normally quite small. However, if one of the components melts to flow around the surfaces of the other particles, there is a great increase in the number of atoms in contact; see the bottom illustration of Figure 12.

Accordingly, melting can have a significant effect on the likelihood of ignition. The potential effect on ignition is outlined in Figure 13. If the percentage of atoms in physical contact increases upon the melting of one component, then more atoms with energies exceeding the activation-energy barrier will be in contact with one another. That means the reaction rate will then be greater, and with it the rate of production of thermal energy, which means that thermal run-away and ignition can occur at a lower temperature. Thus it is suggested that if a composition is nearing its ignition temperature, and one component of the composition melts, that could result in ignition occurring at that lower temperature. For example, the melting point of potassium nitrate and the ignition temperature of Black Powder are effectively the same.^[12b]

Melting can be thought of as occurring when the thermal vibrations of a solid are so strong that some of the bonds, which had been holding the solid together, are broken. While for most pure chemicals melting has a sudden onset at a

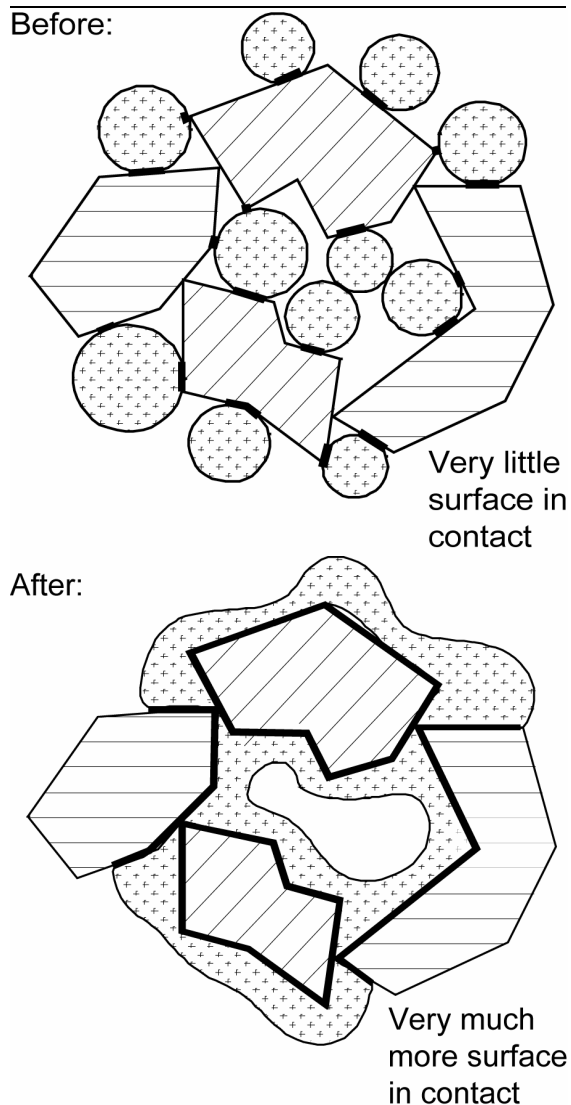


Figure 12. An illustration of the great increase in contact between fuel and oxidizer after one component melts.

specific temperature, the vibrations of the atoms in the solid become increasingly strong as the temperature is increased toward the melting point. This can be thought of as the loosening

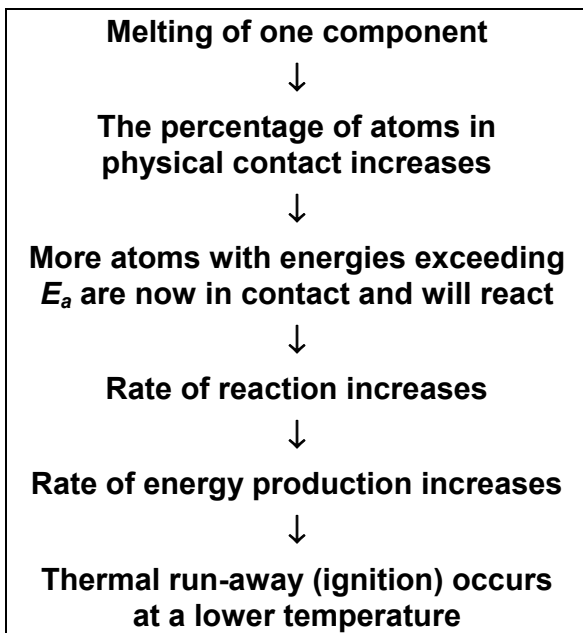


Figure 13. An outline of the effect of melting on thermal run-away and ignition temperature.

of the bonds holding the solid together. It has been suggested that at an absolute temperature halfway to the melting point, the bonds become so loose that there can be a significant commingling of the atoms of particles that are in direct contact.^[8b] This temperature is called the Tamman temperature after the researcher making this observation.

Tamman temperatures are of interest because samples at or above these temperatures demonstrate significantly increased sensitivity to accidental ignition. Table 3 lists the Tamman temperatures for some common pyrotechnic oxidizers.

Table 3. Tamman Temperatures for Common Pyrotechnic Oxidizers.^[12c]

Oxidizer	Tamman Temp. (°C)
Sodium nitrate	17
Potassium nitrate	31
Potassium chlorate	42
Strontium nitrate	149
Barium nitrate	160
Potassium perchlorate	168
Lead chromate	286
Iron(III) oxide	646

Propagation and the Propagation Inequality

Having successfully ignited a pyrotechnic composition is no guarantee that the reaction will propagate throughout. This is because the application of an external stimulus, such as a flame, typically provides thermal energy to only a small portion of the composition, and the ignition stimulus is usually of relatively short duration. After its application, the pyrotechnic combustion reaction will continue to propagate through the composition only so long as the pyrotechnic reaction provides sufficient energy to the unreacted composition. What is needed is sufficient energy to raise the unreacted composition above its ignition temperature. This process is illustrated in Figure 14. The portion of the rod of pyrotechnic composition to the extreme right has already been consumed by burning. Just to the left of that is shown a thin disk of composition that has ignited and is still reacting (burning). Just left of that is another thin disk of composition, labeled “pre-reacting material”, which has not yet ignited. This disk of pre-reacting material will only ignite if it is raised above its ignition temperature, which means that a significant number of its atoms and molecules will have received at least the required activation energy E_a .

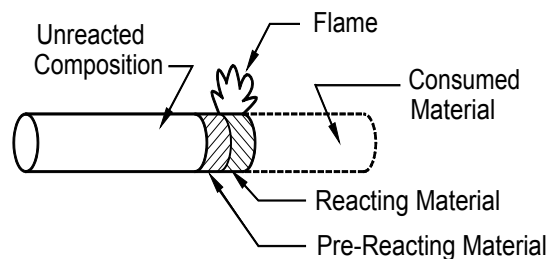


Figure 14. Illustration of a propagating rod of pyrotechnic composition.

Most of the energy being produced by the reacting material (the heat of reaction ΔH_r) is lost to the surroundings. However, some fraction F_{fb} of the energy will be fed back from the reacting layer to the pre-reacting layer. The actual amount of energy fed back is just the product of the heat of reaction and this fraction (i.e., $\Delta H_r \cdot F_{fb}$). Propagation will occur providing more

energy is fed back than is required for ignition of the pre-reacting disk of composition. This statement, then, gives rise to something that could be called the “propagation inequality”

$$\Delta H_r \cdot F_{fb} > E_a \quad (4)$$

Obviously, the probability of successful pyrotechnic propagation is increased by anything that results in more energy being produced by the burning composition, a greater percentage of that energy being fed back, or a reduction of the activation energy requirement. The heat of reaction and the activation energy are determined by the chemical nature of the composition; however, a thorough discussion is beyond the scope of this article.^[g] Energy is fed back to the pre-reacting layer through any combination of conduction, convection, or radiation. These are more fully described in Figure 15, where some of the factors influencing the efficiency of these mechanisms are also presented.

Figure 16 is similar to Figure 14 but provides a more complete description of the propagation process, including information on the relative temperatures expected. Zone (a) is unreacted pyrotechnic composition, which has thus far been unaffected and remains at ambient temperature. Zone (b) is described as the warm-up zone, where the temperature has started to rise above ambient, as a result of thermal conduction and possibly convection. It is in this zone where reaction rates are first beginning to increase. These reactions are sometimes referred to as “pre-ignition reactions”^{[8c][h]} and contribute relatively little thermal energy. In Zone (c), the temperature has risen significantly, at least one component of the composition has melted, and some gaseous materials may be bubbling to the surface. Because of the rise in temperature and the greatly increased contact between fuel and oxidizer, the reaction rate in Zone (c) and the production of heat is greatly increased. In Zone (d), much of the reaction is occurring in the gas phase; however, some droplets of reacting composition ejected from the surface may be present. Again the reaction rate and the thermal energy being produced has increased substantially from the previous zone, and the temperature has peaked. In the final region, Zone (e), the energy producing reactions have ceased, and as a result of heat loss to the sur-

Conduction:

- **Thermal energy (molecular vibration) is conducted along solids, from hotter to cooler.**
- **Factors maximizing conductive feedback:**
 - **Compacted composition**
 - **Metal fuels**
 - **Metal casing or core wire**

Convection:

- **Hot gases penetrate the solid composition along spaces between grains (fire paths).**
- **Factors maximizing convective feedback:**
 - **Uncompacted composition**
 - **Granulated composition**

Radiation:

- **Thermal (infrared) radiation, emitted from flame and glowing particles, is absorbed by incompletely reacted composition.**
- **Factors favoring radiative feedback:**
 - **Solid or liquid particles in flame**
 - **Dark or black composition**

Figure 15. Outline describing the mechanisms of pyrotechnic energy feed back and the factors that affect them.

roundings, the temperature begins to fall significantly.

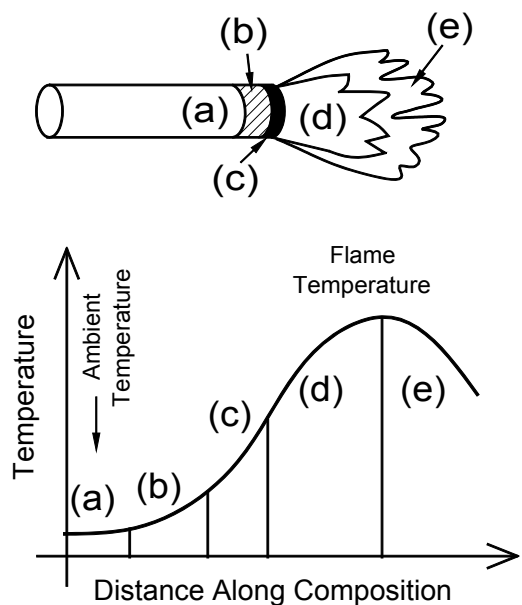


Figure 16. A more complete description of the processes of pyrotechnic propagation: *a*, unreacted composition; *b*, warm-up zone; *c*, condensed phase reactions; *d*, gas phase reactions; and *e*, reactions complete. (Reference based on 5d.)

Conclusion

The subjects of ignition and propagation could have been dealt with much more expeditiously. Specifically, it could simply have been stated that ignition requires raising at least a portion of a pyrotechnic composition to its ignition temperature, and that propagation requires the feed back of sufficient energy for continuing self-ignition of the composition. However, while this would have saved much time, it would have provided little understanding of the important principles involved. Accidents caused by unintentional ignitions continue to plague the pyrotechnics industry. In addition, ignition failures with fireworks, whether leaving an unfired-aerial shell in a mortar that needs to be cleared or resulting in a dud shell left after a fireworks display, have serious potential for accidents as well. Ignition failures with signaling smokes or flares may cause someone to not be rescued. It is through a more thorough understanding of the basis for ignition and propagation, that pyrotechnists will be better able to solve potential problems before accidents occur.

Acknowledgments

The authors gratefully acknowledge the technical and editorial assistance of J. Domanico and L. Weinman in the preparation of this article.

Notes

- [a] More recent usage of this term is “Enthalpy of Reaction”.
- [b] The use of the term “activation energy” in the context of solid-phase pyrotechnic compositions has a slightly different meaning than in aqueous or gas-phase chemistry. In aqueous and gas-phase chemistry, molecules can be thought of as reacting individually, or at least in small groups. In that case, activation energy can be thought of as the amount of energy needed for a collision between two individual molecules to cause them to react. However, a typical pyrotechnic composition is composed of solid particles of fuel and oxidizer, with each particle comprised of many billions of atoms or molecules. In this case, activation energy takes on much more of a macroscopic and less precise meaning. For the purpose of this article, activation energy of solid-phase pyrotechnic compositions is generally taken to mean that amount of thermal energy needed to induce a sustained exothermic reaction within a tiny portion of the composition.
- [c] Pyrotechnic compositions, especially those of dark color, exposed to bright sunlight may be an exception to the generalization about the highest temperature expected to be in the middle of the composition.
- [d] Note that it is assumed the composition is physically at rest (i.e., it is not being mixed, which adds energy to the system).
- [e] In some texts thermal run-away temperature is called the critical temperature^[1] or the reaction temperature.^[8a]
- [f] Wood’s metal is a eutectic alloy of bismuth, lead, tin and cadmium. It melts at 70 °C.
- [g] Some oxidizers are known for producing compositions with low activation energies (e.g., chlorates), while other oxidizers tend to produce compositions with high activa-

tion energies (e.g., oxides and sulfates). Fuels with low melting points or low decomposition temperatures (e.g., sulfur, lactose and acaroid resin) tend to form compositions with low activation energies. Metal fuels tend to produce compositions with high heats of reaction.

- [h] Pre-ignition reactions are typically reactions taking place in the solid state. While such reactions can be a source of energy, they generally only contribute in a minor way to promoting ignition. This is because solid-state reaction rates are constrained by the difficulty of fuel and oxidizer commingling while both remain solid.

References

- 1) A. G. Merzhanov and V. G. Abramov, "Thermal Explosion of Explosives and Propellants, A Review", *Propellants and Explosives*, Vol. 6, 1981, pp 130–148.
- 2) A. G. Merzhanov and V. G. Abramov, "The Present State of Thermal Ignition Theory: An Invited Review", *Combustion and Flame*, Vol. 16, 1971, pp 89–124.
- 3) *The Illustrated Dictionary of Pyrotechnics*, Journal of Pyrotechnics, 1995, p 64.
- 4) Any General Chemistry Text, e.g., B. H. Mahan, *University Chemistry*, Addison-Wesley, 1965, pp 329–334.
- 5) A. A. Shidlovskiy, *Principles of Pyrotechnics*, reprinted by American Fireworks News, 1997; [a] pp 64–65; [b] pp 61–63; [c] p 84; [d] p 96–98.
- 6) W. D. Smith, "Estimating the Distribution of Molecular Energies", *Journal of Pyrotechnics*, No. 6, 1997.
- 7) Any General Physics Text, e.g., F. W. Weston and M. W. Zemansky, *University Physics*, Addison-Wesley, 1970, p 239.
- 8) J. H. McLain, *Pyrotechnics, From the Viewpoint of Solid State Chemistry*, Franklin Institute Press; 1980; [a] p 186; [b] p 30 and 40; [c] pp 3–6.
- 9) R. N. Rogers and E. D. Morris, "On Estimating Activation Energies with a Differential Scanning Calorimeter", *Analytical Chemistry*, Vol. 38, 1966, pp 412–414.
- 10) H. Henkin and R. McGill, "Rates of Explosive Decomposition", *Industrial and Engineering Chemistry*, Vol. 44, 1952, pp 1391–1395.
- 11) D. B. Olsen, "Gas Evolution, Henkin and 1-Liter Cook-Off Tests", *Explosives Firing Site and Laboratory Safety Course Notes*, Center for Explosives Technology Research, New Mexico Tech, 1990.
- 12) J. A. Conkling, *Chemistry of Pyrotechnics*, Marcel Dekker, 1985; [a] p 97; [b] p 43 & 103; [c] p 102.
- 13) B. T. Fedorff, O. E. Sheffield, and S. M. Kaye, *Encyclopedia of Explosives and Related Terms*, Picatinny Arsenal, 1975, Vol. 7, pp 12 – 129.
- 14) T. J. Barton, N. Williams, E. L. Charsley, J. Ramsey and M.R. Ottaway, "Factors Affecting the Ignition Temperature of Pyrotechnics", *Proceedings of the 8th International Pyrotechnics Seminar*, 1982, p 100.

Studies of the Thermal Stability and Sensitiveness of Sulfur/Chlorate Mixtures

Part 1. Introduction

D. Chapman*, R. K. Wharton* and G. E. Williamson**

* Health and Safety Laboratory, Harpur Hill, Buxton, Derbyshire, SK17 9JN, United Kingdom

** HM Explosives Inspectorate, Health and Safety Executive, Magdalen House, Trinity Road, Bootle, Merseyside, L20 3QZ, United Kingdom

ABSTRACT

The presence of sulfur/chlorate mixtures in fireworks compositions has been proposed as the cause of numerous accidents in production and storage. A series of accidents after the introduction of the 1875 Explosives Act led to additional legislation to prohibit such mixtures in the UK. In this paper, as part of an ongoing programme to quantify the hazards associated with the presence of the mixture in fireworks compositions, we have reviewed previously published work and give an outline of the approach we will take in our current research.

Keywords: sulfur, chlorate, pyrotechnics, fireworks, reactivity, accidents, safety

Introduction

Sulfur/chlorate mixtures have, for many years, been known as potential causes of the accidental initiation of pyrotechnics. In the period 1875 to 1894 there are numerous incidents recorded in the United Kingdom (UK) HM Inspectors of Explosives reports that are attributed to the presence of sulfur/chlorate mixtures. The majority of these incidents, which resulted in 11 deaths along with many injuries, were believed to be caused by the spontaneous ignition of the mixture while the remainder were thought to be due to the sensitiveness^[1] of the mixtures.

An accident^[2] in 1887 was attributed to a green star composition where both barium and potassium chlorates were present with sulfur (KClO_3 47%, $\text{Ba}(\text{ClO}_3)_2$ 9%, $\text{Ba}(\text{NO}_3)_2$ 24%,

S 14%, shellac 4%, charcoal 2%), whereas an accident^[3] in 1890 was attributed to a green lance manufactured using two compositions. These comprised a green fire which contained both potassium and barium chlorates and a white fire containing sulfur. It was believed that filling was not carried out carefully and that the two compositions were able to mix and form a sulfur/chlorate mixture. Similar ignitions were reported^[4] involving a green fire composition containing 62% barium chlorate with 8% sulfur.

The acidic nature of the materials used at that time was proposed as a possible cause of the accidents.^[5] The occurrence of such events led to an Order in Council in 1894 prohibiting the manufacture, import, keeping, conveyance or sale of fireworks containing mixtures of sulfur with any chlorate except with the consent of a Government Inspector. Such restrictions on fireworks have been and continue to be in place for fireworks manufactured in or imported into the UK.

In a more recent review of accidents, in this case to minors from chemical experimentation in the 1950s, Burns^[6] reported that 36% of the incidents were attributed to handling sulfur/chlorate mixtures in conjunction with carbon.

In recent years a number of fireworks have been examined by the Health and Safety Laboratory for the presence of sulfur/chlorate mixtures, both qualitatively^[7] and quantitatively.^[8] A proportion of the fireworks tested was found to contain sulfur/chlorate mixtures to different extents within a component composition, and in many cases this necessitated both removal of

the item from sale and destruction of the fireworks. While there have been no recent reported manufacturing or storage incidents in the UK, there are reports of accidents with pyrotechnic materials in many countries (e.g., Peru,^[9] China^[10,11] and India^[12] that could be attributable to the presence of sulfur/chlorate mixtures.)

Role of Sulfur and Chlorate in Fireworks

Sulfur is one of the commonly used fuels in fireworks manufacture and is said to act as a “tinder”, and its low temperature exothermic reactions with a variety of oxidisers are used to initiate other higher temperature reactions.^[13]

Chlorates are present in compositions to either:

- a) act as an oxidiser and/or
- b) act as a chlorine source.

The presence of chlorate is said to generate compositions with relatively low ignition temperatures, in the region of 200 °C for many compositions.^[14] Conkling reports a strong exotherm for sulfur/potassium chlorate mixtures corresponding to ignition at temperatures well below 200 °C.^[15] It is further suggested by Conkling that the low Tammann temperature (defined as 0.5 T where T is the melting temperature in Kelvin) of 42 °C, the exothermic decomposition of potassium chlorate, and the melting temperature of sulfur of 119 °C are responsible for the low ignition temperature. At the Tammann temperature, a solid has 70% of the vibrational freedom present at the melting temperature and considerable diffusion into the lattice is likely. Similar ignitions have been observed with thiourea/potassium chlorate mixtures in processing^[16] where reactivity was attributed to migration of loosely bound sulfur from thiourea into the potassium chlorate lattice producing a material that was both highly sensitive to mechanical stimulus and had temperatures of ignition of about 150 °C.

Previous Work

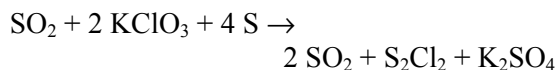
Several previous studies have investigated the reaction of sulfur and metallic chlorates. All workers have found the mixtures to be readily ignited at low temperature or with low mechanical stimulus. As early as 1881, acidity of the sulfur was cited by Dupré^[17] as a major contributing factor in the auto-ignition of sulfur/chlorate mixtures. Additionally, where barium salts were present under moist conditions with potassium chlorate, a double decomposition reaction could occur to produce barium chlorate. Barium chlorate was also shown to be more susceptible to auto-ignition than the potassium salt when mixed with sulfur. Later work by Dupré^[18] concluded that under conditions of heat retention it was a matter of when not if mixtures containing sulfur and chlorate would spontaneously ignite.

Amiel^[19] attributed the spontaneous ignition of chlorates and sulfur to the production of chlorine dioxide (ClO₂). Chlorates, other than alkali-metal chlorates, were shown to produce ClO₂ at temperatures around 60 °C in the presence of water. Additionally, the chlorates of magnesium, nickel, cobalt, cadmium and zinc were reported to react very suddenly.

Taradoire^[20] focused his studies on potassium, barium and lead chlorates. Under wet conditions the production of sulfuric acid followed by the formation of chloric acid (HClO₃) was proposed as the cause of spontaneous ignition of mixtures. The mixtures formed by sulfur with the chlorates of barium and lead were said to ignite at “ordinary” temperatures.

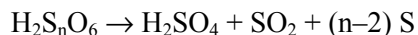
In a further paper, Amiel^[21] reported the effect of sample size, indicating that for large (unspecified) quantities, self-reaction was immediate rather than taking minutes or hours as for smaller (unspecified) quantities.

Tanner^[22] has demonstrated that sulfur dioxide can initiate sulfur/chlorate mixtures. He proposed that the exothermic reaction:



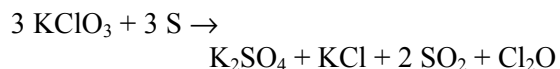
was responsible for the ignition of the material. This chain reaction would be capable of self sustaining once the initial sulfur dioxide had

been generated from polythionic acids ($H_2S_nO_4$) by the equation:



Polythionic acids form on the surface of sulfur crystals, particularly at elevated temperatures due to surface oxidation. Decomposition of polythionic acids occurs when evaporation of surface moisture or a temperature rise make the acid unstable.

An alternative mechanism was proposed by Rudloff^[23] from thermal analysis work carried out on the reaction of sulfur vapour and potassium chlorate. The overall reaction for the complex mechanism was reported as:



Storey^[24] reported friction sensitiveness of sulfur/chlorate mixtures and the results of a number of thermal techniques that were used to assess the likelihood of the ignition of sulfur/chlorate mixtures. Stoichiometric mixtures of sulfur and potassium chlorate were shown to have a Figure of Friction 0.12, compared to 0.84 for lead azide. Since low Figure of Friction values indicate a more sensitive composition, this illustrates that under certain circumstances sulfur/chlorate mixtures can be more sensitive to friction than primary explosives commonly used as initiator compositions. Mixtures containing less than 2.5% sulfur with potassium chlorate were shown to be insensitive to friction.

Hot stage microscopy of mixtures containing 1–5% sulfur with potassium chlorate indicated that they started to decompose at temperatures in the range 165–178 °C, dependent on sample size and percentage of sulfur. Differential thermal analysis on 20 mg samples reduced the initiation temperature to the range 130–155 °C for similar mixtures, again depending on the percentage of sulfur and, in this case, the source of the sulfur. Times to autoignition for stoichiometric mixtures were also considered. Sulfur/potassium chlorate mixtures (1 g samples) were sealed in glass test tubes and the time to ignition was recorded. Sulfur from two sources produced similar results taking 2.5–3 hours for ignition at 90 °C, while the sulfur from a third source ignited in 13.5 minutes at the same temperature. The sulfur samples were

from three different UK manufacturers and were representative of the materials used in fireworks manufacture. Unfortunately no measurement of acidity was reported.

Calorimetry (Seteram C80) on 0.5 g samples of stoichiometric sulfur/potassium chlorate mixtures indicated that exothermic reactions were initiated within a few hours at temperatures below 60 °C under isothermal conditions. Using a heating rate of 0.1 °C min⁻¹, exotherms were observed for similar mixtures at temperatures as low as 62 °C. Mixtures with low sulfur percentage showed higher onset temperatures, but generally these were below the sulfur melting temperature. The addition of sulfur dioxide to a mixture was shown to initiate the reaction almost instantaneously.

Research Plan

Thermal Studies

The early papers by Amiel and Tara-doire^[19,20,21] do not report the sizes of the samples taken, the ratio of sulfur to chlorate in the experiments, nor the conditions under which the experiments were carried out. However, they do indicate an early appreciation of the thermal instability of this mixture. Tanner's work^[22] utilised an almost stoichiometric mixture (33:67) and the acidity of the sulfur was measured.

A previous study,^[24] which defines the conditions employed for the experimental work, used samples contained in glass or metal containers, many of which were sealed systems. The use of a sealed system will prevent the dispersion of any sulfur dioxide produced which could in turn accelerate the autocatalytic reaction yielding unrealistically low reaction temperatures or times to ignition. Tanner's work,^[22] on the other hand, utilised cardboard tubes made from match books after the striker composition had been torn off. This provided an open containment system and the samples tested would therefore not suffer from any effects of confinement. However, his use of a heat lamp and thermocouple positioned in the centre of the sample may have led to unrepresentatively low measured temperatures of ignition since the reaction surface of the material would have

been at a significantly higher temperature than that indicated by the thermocouple. Additionally, it may be possible that some phosphorus contamination remained from the matches.

Our studies will investigate the initiation of sulfur/chlorate mixtures in containers that are similar to those used in the fireworks industry (i.e., cardboard tubes sealed with a clay plug at the bottom and either open at the top or sealed with a further clay or cardboard disk.) Temperature measurement of the samples will be made using a thermocouple inserted into the composition. The cardboard tubes will be heated in a metal block to achieve uniform temperature throughout the sample. To fully understand the reactivity of sulfur/chlorate mixtures in fireworks a number of variables will be systematically examined. These include:

1. the acidity of the sulfur,
2. the stoichiometry of the mixture,
3. the size of sample,
4. the degree of sample compaction,
5. the moisture content of the mixture,
6. the particle size of the components of the mixture, and
7. the inclusion of other fireworks materials such as barium or strontium salts and metal particles.

Sensitiveness Studies

While the majority of accidental ignitions of compositions containing sulfur/chlorate mixtures have been attributed to thermal instability, Dupré^[2] reported that he could initiate a sulfur/chlorate containing "green Roman" composition by friction using the wooden plunger used in filling, particularly when the material had been heated. He concluded that the composition "possesses a degree of sensitiveness which renders it in the highest degree a hazardous composition to deal with especially in hot weather". Therefore, in parallel with our proposed thermal studies, the sensitiveness of different sulfur/chlorate mixtures to mechanical stimuli will also be quantified using the same matrix of variables identified for the thermal stability work.

Friction has previously been shown to be a major cause of accidental ignitions for explo-

sives in general^[25] and pyrotechnics^[26] in particular. However, for completeness both friction and impact sensitiveness will be examined. This will be carried out using the BAM friction and BAM Fallhammer apparatus to gain data using the UN recommended test methods^[27] for friction and impact, respectively.

Future Work

This paper has outlined the problems associated with the presence of sulfur/chlorate mixtures in fireworks and forms the introduction to a series of papers where we intend to report the findings of our research programme. Part 2^[28] will deal with the early work carried out on dry stoichiometric mixtures. Future papers will cover other variables considered in the study.

References

- 1) R. K. Wharton and D. Chapman, "Use of the Term Sensitiveness to Describe the Response of Pyrotechnic Compositions to Accidental Stimuli", *Journal of Pyrotechnics*, in press.
- 2) Special Report of HM Explosives Inspectors LXXX, 1887.
- 3) Special Report of HM Explosives Inspectors XCIV, 1890.
- 4) Special Report of HM Explosives Inspectors CII, 1892.
- 5) R. Lancaster, "Chlorate: Can We Really Exist without It?", *Proceedings of the 3rd International Symposium on Fireworks*, Walt Disney World® Resort, Lake Buena Vista, Florida, September 16–20, 1996, p 272.
- 6) C. Burns, "Chemical Accidents Involving Minors", *Journal of Chemical Education*, Vol. 33, 1956, p 508.
- 7) BS7114: Part 3: Appendix C, 1988, p 23. (ISBN 0 580 17028 4)
- 8) D. Chapman, "Techniques for the Quantitative Analysis of Sulfur and Chlorate in Fireworks Compositions", *Journal of Pyrotechnics*, No. 5, 1997, p 25.

- 9) Reuter Economic News, "Two Dead, 17 Hurt in Peru Fireworks Factory Blast", November 8, 1995.
- 10) Lloyds List, Lloyds Information Casualty Report, "China: Fires and Explosion; Firework Factory, Linquan, China", October 31, 1996.
- 11) Reuter-News-Services-Far-East Report "Explosion in Store for Materials Used in Fireworks", Xichong, China, February 4, 1997.
- 12) Lloyds List, Lloyds Information Casualty Report, "Fires and Explosion; Fireworks Factory, Southern India", May 6, 1997.
- 13) J. A. Conkling, *Chemistry of Pyrotechnics*, Marcel Dekker, New York, 1985, p 70.
- 14) K. L. Kosanke, B. J. Kosanke, C. Jennings-White and W. D. Smith, *Lecture Notes for the Chemistry of Pyrotechnics, Pyrotechnic Reference Series No. 2*, Journal of Pyrotechnics, 1996, p II-22.
- 15) Ref. 13, p 102.
- 16) R. K. Wharton and A. J. Barratt, "Observations on the Reactivity of Pyrotechnic Compositions containing Potassium Chlorate and Thiourea", *Propellants, Explosives and Pyrotechnics*, Vol. 18, 1993, p 77.
- 17) Annual Report of HM Explosives Inspectors, 1881.
- 18) Annual Report of HM Explosives Inspectors, 1892.
- 19) J. Amiel, "Action of Chlorates on Sulfur, Selenium and Tellurium", *Comptes Rendus de l'Académie des Sciences*, Vol. 198, 1934, p 1033.
- 20) F. Taradoire, "Action of Sulfur on Chlorates" *Comptes Rendus de l'Académie des Sciences* Vol. 199, 1934, p 603.
- 21) J. Amiel, "Damp Mixtures of Chlorates and Sulfur and Some Other Reactions of Damp Chlorates", *Comptes Rendus de l'Académie des Sciences* Vol. 199, 1934, p 787.
- 22) H. G. Tanner, "Instability of Sulfur-Potassium Chlorate Mixture", *Journal of Chemical Education*, Vol. 36, 1959, p 58.
- 23) W. K. Rudloff, "Thermal Analysis of the Reaction between Sulfur Vapor and Chlorates", *Proceedings of the 4th International Conference of Thermal Analysis*, Budapest, 1974, p 555.
- 24) P. D. Storey, "Identification and Assessment of Hazardous Mixtures in Pyrotechnics", *Proceedings of the 13th International Pyrotechnics Seminar*, Grand Junction, Colorado, USA, July 1988, p 765.
- 25) A. Bailey, D. Chapman, M.R. Williams and R. Wharton, "Handling and Processing of Explosives", *Proceedings of the 18th International Pyrotechnics Seminar*, Breckenridge, Colorado, USA, 13-17 July 1992, p 33.
- 26) F.L. McIntyre, "Incident/Accident Survey of Pyrotechnic Compositions", *Proceedings of the 6th International Pyrotechnics Seminar*, Denver, Colorado, USA, 1978, p 392.
- 27) "Recommendations on the Transport of Dangerous Goods, Manual of Tests and Criteria", ST/SG/AC.10/11/Rev 2, 2nd revised ed., United Nations, New York and Geneva, 1995, p 105-6.
- 28) D. Chapman, R. K. Wharton, J. E. Fletcher and G. E. Williamson, "Studies of the Thermal Stability and Sensitiveness of Sulfur/Chlorate Mixtures. Part 2. Dry Stoichiometric Mixtures", *Journal of Pyrotechnics*, in press.

Events Calendar

Pyrotechnics

Pyrotechnic Chemistry Course — UK

April 27–29, 1998, DERA, Sevenoaks, Kent, UK

Contact: Ken Kosanke, PyroLabs
1775 Blair Road
Whitewater, CO 81527, USA

Phone: 970-245-0692
FAX: 970-245-0692
e-mail: kosankes@compuserve.com

ADPA/NSIA — 42nd Annual Fuse Conference; Munitions Technology Symposium V; and Statistical Process Control Meeting (concurrent meetings)

April 28–29, 1998, San Diego Princess Resort,
San Diego, CA USA

Contact: jkohlmeier@ndia.org
ADPA/NSIA
2101 Wilson Boulevard
Arlington, VA 22201-3061
Web Site: www.adpansia.org

1998 Summer Pyrotechnic Seminars:

The Chemistry of Pyrotechnics & Explosives

July 19–24, 1998, Chestertown, MD, USA

Advanced Pyrotechnic Seminar: A Survey of Highly Reactive Systems-Explosives, Propellants, and Pyrotechnic Gas Generants

July 26–31, 1998, Chestertown, MD, USA

Contact: John Conkling
PO Box 213
Chestertown, MD 21620, USA

Phone: 410-778-6825
FAX: 410-778-5013
e-mail: John.Conkling@washcoll.edu

Pyrotechnic Chemistry Course — USA

Tentative Oct. 10–13, 1998, Purdue University,
West Lafayette, IN USA

Contact: Ken Kosanke, PyroLabs
1775 Blair Road
Whitewater, CO 81527, USA

Phone: 970-245-0692
FAX: 970-245-0692
e-mail: kosankes@compuserve.com

Fireworks

Western Winter Blast IX

February 13–15, 1998, Lake Havasu, AZ, USA

Contact: Steve Rhoads
Phone/FAX: 909-685-2896
e-mail: remains4u@aol.com
Web Site: www.pyrotechnics.org/~wpa

Pyrotechnics Guild International Conv.

August 9–14, 1998, Gillette, WY USA

Contact: Bruce Burns, Chairman
PO Box 6027
Sheridan, WY 82801
Phone: 307-674-7376
e-mail: bburns@cyperhighway.net

Events are continued on Page 64.

Hydrazinium Nitroformate: A High Performance Next Generation Oxidizer

Jeroen Louwers

TNO Prins Maurits Laboratory, Research Group Rocket Technology,
P.O. Box 45, 2280 AA Rijswijk, The Netherlands [e-mail: louwers@pml.tno.nl]

ABSTRACT

The use of chlorine-free high performance oxidizers in solid rocket propellants may reduce launch costs, while producing less polluting exhaust products. Hydrazinium nitroformate (HNF) is a candidate for such a next generation oxidizer. In this article the properties of HNF are addressed. Its combustion and decomposition characteristics, and its application in rocket propellants are discussed.

Keywords: oxidizer, hydrazinium nitroformate, HNF, monopropellant, composite propellant, decomposition

Introduction

Solid rocket propellants can be divided into two main categories. Double-base propellants, which are *homogeneous* mixtures, with main ingredients nitroglycerin and nitrocellulose. Another group consists of the so-called composite propellants, which are *heterogeneous* mixtures of oxidizer and fuel. The oxidizer is an inorganic salt, which is held together by a polymer matrix, which also acts as a fuel. Double-base propellants are mostly used in small military missiles. The mechanical properties and performance of composite propellants are better than those of double-base propellants. Therefore, most larger systems (e.g., the boosters of the Space Shuttle) are based on composite propellants.

The majority of the composite propellants use hydroxyl-terminated polybutadiene (HTPB, $\sim\text{CH}_{1.5}$) as binder and ammonium perchlorate (AP, NH_4ClO_4) as the oxidizer.^[1] Often fine aluminum is added as a fuel to increase the

combustion temperature and hence performance. These types of composites are cheap, reliable, and can be tailored to a large range of regression rates by using burn-rate modifiers and varying AP particle-size distribution. However, there is a lot of research on new oxidizers to replace AP. Reasons for this are:

- By replacing AP composites with more energetic composite propellants, launch costs can be decreased dramatically. Reduction of launch costs is important in the current period of increased competition between launcher organizations.
- AP-based composites are characterized by a large amount of hydrochloric acid (HCl) in their exhaust products. During each launch of the Space Shuttle, 162 metric tons of HCl are ejected into the earth's atmosphere! HCl is known for its ozone depletion properties.
- The presence of HCl causes a large smoke trail behind missiles. This so-called secondary smoke consists of condensed water. (Primary smoke is caused by solid particles in the exhaust products, for example, aluminum oxide and soot.) In the presence of HCl, water condenses more easily, as HCl decreases the effective saturation pressure of water (like the white trail behind airplanes). The secondary smoke increases the signature of a missile and is therefore unwanted.

New Oxidizers

The introduction explains the search for new oxidizers that may replace AP. Several alternatives have been identified, and some of them have already been applied in actual systems.

Ammonium nitrate (AN, NH_4NO_3) is an oxidizer that does not contain chlorine. AN-based composite propellants are characterized by their low flame temperature. This makes them ideal for gas generator applications. However, their performance is lower than that of AP-based composite propellants.

The cyclic nitramines, cyclotrimethylenetri-nitramine (RDX, $\text{C}_3\text{H}_6\text{N}_6\text{O}_6$) and cyclotetra-methylene tetranitramine (HMX, $\text{C}_4\text{H}_8\text{N}_8\text{O}_8$), are not real oxidizers, as they are stoichiometrically balanced. Both nitramines have a high flame temperature and generate combustion products with a low molecular weight. By replacing AP in AP-based composites with these nitramines, the performance may be increased. RDX- and HMX-based propellants do not show a strong particle-size dependent burning rate.^[2] This has been attributed to the melt layer formed during decomposition of these materials. Regression rates of nitramine-based composites can therefore not be tailored by particle-size distribution control. Also combustion catalysts have only been proven partially successful. AP is therefore often only partially replaced by HMX or RDX. The performance gain of nitramine composites is still not the maximum that can be obtained as the binder decomposition products cannot be oxidized, because the nitramines are stoichiometrically balanced.

A new energetic filler is CL20 or hexanitro-hexaazaisowurtzitane (HNIW, $\text{C}_6\text{H}_6\text{N}_{12}\text{O}_{12}$).

Unlike RDX and HMX, CL20 is not yet used in operational systems. Its main advantage over the cyclic nitramines is its high density, 2.04 g/cm^3 . CL20 research is carried out in France and the United States.

Ammonium dinitramine [ADN, $\text{NH}_4\text{N}(\text{NO}_2)_2$] and hydrazinium nitroformate [HNF, $\text{N}_2\text{H}_4\text{C}(\text{NO}_2)_3$] are two “new” high-performance oxidizers that do not contain chlorine and have a positive oxygen balance. In the United States, research focuses on the development of ADN-based propellants. There are also ADN programs in France and Sweden. There are indications that Russian rocket engines based on ADN have already been operational for many years.^[3] However, ADN is hampered by its low melting point ($93 \text{ }^\circ\text{C}$) and hygroscopicity.^[4]

HNF was part of a large research project for new high-performance propellants in the 1960s in the United States. HNF appeared to be incompatible with the double bonds in unsaturated binders like HTPB.^[5] The recent commercial production of saturated energetic binders, like glycidyl azide polymer (GAP), led to a renewed interest in HNF. The theoretical performance of HNF-based composites is unmatched by any other energetic material. Because of HNF's high performance, the European Space Agency (ESA) decided to fund HNF research.

Several properties of the oxidizers discussed are summarized in Table 1.^[6,7] The performance of some typical propellants with some of these oxidizers is given in Figure 1.

Table 1. Properties of Several Oxidizers and Energetic Fillers.^[6,7]

	AN	AP	RDX	HMX	HNF	ADN	CL20
Molecular weight [kg/mol]	80	117.5	222	296	183	124	438
Density [kg/m ³]	1720	1950	1820	1960	1860	1800	2040
Heat of formation [kcal/kg]	-1028	-601	+72	+61	-94	-282	+208
Melting point [°C]	169	230	>170	275	124	93	>195
Oxygen balance CO+O ₂ [%]	20	34	0	0	21.8	25.8	10.9
BAM friction sensitivity [N]	353	>100	120	120	18-36	350	90-120
BAM impact sensitivity [Nm]	49	15	7.5	7.4	2-4	3-6	3.5-13

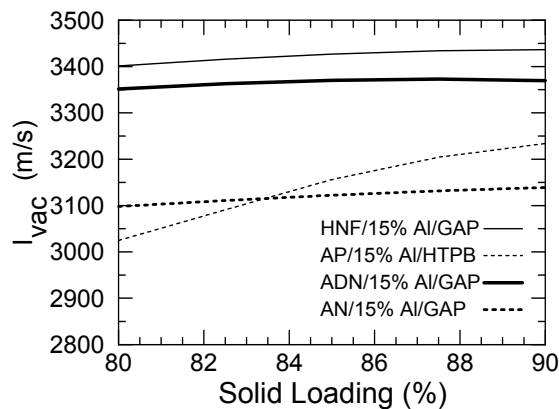
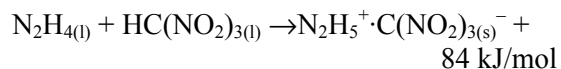


Figure 1. Performance of several propellants (Chamber pressure 10 MPa, expansion ratio 100, equilibrium flow).

Hydrazinium Nitroformate

HNF is an orange-yellow solid of formula $N_2H_5^+C(NO_2)_3^-$. HNF is made by a precipitation reaction between hydrazine (N_2H_4) and nitroform [$HC(NO_2)_3$]:



As this reaction is exothermic, the process vessel must be thoroughly cooled. After reac-

tion, the HNF crystals are recrystallized, to improve the purity of the raw HNF and to obtain different particle sizes. HNF is now commercially produced in batch quantities by Aerospace Propulsion Products (APP) in Hoogerheide, The Netherlands. At the moment, about 50 kg of HNF are produced each year.

Purity is an important factor for the stability of HNF. Friction and impact sensitivity increase in the presence of even trace impurities. Also, the melting point and thermal stability are very sensitive to the purity of the HNF. Because of this sensitivity, the melting point of HNF is used as a simple method to determine its purity.

HNF particles tend to crystallize into needle-shaped crystals, with large length to diameter ratio's (L/D). Needle-shaped HNF is more sensitive to impact and friction and is not desirable for propellant production. Furthermore, the rheology of needle-shape-based propellants prevents the manufacturing of propellants with high solid loadings. Cubic or spherical crystals would be ideal for both sensitivity and casting properties. By recrystallization, the L/D ratio can be reduced to values between 4 and 5 (see Figure 2), and the different processes also influence the mean particle size. At the moment it is possible to manufacture HNF crystals with particle size varying between 5 and 2000 μm .

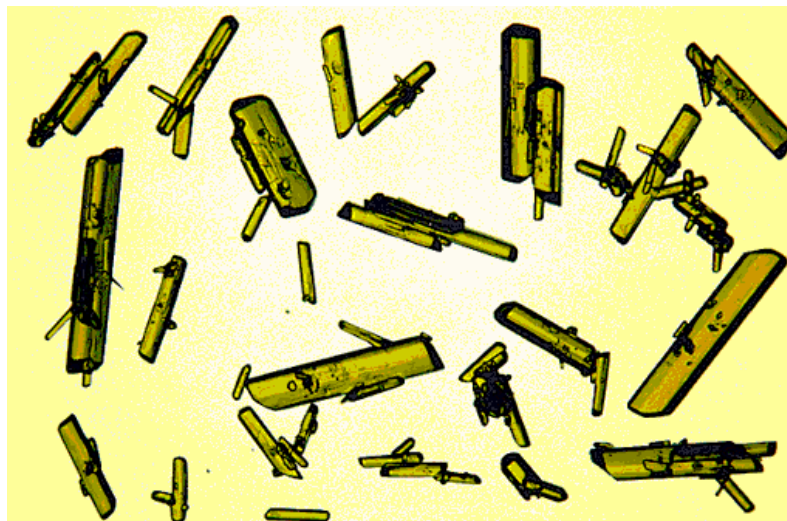


Figure 2. Recrystallized HNF with length to diameter ratio's between 4 and 5, mean diameter about 500 μm .

Monopropellant Combustion

Because of the highly exothermic HNF decomposition, self deflagration of pressed neat HNF is possible, at least in the experimental pressure range of 0.025 to 10 MPa.^[8,9] The regression rate, r_b , of HNF monopropellants was determined by McHale and von Elbe.^[10] They determined the burning rate of HNF-filled Pyrex tubes at approximately 75% of the theoretical maximum density (TMD). For safety reasons, the HNF was only loosely packed in the Pyrex tubes and not pressed. More recently, regression rates of pressed HNF at 96% TMD were measured.^[9,11] The results of both measurements are shown in Figure 3. Neat HNF regression rates are high, reaching more than 40 mm/s at 10 MPa. HNF also burns nicely at subatmospheric pressures down to 0.025 MPa.

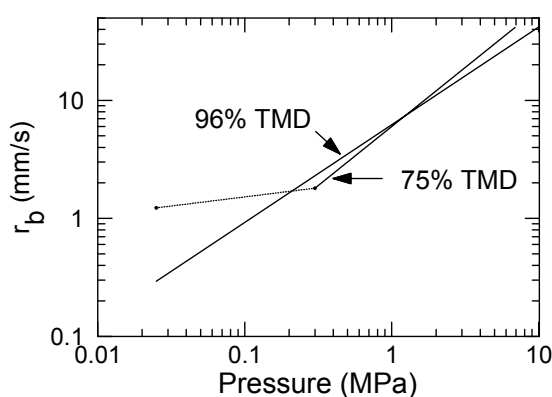


Figure 3. Experimentally determined regression rates of HNF monopropellants for two different TMD values. The beginning and ending points of the lines indicate the experimental pressure range.

Parr and Hanson-Parr measured the species profiles of HNF flames using several optical techniques.^[11] The transient combustion of HNF was studied by Finlinson using a laser recoil method.^[12] The HNF oscillations were found to be of the same order of magnitude as HMX.

Decomposition

To study the decomposition behavior of HNF under combustion-like conditions, temperature-jump (T-jump) experiments were conducted by

Williams and Brill.^[13] Species were detected with a Fourier Transform Infra-Red (FT-IR) apparatus.

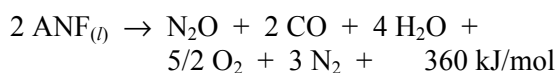
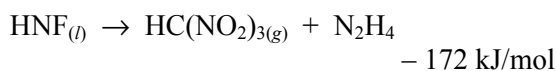
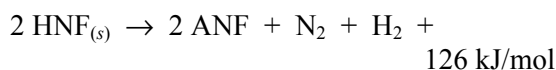
The T-jump studies show a strong dependence of the species formed during decomposition on temperature. It was found that the same three temperature regions as for HNF monopropellant combustion can be distinguished:

1) Decomposition below 123 °C:

Below the melting temperature of HNF, preheating only; no decomposition occurs.

2) Decomposition from 123 to 260 °C:

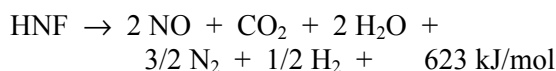
This temperature range corresponds with the foam zone found during HNF monopropellant combustion. Ammonium nitroformate (ANF, $\text{NH}_4\text{C}(\text{NO}_2)_3$) aerosol, $\text{HC}(\text{NO}_2)_3$, N_2H_4 , N_2O , H_2O , and CO were detected in the gaseous phase. HNF aerosol was not detected; so the evaporation of HNF followed by gas decomposition was concluded to be negligible. The following reaction scheme was proposed:



Taken together, the reactions above yield 314 kJ/mol of HNF. This exothermicity is confirmed by the thermocouple experiments; this might explain the self-sustained combustion of HNF at subatmospheric pressures.^[8]

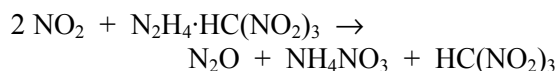
3. Decomposition above 260 °C:

This temperature region corresponds with the combustion zone found during HNF monopropellant combustion. Above 260 °C, the formation of CO_2 is observed for the first time. The amount of CO_2 increases with increasing temperature; hence, the exothermicity increases with temperature. Above 350 °C, the amount of ANF, N_2O , and CO decreases. At 400 °C, the reaction can be described by

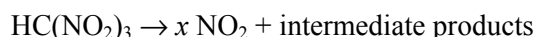


This reaction is the most strongly exothermic of the above reactions. The products of this reaction are not in the thermodynamic equilibrium concentrations that exist at the theoretical, adiabatic flame temperature. Further reaction at higher temperature is expected.

The above reaction pathways differ from those proposed by von Elbe et al.^[8] By simple analytical techniques, they determined that NO₂ was released during HNF monopropellant combustion. This NO₂ reacts with the hydrazine component of HNF, liberating nitroform, according to



Because the free nitroform is unstable well below 120 °C, this reaction is immediately followed by



where x is presumably >1 , but cannot exceed 3. It was concluded that at elevated temperatures, confinement of HNF in a closed container constitutes a severe explosion hazard, because a run-away increase of the NO₂ concentration, terminating in an explosion, may be expected. Effective venting of the container to remove trace amounts of NO₂ would mitigate this hazard.

The difference between the results from Williams and von Elbe is remarkable. During combustion von Elbe found that NO₂ plays an important role, whereas Williams found no evidence of NO₂ in T-jump experiments at combustion-like temperatures and temperature gradients. These differences may be explained by the fact that NO₂ is very unstable and might not be detected above the platinum filament, because it is already reduced to NO by, for example, the released hydrazine. The decomposition to NO in one step is very unlikely, for example, HMX and RDX also decompose into NO₂ first.

HNF Propellants

Compatibility of HNF with Propellant Ingredients

Application of HNF in a composite rocket propellant requires the use of energetic binders for two reasons. As stated earlier, HNF is incompatible with the double bonds in conventional solid propellant binders like HTPB. Modern energetic binders do not show this incompatibility as they do not contain double bonds. However, apart from the binder prepolymer, HNF has also shown incompatibility with many isocyanates, which are used for curing the binder.^[14] A reaction between the hydrazine moiety of HNF and the isocyanate groups seems most logical, as similar effects were also found with hydrazine diperchlorate.

As HNF is not a very strong oxidizer like AP (oxygen balance +21.8 and +34%, respectively) performance with hydrocarbon binders like HTPB is not maximized due to lack of oxygen for binder combustion. Energetic binders have energetic groups attached to their backbones and often contain oxygen. This reduces the amount of oxygen needed to fully oxidize the binder decomposition products. Glycidyl azide polymer (GAP) is the only energetic binder that is produced in large quantities. Therefore GAP was chosen as the binder for propellant testing, although better performance may be obtained with some of the new binders like polyNIMMO and polyGLYN, produced by ICI Explosives.

The azido group in GAP contributes to its energy content (Figure 4). During combustion, the exothermic scission of the $-\text{N}_3$ bond structure forms $\text{N}_{2(g)}$, releasing 685 kJ/mol. Due to this highly exothermic decomposition, neat GAP gumstock is able to sustain combustion with appreciable regression rates (more than 10 mm/s at 10 MPa).^[15]

Propellant Combustion

At the moment there is little experimental regression rate data on HNF propellants. TNO-PML has tested several propellant combinations. The most important are summarized in Table 2.^[14] Due to the crystal-shaped oxidizer particles, the high mixture viscosity made casting impossible; therefore, the propellants were

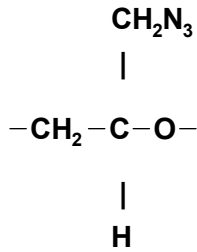


Figure 4. Molecular structure of glycidial azide polymer (GAP).

pressed. Figure 5 shows the regression rates for two different propellants, as measured in a chimney burner. The uncatalyzed propellant has a very high combustion exponent of 0.81. This makes the propellant unsuitable for application in rocket engines. By introducing a combustion modifier (catalyst), the regression rates are increased in pressure from 0.1 to 10 MPa. No data above 10 MPa are available, but it is expected that the catalytic effect will disappear above this pressure, and regression rates will become similar. Due to the higher regression rates at lower pressure, the pressure exponent decreased from 0.81 to 0.59.

Experiments have been conducted to compare the specific impulse of the HNF/Al/GAP propellants to that of conventional AP/Al/HTPB propellants.^[14] These experiments have confirmed the theoretical calculations.

Conclusions

HNF-based composite rocket propellants have a higher performance than any other solid rocket propellant at the moment. This, and the fact that its exhaust gases are chlorine-free, makes it a very likely candidate for replacement of AP in many commercial and military solid-propellant rocket engines. HNF has a high sensi-

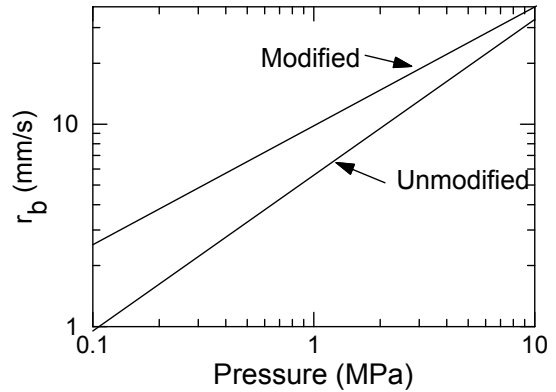


Figure 5. Experimentally determined regression rates of HNF-based propellants.

tivity and has shown incompatibility with many usual propellant ingredients. Therefore, much research still has to be conducted. This makes the application of HNF in operative systems very unlikely in the short term. However, HNF's advantages are many, and its use as a next-generation, solid-propellant oxidizer is promising.

References

- 1) R. R. Sobczak, "Ammonium Perchlorate Composite Basics", *J. Pyrotechnics*, No. 3, 1996, p 35.
- 2) K. Klager and G. A. Zimmerman, "Steady Burning Rate and Affecting Factors: Experimental Results", In: *Nonsteady Burning and Combustion of Solid Propellants*, AIAA Inc., New York, Vol. 143, 1992, p 59.
- 3) Z. Pak, "Some Ways to Higher Environmental Safety of Solid Rocket Propellant Application", AIAA, 1993, Paper 93-1755.
- 4) M. D. Pace, "Nitrogen Radicals from

Table 2. Two Typical HNF-Based Propellants Tested at TNO-PML.

Propellant Composition		Regression rate (in mm/s, pressure in MPa)
Baseline	59% HNF, 18% Al, 23% GAP binder	$5.75 \cdot p_c^{0.81}$
Modified	59% HNF, 14% Al, 4% catalyst, 23% GAP binder	$9.86 \cdot p_c^{0.59}$

- Thermal and Photochemical Decomposition of Ammonium Perchlorate, Ammonium Dinitramine, and Cyclic Nitramines”, *Mat. Res. Soc. Symp. Proc.*, Vol. 296, 1993, p 53.
- 5) G. M. Low, Hydrazinium Nitroformate Propellant with Saturated Polymeric Hydrocarbon Binder, U.S. Patent 3,708,359, Jan 2, 1973.
 - 6) G. Doriath and B. d’Andrea, “New Solid Propellants Formulations and Production Processes”, *5th Int. Symp. Propulsion in Space Technology*, Paris, 1996.
 - 7) J. Köhler and R. Meyer, *Explosives*, 4th rev. & extended ed., VCH, Weinheim, Germany, 1993.
 - 8) G. von Elbe, R. Friedman, J. B. Levy, and S. J. Adams, *Research on Combustion in Solid Rocket Propellants: Hydrazine Nitroform as a Propellant Ingredient*, Atlantic Research Corp., Technical Report DA-36-034-AMC-0091R, 1964.
 - 9) J. Louwers, G. M. H. J. L. Gadiot, M. Q. Brewster, and S. F. Son, “A Model for Steady-State HNF Combustion”, *International Workshop on Combustion Instability of Solid Propellants and Rocket Motors*, Milan, Italy, 16–18 June 1997.
 - 10) E. T. McHale and G. von Elbe, “The Deflagration of Solid Propellant Oxidizers”, *Combustion Science and Technology*, Vol. 2, 1970, p 227.
 - 11) T. Parr and D. Hanson-Parr, “HNF: Neat and Diffusion Flame Structure”, *32nd JANNAF Combustion Subcommittee Meeting*, 1995.
 - 12) J. C. Finlinson, “Laser Recoil Combustion Response of HNF Oxidizer from 1 to 6 atm”, AIAA Paper 97-3342, 1997.
 - 13) G. K. Williams and T. B. Brill, “Thermal Decomposition of Energetic Materials 67. Hydrazinium Nitroformate (HNF) Rates and Pathways under Combustionlike Conditions”, *Combustion and Flame*, Vol. 102, 1995, p 418.
 - 14) H. F. R. Schöyer, A. J. Schnorhk, P. A. O. G. Korting, and P. J. van Lit, “First Experimental Results of an HNF/Al/GAP Propellant”, AIAA Paper 97-3131, 1997.
 - 15) N. Kubota and T. Sonobe, “Combustion Mechanism of Azide Polymer”, *Propellants, Explosives, Pyrotechnics*, Vol. 13, 1988, p 172.
-

A Thermodynamic Properties Estimation Method for Isocyanates

Will Meyerriecks

702 Leisure Avenue, Tampa, FL 33613, USA

ABSTRACT

The accurate estimation of the adiabatic flame temperature is necessary when evaluating a composite propellant. This in turn requires additional formulation and properties data including the reactant percentages, chemical formulas, and formation enthalpies, where the latter is sometimes difficult to obtain. When experimental data is not available, one must use estimation methods. The estimation method or its software implementation may not completely describe all components or properties of interest, however. This is often the case with isocyanates. The author has assembled thermodynamic data for a variety of isocyanates and, from this, has derived Benson Group values that may be used in estimating isocyanate properties when experimental data is unavailable. Application of these estimates and their effect on the estimation of the adiabatic flame temperature is considered.

Keywords: isocyanate, diisocyanate, urethane, enthalpy of formation, Benson group, estimation, adiabatic flame temperature

Introduction

There are many properties of a composite propellant that are of interest to the energetics chemist. These include, but are not limited to, the chemical formulation, adiabatic flame temperature, and the resulting products gas composition and properties as a function of pressure. Generally, the chemical composition of the propellant ingredients is well established. What is sometimes unknown is the formation enthalpy ($\Delta_f H^\circ$) of a particular ingredient. This property represents the energy required to form this molecule from its constituent elements in

their standard states.^[1] When the combustion reaction takes place, and one assumes an adiabatic condition, where no heat is gained or lost in the system,^[2a] the enthalpy of the products equals that of the reactants. This is the adiabatic, or maximum theoretical, flame temperature. Thus, knowledge of the reactant formation enthalpies is required to accurately estimate the flame temperature and combustion properties at this temperature.

Many composite propellants utilize polymers to bind together the oxidizer and metal fuel particles, and these polymers contribute to the combustion process as a fuel source. Polyurethanes are frequently used in this capacity due to their relatively low cost, high performance, and rheological properties. A polyurethane, put quite simply, is a thermoplastic polymer produced by the condensation reaction of an isocyanate and a hydroxyl-containing material.^[2b] An isocyanate (NCO) is a nitrogen, carbon, and oxygen double bonded together, and this functional group is bonded to a "base" molecule.^[2c] A hydroxyl (OH) is a hydrogen bonded to an oxygen, which is in turn bonded to a "base" molecule.^[2d] See Figure 1.

A common propellant binder composition includes the long chain hydrocarbon HTPB (hydroxyl-terminated polybutadiene) and the diisocyanate IPDI (isophorone diisocyanate). The diisocyanate differs from the isocyanate in that each molecule contains two of the isocyanate functional groups. Examples of both iso- and diisocyanates are in Figure 2 (located after references). HTPB (see Figure 3) has a hydroxyl (OH) group at both ends of the molecule, and IPDI has two isocyanate groups (NCO). In the process of reaction, the HTPB and IPDI form a urethane bond (see Figure 1) that unites them, and a synthetic rubber results.

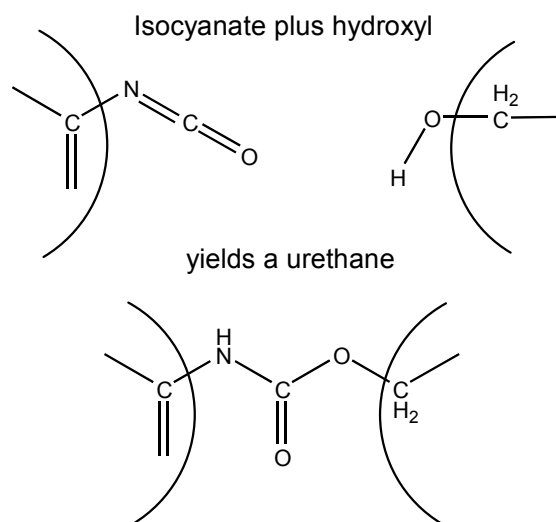


Figure 1. Urethane bond between an isocyanate and a hydroxyl.

Data

For many isocyanates there is little thermodynamic data available despite the use of these chemicals in tremendous quantities in the plastics and coatings industries. The urethane condensation reaction mechanism is poorly understood,^[3] and the availability of critically evaluated experimental data is in short supply.^[4]

A search for thermodynamic data can sometimes be a lesson in frustration. What is available at a conventional library is minimal at best, difficult to locate, and often disappointing in scope. Fortunately, there are sources of data

that are readily available—ones that provided most of the data presented here.

In particular is an Internet web site maintained by the National Institute of Standards and Technology (NIST), *NIST Chemistry Web-Book*.^[5] This online database includes thermodynamic data for many molecules, of which a few are iso- and diisocyanates. As of this writing, the ability to search for specific compounds is limited to full chemical names, Chemical Abstract Registry (CAS) numbers, and partial formulas.

Another web site, CambridgeSoft's *Chem-Finder*,^[6] has a large database of organic molecules, and this search engine allows partial name searches. When "isocyanate" is used as a partial name search, up to 25 "hits" are displayed. Selecting any of these items displays the chemical structure (if known), formula, CAS registry number, and other properties information. This proved useful in determining the CAS numbers for particular isocyanates. The NIST site was then used to cross reference the thermodynamic properties when they were available. In addition, the structural drawing found on *ChemFinder* proves valuable too, as described later. The 25 hits limit of the *Chem-Finder* web site was eliminated by use of *Chem-Office Ultra*,^[7] which includes the complete database found on the web site.

The data and sources are listed in Appendix 1. All data presented is referenced at 298.15 K. Temperatures are in Kelvin. Units are kJ/mol for $\Delta_f H^\circ$ (enthalpy), and J/(mol·K) for C_p° (heat ca-

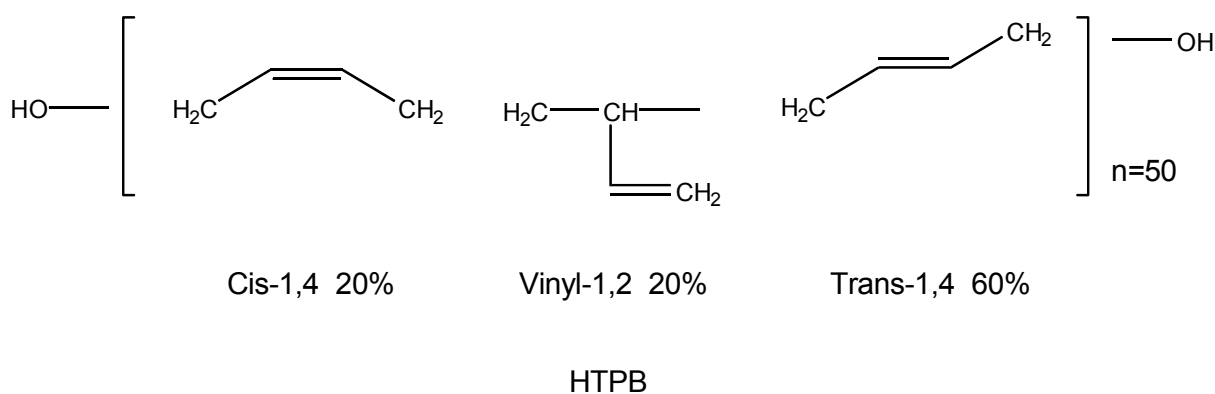


Figure 3. HTPB (hydroxyl terminated polybutadiene).^[22]

capacity) and S° (entropy). In the gas phase, only $\Delta_f H^\circ$ was found; some of these values are estimates as noted in the data. In the liquid and solid phases, only $\Delta_f H^\circ$ and C_p° were found with three exceptions for S° . Some of the data was contradictory or apparently erroneous and is so noted. Of primary importance in estimating the adiabatic flame temperature is the liquid phase $\Delta_f H^\circ$; the isocyanates and hydroxyl-terminated polymers used in propellants are liquids and react to form a viscoelastic fluid as opposed to a crystalline solid. The majority of the $\Delta_f H^\circ$ data found is for the solid phase.

The Benson Group Additivity Method

Where experimental data does not exist, one must estimate the required properties. There are a variety of methods available for the gas phase. The interested reader is directed to reference 8 for lucid descriptions and sample calculations of five methods, including that of Benson. For composite solid propellant evaluation, the liquid phase is generally of most interest. The method of Benson has been extended to the liquid and solid phases by Domalski and Hearing,^[9] and is available from NIST as the software database program *THERM*.^[10] This program was used extensively in evaluating the thermodynamic data presented herein.

The Benson Group method assigns thermodynamic values to specific groupings of atoms that are commonly found in organic molecules containing the elements C, H, N, O, S, Cl, Br, I, and F, for which a large body of experimental thermodynamic data is available. Specifically, the molecule is broken down into groups where each group is generally the non-hydrogen atom of interest and the atoms immediately bonded to it. For example, methane, CH_4 , is a carbon atom with 4 hydrogens bonded to it. In Benson Group notation, this is equivalent to $\text{C}-(\text{H})_4$. Methanol, CH_3OH , has 2 groups: a carbon bonded to 3 hydrogens and an oxygen, $\text{C}-(\text{H})_3(\text{O})$, and an oxygen bonded to a carbon and a hydrogen, $\text{O}-(\text{H})(\text{C})$. Carbons that have single, double, triple, and resonant bonds are given the notations C , C_D , C_T , and C_B , respectively. Unsubstituted benzene, for example, would be six $\text{C}_\text{B}-(\text{H})(\text{C}_\text{B})_2$ groups. There are corrections for a variety of molecular configurations. Hexane,

C_6H_{12} , when formed into the ring structure cyclohexane, imparts additional strain on the carbon bonds. The notation used is still six $\text{C}-(\text{H})_2(\text{C})_2$ groups, but then a "correction" group "Cyclohexane, RSC" is included to account for this strain. When substitutions are made on a "base" structure, their proximity to other groups can impart additional strain. Examples of this include methyl substitution (a " $-\text{CH}_3$ correction"), and the neighboring interaction ortho and meta substitutions, such as *o*-xylene and *m*-xylene.^[10a]

After all of the component groups are identified, their respective contributions are arithmetically summed, corrections are applied when required, and the resulting values are the estimates of the thermodynamic properties. This method and its extension to liquid and solid phases is surprisingly accurate despite its apparent simplicity.^[9] The primary problem in evaluating the properties of isocyanates using this method is that no values for the NCO group have yet been defined^[9] due to the lack of critically evaluated data.^[4]

NCO Group Estimation

The NCO group contributions are required to complete the estimation of the isocyanate properties. Based on the chemical structures for which thermodynamic data was available (see Figure 2) only three variations of the NCO group are considered based on the specific type of carbon-nitrogen bond: a carbon, C , a resonant carbon C_B , and a doubly bonded carbon C_D . The group notations used for these three cases are $\text{N}-(\text{C})(\text{C}_\text{O})$, $\text{N}-(\text{C}_\text{B})(\text{C}_\text{O})$, and $\text{N}-(\text{C}_\text{D})(\text{C}_\text{O})$. The introduction of the (C_O) nomenclature is to suggest that the CO group is itself double bonded to the nitrogen via the carbon rather than using the notation $(\text{CO})_2$ which indicates that two separate CO groups bond to the nitrogen. This was also adopted so as not to create confusion with the N_A and N_I nomenclature used for azo and imino nitrogen bonding.

Estimating the properties of the NCO group is straightforward: using a structural diagram of the molecule, like that found on the *Chem-Finder* database, sum the respective contributions of all of the other (known) groups in the molecule, and then subtract this sum from the

cited value. The contribution of the NCO group is the remainder. In the case of the molecule being a diisocyanate, the remainder is divided by two, half for each contributing NCO group. Diisocyanates such as IPDI were not used in estimating the NCO group values due to the molecule having multiple C–NCO bond types. The tabulated results are presented in Table 1 (located after references) and are organized by phase—gas, liquid, and solid, and by property type—formation enthalpy ($\Delta_f H^\circ$), heat capacity (C_p°), and entropy (S°). Arithmetic averages appear for the various properties and bond types. Due to the limited number of data points available, no statistical methods were applied to the data. One value, as noted, was excluded due to its inconsistent and possibly inaccurate value. Appendix 2 outlines a brief study of para, meta, and ortho group substitutions effects.

Urethane Reaction Estimate

One may wish to consider the reaction between the component isocyanate and hydroxyl compounds that result in a urethane. There are no values for the CO–(O)(N) group, however.^[9,10] The gas and liquid phase $\Delta_f H^\circ$ contributions for this group were estimated from the two urethanes listed in Table 2. Due to this very sparse data, and for the sake of completeness, the author used a different approach to “fill in the gap” for the solid phase $\Delta_f H^\circ$, as detailed in Table 2. The differences between these single-atom estimates and those estimated from the two urethanes were 0.82 kJ/mol_{gas} and –9.33 kJ/mol_{liquid} for $\Delta_f H^\circ$. This agreement lends confidence to the solid phase $\Delta_f H^\circ$ estimate. These are all tentative figures, nonetheless, and should be treated as such.

As an example of this reaction, when a mole of HTPB and a mole of IPDI completely react, the resulting urethane $\Delta_f H^\circ$ does not equal that of the reactants due to the rearrangement of the atoms taking place in the urethane bond. For this particular case, and using the $\Delta_f H^\circ$ values in Table 3 combined with the estimated CO–(O)(N) group value and bond rearrangements, the resulting rubber has a $\Delta_f H^\circ$ of –230.63 kJ/mol_{liquid} as compared to the combined reactants respective $\Delta_f H^\circ$ of 17.65 kJ/mol_{liquid}—a

heat of reaction^[2e] of –248.28 kJ/mol_{liquid}. This difference represents two moles of urethane bonds due to the reactants having a functionality of two. Thus, the estimated, exothermic heat of reaction per mole of urethane bonds, in this case, is –124.14 kJ/mol_{liquid}.

Application of Results

From these tabulated values, one can estimate the properties for other isocyanates. As an example, estimates for IPDI agree reasonably well with reference 16 rather than reference 19 or 21. Appendix 3 compares a sample of estimated isocyanate enthalpies to values used in the propulsion industry. There are significant differences in some cases. This leads one to consider how the isocyanate $\Delta_f H^\circ$ estimate impacts the prediction of the adiabatic flame temperature of a composite propellant.

To evaluate this, simulations were run using the author’s free energy minimization program.^[11] Each simulation was run six times: once each for the two cited values for IPDI, and once each for the as-estimated $\Delta_f H^\circ$ value, this value divided by two, this value multiplied by two, and for the urethane system described above that represents the cured (reacted) isocyanate and hydroxyl-terminated polymer.

Two generic propellants were used in this evaluation, and their formulations and test results are presented in Table 3. The diisocyanate contributes only a small percentage to the mass of the propellant, and thus its overall contribution to the propellant enthalpy is minor. Even so, the intentionally poor $\Delta_f H^\circ$ estimates (times 2, divided by 2) indicate that there is a subtle, but definite, effect on the flame temperature. Although it is a small variation, it should not be ignored. Accounting for the urethane reaction enthalpy resulted in a change to the estimated flame temperature that is almost as significant as that of the intentional errors in the isocyanate enthalpy for these particular formulations.

Conclusion

Experimental thermodynamic data for isocyanates may be hard to find, but with the data that is available, reasonable NCO group values may be estimated. These Benson Group NCO values accommodate the estimation of some of the thermodynamic properties of the arbitrary isocyanate, which may then be considered in evaluating the composite propellant as a whole. The overall effect of the isocyanate enthalpy on the adiabatic flame temperature is minimal; even so, every effort should be made to acquire or estimate accurate $\Delta_f H^\circ$ values, especially in situations where the effective enthalpy contribution is greater. The effect of the urethane reaction should not be overlooked or ignored either, as it is relatively easy to estimate and account for using similar group additivity methods.

References

- 1) William L. Masterson and Emil J. Slowinski, *Chemical Principles*, Fourth Edition, W. B. Saunders Company, 1977, p 66.
- 2) Richard J. Lewis, Sr., *Hawley's Condensed Chemical Dictionary*, 12th ed., Van Nostrand Reinhold Company,, 1993; [a] p 24, [b] p 942, [c] p 654, [d] p 623, [e] p. 586.
- 3) Jerry March, *Advanced Organic Chemistry*, 3rd ed., John Wiley and Sons, 1985, p 792.
- 4) Eugene Domalski, National Institute of Standards and Technology, Personal Conversation, March 1996. See reference 9.
- 5) National Institute of Standards and Technology, *WebChem*, <http://webbook.nist.gov>.
- 6) CambridgeSoft Corporation, *ChemFinder*, <http://www.camsoft.com>.
- 7) *ChemFinder Pro*, CSData database, *ChemOffice Ultra* software, CambridgeSoft Corporation. Version 3.01.
- 8) Robert C. Reid, John M. Prausnitz and Bruce E. Poling, *The Properties of Gases and Liquids*, 4th ed., McGraw-Hill, Inc., 1987, Chapter 6.
- 9) Eugene S. Domalski and Elizabeth D. Hearing, "Estimation of the Thermodynamic Properties of C-H-N-O-S-Halogen Compounds at 298.15 K", *J. Phys. Chem. Ref. Data*, Vol. 22, No. 4, 1993, pp 805–1159; Erratum, *J. Phys. Chem. Ref. Data*, Vol. 23, No. 1, 1994, pp 157–159.
- 10) National Institute of Standards and Technology, *NIST Database 18: NIST THERM/EST V.5.2*, Standard Reference Data Program. Version 5.2, 1994; [a] Users Guide pp 47–90.
- 11) Will Meyerriecks, *CEQ Chemical Equilibrium*, Version 36E.
- 12) *CS MOPAC Pro*, *ChemOffice Ultra* software, CambridgeSoft Corporation, Version 3.51.
- 13) *ChemDraw Pro*, *ChemOffice Ultra* software, CambridgeSoft Corporation, Version 4.01.
- 14) *Chem 3D Pro*, *ChemOffice Ultra* software, CambridgeSoft Corporation, Version 3.51.
- 15) *Chemistry Webbook*, <http://webbook.nist.gov/chemistry> National Institute of Standards and Technology.
- 16) Courtesy of Mr. J. D. Mockenhaupt, Aerojet General Corporation, Sacramento, CA.
- 17) J. B. Pedley, R. D. Naylor and S. P. Kirby, *Thermodynamic Data of Organic Compounds*, 2nd ed., Chapman and Hall, 1986, p 186.
- 18) *CRC Handbook of Chemistry and Physics*, 75th Edition, CRC Press, 1995; [a] Chap. 5, p 27; [b] Chap. 5, p 9.
- 19) Eli Freedman, *Thermodynamic Properties of Military Gun Propellants*, p 124, Chapter 5 of *Gun Propulsion Technology, Volume 109* of the *Progress in Astronautics and Aeronautics* Series, American Institute of Aeronautics and Astronautics, 1988.
- 20) D. R. Stull, E. F. Westrum and G. C. Sinke, *The Chemical Thermodynamics of Organic Compounds*, John Wiley and Sons, 1969, pp 642 and 647.

- 21) *PEPCODED.DAF* database, *MicroPEP* software, Martin Marietta Corporation, 1987.
- 22) *General Bulletin, Hydroxyl terminated Poly bd® resins, functional liquid polymers*, 10M-3/89 U/C MT, Atochem, Inc., 1989, p 2.

made to convert to the molecular weight of the molecule and then to kJ/mol. None of this data was used in the estimates as the original sources of these values are unknown, and sometimes the phase was unknown as indicated. (Estimates based on the methods outlined were used to compare against some of these compounds for illustrative purposes. See Appendix 3.)

Notes on References

Data for references 16 and 21 is in an unusual format that seems to be prevalent in the propulsion industry: enthalpy values are expressed in kCal/100 g, and it is rounded to integer values in reference 21. The appropriate steps were

Figure 2. Isocyanate and urethane molecular structures.

<p>1 Benzene, 1,1'-methylenebis[4-isocyanato- 101-68-8</p>	<p>2 Benzene, 1,2-dichloro-4-isocyanato- 102-36-3</p>	<p>3 Benzene, isocyanato- 103-71-9</p>
<p>4 Benzene, 1-chloro-4-isocyanato- 104-12-1</p>	<p>5 Benzene, 1,4-diisocyanato- 104-49-4</p>	<p>6 Ethane, isocyanato- 109-90-0</p>
<p>7 Benzene, 1-isocyanato- 111-36-4</p>	<p>8 Octadecane, 1-isocyanato- 112-96-9</p> <p>9 2,4,4-Trimethylhexamethylene diisocyanate 15646-96-5</p>	
<p>10 Toluene diisocyanate 26471-62-5</p>	<p>11 4,4'-Biphenyldiisocyanate 2761-22-0</p>	<p>12 Benzene, 1-chloro-3-isocyanato- 2909-38-8</p>

Figure 2. Continued.

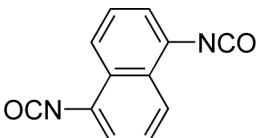
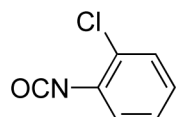
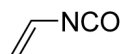
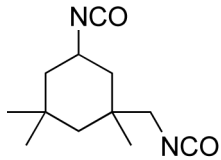
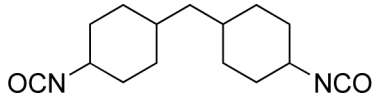
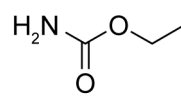
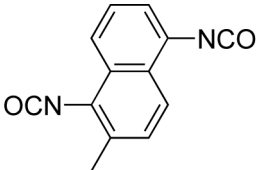
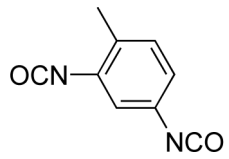
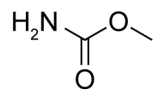

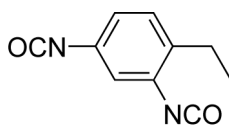
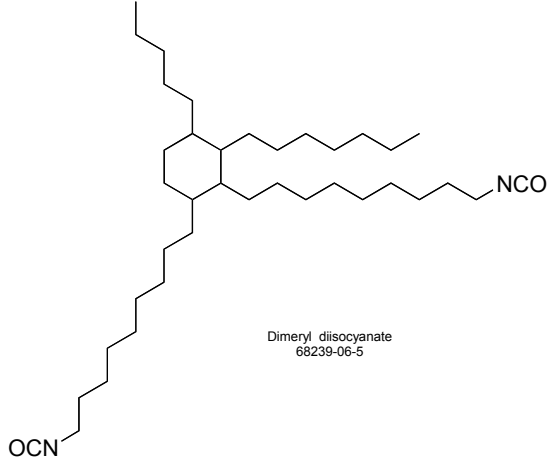
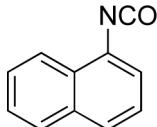
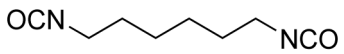
 <p>13 Naphthalene, 1,5-diisocyanato- 3173-72-6</p>	 <p>14 Benzene, 1-chloro-2-isocyanato- 3320-83-0</p>	 <p>15 Ethene, isocyanato- 3555-94-0</p>
 <p>16 Isophorone Diisocyanate 4098-71-9</p>	 <p>17 Cyclohexane, 1,1'-methylenebis[4-isocyanato- 5124-30-1</p>	 <p>18 Urethane 51-79-6</p>
 <p>19 2-Methyl-1,5-naphthalene diisocyanate 56775-58-7</p>	 <p>20 Benzene, 2,4-diisocyanato-1-methyl- 584-84-9</p>	 <p>21 Carbamic acid, methyl ester 598-55-0</p>
 <p>22 Methane, isocyanato- 624-83-9</p>	 <p>23 Ethyl-m-phenylene diisocyanate 64711-83-7</p>	 <p>Dimeryl diisocyanate 68239-06-5</p> <p>24 Dimeryl diisocyanate 68239-06-5</p>
 <p>25 Naphthalene, 1-isocyanato- 86-84-0</p>	 <p>26 1,6-Hexamethylene diisocyanate 822-06-0</p>	

Table 1. NCO Benson Group Contribution Estimates.

N-(C_B)(_DCO)

Fig. 2 Diag. No.	CAS #	Gas	Liquid			Solid		
		$\Delta_f H^\circ$	$\Delta_f H^\circ$	C_p°	S°	$\Delta_f H^\circ$	C_p°	S°
25	86-84-0					-57.66		
1	101-68-8	40.14 ^[a]	-53.0			-65.55	48.71	106.90
						-66.85		106.90
						-65.45		
2	102-36-3					-92.84		
3	103-71-9	-57.75 ^[b]	-76.2	57.78				
4	104-12-1					-87.57	83.83	
5	104-49-4						52.59	
20	584-84-9			88.06				
11	2761-22-0					-78.00		
12	2909-38-8			45.99		-88.67		
13	3173-72-6						36.11	
14	3320-83-0					-83.37		
19	56775-58-7					-91.59		
23	64711-83-7	-67.25	-86.74					
	Average:	-62.50	-71.98	63.94	N/A	-77.76	55.31	106.90

Units $\Delta_f H^\circ$ kJ/mol
 C_p° kJ/(mol•K)
 S° kJ/(mol•K)

N-(C)(_DCO)

6	109-90-0	-79.94 ^[b]	-39.61					
7	111-36-4	-88.18 ^[b]						
8	112-96-9					-67.10		
22	624-83-9	-87.74	-44.39					
			-42.37					
26	822-06-0			55.74	112.91		45.99 ^[c]	51.97 ^[c]
17	5124-30-1	-44.41				-78.38		
	Average:	-75.07	-42.12	55.74	112.91	-72.74	45.99	51.97

N-(C_D)(_DCO)

15	3555-94-0	-40.32 ^[b]	N/A	N/A	N/A	N/A	N/A	N/A
----	-----------	-----------------------	-----	-----	-----	-----	-----	-----

[a] Value is possibly not accurate and has been excluded from the average.

[b] These gas phase enthalpies are based on estimates.

[c] CAS 28182-81-2, 1,6-Hexamethylene diisocyanate C₈H₁₂N₂O₂.

Table 2. CO-(O)(N) – Group Estimates.

Estimated Values for the Group CO-(O)(N) Experimental Data

Fig. 2 Diag. No.	CAS #	Gas ($\Delta_f H^\circ$)	Liquid ($\Delta_f H^\circ$)	Solid (C_p°)
18	51-79-6	-446.30	-497.30	156.43
21	598-55-0	-425.30	-472.70	N/A

The resulting CO-(O)(N) contribution:

CAS #	Gas ($\Delta_f H^\circ$)	Liquid ($\Delta_f H^\circ$)	Solid (C_p°)
51-79-6	-119.27	-153.97	88.56
598-55-0	-131.17	-165.17	N/A
Average:	-125.22	-159.57	88.56

Known Benson Group/Single-Atom Contribution Estimates

The following *THERM* Groups were used to derive the average contribution of a single-atom to a CO (carboxyl) group for $\Delta_f H^\circ$:

CAS #	Gas ($\Delta_f H^\circ$)	Liquid ($\Delta_f H^\circ$)	Solid ($\Delta_f H^\circ$)
Group 121, CO-(C) ₂	-132.67	-152.76	-157.95
Group 116, CO-(O) ₂	-111.88	-122.00	-123.00
Group 289, CO-(N) ₂	-111.00	-190.50	-203.10

Dividing each of the above by 2 gives the single-atom contribution. Adding these single-atom values, then subtracting this from the known value for the actual group gives the methods residual error:

CAS #	Gas ($\Delta_f H^\circ$)	Liquid ($\Delta_f H^\circ$)	Solid ($\Delta_f H^\circ$)
Group 114, CO-(C)(O)	-137.24	-149.37	-153.60
Single-atom contributions	<u>-122.28</u>	<u>-137.38</u>	<u>-140.48</u>
error	- 14.96	- 11.99	- 13.12
Group 239, CO-(C)(N)	-133.26	-185.00	-194.60
Single-atom contributions	<u>-121.34</u>	<u>-171.63</u>	<u>-180.53</u>
error	- 11.92	- 13.37	- 14.07
Average error:	- 13.44	- 12.68	- 13.60

The error is evenly distributed, and for all phases it is -13.24.

The atoms are added together, and the average error added to that sum to yield values for an **estimated Group CO-(O)(N) $\Delta_f H^\circ$** :

CAS #	Gas ($\Delta_f H^\circ$)	Liquid ($\Delta_f H^\circ$)	Solid ($\Delta_f H^\circ$)
O and N contributions	-110.94	-156.25	-163.05
error contribution	<u>- 13.44</u>	<u>- 12.68</u>	<u>- 13.60</u>
CO-(O)(N) Group $\Delta_f H^\circ$:	-124.4	-168.9	-176.7

Table 3. Isocyanate $\Delta_f H^\circ$ Estimate Effect on Adiabatic Flame Temperature.

Application of NCO Group Estimates

Propellant Ingredients

Ingredient	Formula	mw	$\Delta_f H^\circ$
HTPB	$C_{200}H_{302}O_2$	2738.60	365.22 kJ/mol ^[a]
IPDI	$C_{12}H_{18}N_2O_2$	222.29	variable
Ammonium Perchlorate	NH_4ClO_4	117.49	-295.3 ^[b]
Aluminum	Al	26.98	0

Propellant Compositions

Ingredient	Propellant One	Propellant Two
Ammonium Perchlorate	70.0 %	80.0%
Aluminum	15.0%	0.0%
HTPB ^[c]	13.875%	18.5%
IPDI ^[c]	1.125%	1.5%

Flame Temperature, K^[d]

IPDI $\Delta_f H^\circ$	Source	One	Two
-371.62	Ref. 16	3280.6	2363.3
-466.21	Ref. 19, 21	3279.2	2360.5
-347.57	Estimate	3280.6	2363.3
-347.57	Urethane ^[e]	3277.8	2354.9
-695.14	Estimate *2	3275.1	2352.1
-173.79	Estimate / 2	3284.8	2370.2

[a] Value estimated by the author using NIST *THERM* (reference 10), based on structure in reference 22. See Figure 3.

[b] Value from reference 18b.

[c] In both propellants, the NCO:OH ratio is 1:1.

[d] Flame temperature is estimated using reference 11 and convergence is computed using a binary subdivision between 298.15 K and 6000 K, until the difference between successive iterations is less than 1.0 degree K as the reactant minus product enthalpies approaches zero.

[e] The *urethane* is equivalent to the estimated HTPB and IPDI reacting to form a urethane, and the resulting product estimate includes the CO-(O)(N) estimated $\Delta_f H^\circ$. The value used in the simulation for the resulting product has the formula $C_{212}H_{320}N_2O_4$, molecular weight 2960.88, and $\Delta_f H^\circ$ of -230.63 kJ/mol.

Appendix 1

CAS Number	Phase	Property	Value	Ref.	Comments
86-84-0	Naphthalene, 1-isocyanato-				
	Solid	$\Delta_f H^\circ =$	26	15	
101-68-8	Benzene, 1,1'-methylenebis [4-isocyanato-				
	Gas	$\Delta_f H^\circ =$	189 (+/-21)	15	** Questionable accuracy
	Liquid	$\Delta_f H^\circ =$	-25.5	17	
	Solid	$\Delta_f H^\circ =$	-53.0	15	
			-55.6	15	
			-52.8	17	
		$C_p^\circ =$	307.0	15	
		$S^\circ =$	332.5	15	
		332.5	15		
102-36-3	Benzene, 1,2-dichloro-4-isocyanato-				
	Solid	$\Delta_f H^\circ =$	-119	15	
103-71-9	Benzene, isocyanato-				
	Gas	$\Delta_f H^\circ =$	10	15	Estimate
	Liquid	$\Delta_f H^\circ =$	33.9	15	** Typographical error?
			-33.9	15	
		$C_p^\circ =$	186.2	15	
104-12-1	Benzene, 1-chloro-4-isocyanato-				
	Solid	$\Delta_f H^\circ =$	-83.7	15	
			$C_p^\circ =$	210.9	15
104-49-4	Benzene, 1,4-diisocyanato-				
	Solid	$C_p^\circ =$	211.7	15	
109-90-0	Ethane, isocyanato-				
	Gas	$\Delta_f H^\circ =$	-150	15	Estimate
	Liquid	$\Delta_f H^\circ =$	-118.02	20	
111-36-4	Butane, 1-isocyanato-				
	Gas	$\Delta_f H^\circ =$	-200	15	Estimate
112-96-9	Octadecane, 1-isocyanato-				
	Solid	$\Delta_f H^\circ =$	-618.4	15	
584-84-9	Benzene, 2,4-diisocyanato-1-methyl-				
	Liquid	$C_p^\circ =$	287.8	15	
624-83-9	Methane, isocyanato-				
	Gas	$\Delta_f H^\circ =$	-130	15	
	Liquid	$\Delta_f H^\circ =$	-92.0	18a	

CAS Number	Phase	Property	Value	Ref.	Comments
822-06-0	1,6-Hexamethylene diisocyanate				
	Liquid	$C_p^\circ =$	294.0	15	
		$S^\circ =$	420.1	15	
	Solid	$C_p^\circ =$	45.59	15	** 28182-81-2
		$S^\circ =$	51.97	15	** 28182-81-2
		$\Delta_f H^\circ =$	-226.18	16	** Phase unknown
	$\Delta_f H^\circ =$	-504.70	21	** Phase unknown	
2761-22-0	4,4'-Biphenyldiisocyanate				
	Solid	$\Delta_f H^\circ =$	-50.2	15	
2909-38-8	Benzene, 1-chloro-3-isocyanato-				
	Liquid	$C_p^\circ =$	187.0	15	
	Solid	$\Delta_f H^\circ =$	-82.80	15	
3173-72-6	Naphthalene, 1,5-isocyanato-				
	Solid	$C_p^\circ =$	223.6	15	
3320-83-0	Benzene, 1-chloro-2-isocyanato-				
	Solid	$\Delta_f H^\circ =$	-74.50	15	
3555-94-0	Ethene, isocyanato-				
	Gas	$\Delta_f H^\circ =$	-30	15	Estimate
4098-71-9	Isophorone diisocyanate				
	Liquid	$\Delta_f H^\circ =$	-466.21	19	
			-466.07	21	
			-371.62	16	
5124-30-1	Cyclohexane, 1,1'-methylenebis[4-isocyanato-				
	Gas	$\Delta_f H^\circ =$	-311 (+/- 12)	15	
	Solid	$\Delta_f H^\circ =$	-440.6	15	
15646-96-5	2,4,4-Trimethylhexamethylene diisocyanate				
		$\Delta_f H^\circ =$	-377.61	16	** Phase unknown
26471-62-5	Toluene diisocyanate, see 584-84-9				
		$\Delta_f H^\circ =$	-24.05	16	** Phase unknown
		$\Delta_f H^\circ =$	-623.17	21	** Phase unknown
56775-58-7	2-Methyl-1,5-naphthalene diisocyanate				
	Solid	$\Delta_f H^\circ =$	-133	15	
64711-83-7	Ethyl- <i>m</i> -phenylenediisocyanate				
	Gas	$\Delta_f H^\circ =$	-135	15	Mixture
	Liquid	$\Delta_f H^\circ =$	-196	15	Mixture
68239-06-5	Dimeryl diisocyanate				
		$\Delta_f H^\circ =$	-1236.33	16	** Phase unknown
		$\Delta_f H^\circ =$	-872.60	21	** Phase unknown

Appendix 2

The groups used in estimating the NCO contributions included corrections where required, such as ortho Cl-Cl, meta, CH₃ tertiary and quaternary substitutions, etc. The available experimental data is too limited to draw any conclusions in terms of the development of additional correction groups for NCO-NCO, CH₃-NCO, and Cl-NCO next-to-nearest neighbor interactions. Nonetheless, *MOPAC*^[12] was used to investigate these interactions. The method used was to draw the structure in *ChemDraw Pro*,^[13] import it into *Chem 3D Pro*,^[14] and then minimize the strain of the structure using the PM3 Hamiltonian.

The two structures studied were benzene and the *chair* conformation of cyclohexane. An NCO group was substituted, and a second group X was substituted in the para, meta, or ortho position relative to the first group. This second group X was either CH₃, Cl, or NCO. The results are tabulated below in both $\Delta_f H^\circ_{\text{gas}}$ and the difference between the para value and that of the current position. The interaction did not become really significant until the ortho position, and in most of the available data, this condition does not arise.

The exception to this, for which $\Delta_f H^\circ_{\text{gas}}$ is available, is a meta NCO-NCO interaction, 64711-83-7, ethyl-*m*-phenylenediisocyanate. The cited $\Delta_f H^\circ_{\text{gas}}$ is -135 kJ/mole. The *MOPAC* estimate is -47.18. This represents a significant difference that cannot be easily evaluated without additional gas phase enthalpy data.

Benzene

Position	CH ₃	Cl	NCO	ΔCH_3	ΔCl	ΔNCO
para	9.86	21.66	1.95	0	0	0
meta	9.97	21.89	1.35	0.11	0.23	-0.6
ortho	18.49	25.83	11.82	8.63	4.17	9.87

Cyclohexane

Position	CH ₃	Cl	NCO	ΔCH_3	ΔCl	ΔNCO
para	-185.04	-182.75	-187.89	0	0	0
meta	-184.96	-182.43	-192.84	0.08	0.32	-4.95
ortho	-174.72	-177.42	-180.33	10.32	5.33	7.56

Appendix 3

Comparison of Estimated and Cited Isocyanate Enthalpies

Fig. 2 Diag. No.	Estimated $\Delta_f H^\circ$			Cited $\Delta_f H^\circ$	Ref
	Gas	Liquid	Solid		
26	822-06-0	1,6-Hexamethylene diisocyanate			
	-289.26	-248.76	-331.12	-226.18 -504.70	16 21
16	4098-71-9	Isophorone diisocyanate			
	-335.15	-347.57	-398.33	-371.62 -466.21 -466.07	16 19 21
9	15646-96-5	2,4,4 Trimethylhexamethylene diisocyanate			
	-362.15	-332.22	-414.13	-377.61	16
10	26471-62-5, Toluene diisocyanate				
	-104.16	-141.67	-142.27	-24.05 -623.17	16 21
24	68239-06-5	Dimeryl diisocyanate			
	-871.45	-972.86	-1125.06	-1236.33 -872.60	16 21

- 1) The phase of the cited values listed is unknown.
- 2) The chemical name of the cited value, and its value, were all that was available for the above. It is assumed to be the same as those presented by CAS registry number.

Appendix 4

Suggested Values for the NIST THERM Database file THERM.COD

The Group Numbers chosen, 800-805, were an arbitrary choice by the author. *Please note that the user takes full responsibility in editing this file.*

800!N-(CB)(DCO)!-62.50!*!-71.98!63.94!*!-77.76!55.31!106.90!!
 801!N-(C)(DCO)!-75.07!*!-42.12!55.74!112.91!-72.74!45.99!51.97!!
 802!N-(CD)(DCO)!-40.32!*!***!***!***!***!!
 805!CO-(N)(O)!-125.22!*!-159.57!*!-176.70!88.56!*!!

A Severe Human ESD Model for Safety and High Reliability System Qualification Testing

Richard J. Fisher

Formerly with Sandia National Laboratories, Albuquerque, NM 87185, USA

ABSTRACT

A severe human electrostatic discharge (ESD) equivalent source model has been developed for use in qualification testing of systems that have stringent safety or very high reliability requirements. The model produces the now-acknowledged worst-case waveform, and the values of the constituent components have been selected from measured human body electrical parameters to maximize the peak amplitude and rate of rise of the short-circuit discharge current and energy transfer to the victim system.

Introduction

Many systems have either stringent safety or very high functional reliability requirements. Often these same systems, military ones in particular, are subject to operations and maintenance in field or repair depot environments where there is no guarantee of ESD source control. This combination of requirements implies the need for a capability to demonstrate system tolerance to severe human ESD.

Most of the broadly accepted existing human ESD simulation circuits, for example those in the MIL-STD-883C, International Electrotechnical Commission (IEC), and European Computer Manufacturers Association (ECMA) models, appear to incorporate average values for equivalent body electrical parameters and initial charge voltages. They therefore correspondingly replicate typical, or moderate, ESD events. While these environments adequately address the testing needs for a large variety of commercial and other systems, they are inadequate for qualification of systems of the type mentioned above.

In the present effort, a database of the better documented measurements of human body electrical parameters—capacitance, resistance, and inductance—and the distribution of acquirable body voltages was assembled from the literature. The data were found to be surprisingly sparse, especially with respect to body voltage. A severe human ESD source model was developed with component values selected from the available data to yield short-circuit discharge parameters with reasonable upper-bound values that could be encountered by a system over its life-cycle under actual conditions.

Elimination of the attachment arc in ESD testing is now widely recognized to enhance both the repeatability of test results and their correlation to failure distributions observed on the same test objects due to actual human ESD.^[1,2] Therefore, the present model is intended for direct connection to the test item, and no elements corresponding to an arc are included.

In this paper, the rationale is given for the form of the model and its component values. For brevity hereafter, the term ESD is used to mean human body ESD unless otherwise indicated.

Equivalent Source Model

Output Waveform

The key aspects of pulsed electrical over-stress transients in general, and ESD in particular, that influence the nature and level of induced effects are peak amplitude, rise rate, and total energy transferred to the victim object. The correlations between effect and the peak amplitude or total energy deposited by the pulse can be readily appreciated. The extreme sensitivity of victim systems (both electronic and

ordnance) to rise rate of the discharge current is perhaps less intuitive, but nonetheless well-documented [e.g., Refs. 1–5]. Effects or failure mechanisms that are sensitive to the derivative of the driving current include radiation from the source current, magnetic field coupling into internal wiring or circuit boards, inductive voltage transients, and others.

ESD events result in a very wide variety of waveshapes. It is now widely accepted, however, that the worst-case waveform is of the type shown in Figure 1, which corresponds to the short-circuit current often observed in discharges from a hand grasping some small metallic object. That this particular shape represents the worst case follows from the presence of the initial narrow spike, which generically reflects the highest peak amplitudes and fastest rise rates observed in the extensive empirical database reported by King, Richman, and others in recent years.^[3,6,7] This waveform was therefore adopted as the desired output of the model.

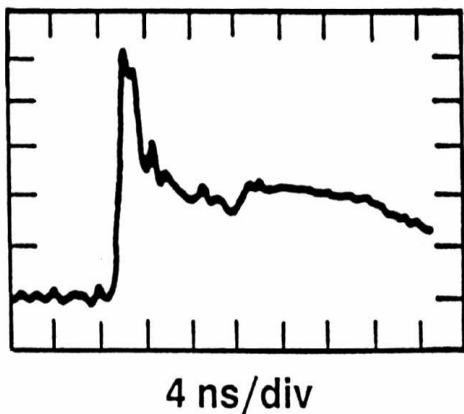


Figure 1. Worst-case human ESD waveform (After Richman^[7]).

Source Circuit Model

The traditional human body ESD equivalent source models have been simple series RLC circuits in which the R corresponds to the resistance of that portion of the body in series with the discharge, L is the similar body inductance,

and C is the capacitance of the body to its surroundings. The body inductance is often neglected, as, for example, in MIL-STD-883C, in apparent tacit recognition of the fact that zero inductance represents the worst case.

Recent refinements to source models have been suggested to account for various observed features in actual ESD currents, such as multiple-pulse discharges^[8] and the important initial narrow spike of Figure 1.^[9] Multiple pulses occur only in discharges involving sparks. Since total energy transferred is the sum of that available to the victim in the individual pulses, worst-case stress can be simulated in a single current pulse from an appropriate source. Comparison of the minimum interval between individual pulses ($\sim 20 \mu\text{s}$ ^[8]) versus the thermal time constants of victim electronics (hundreds of nanoseconds or more) also indicates that the transfer of all available energy from the source in a single pulse represents the worst case.

All ESD source models rely on the Thevenin linear circuit equivalency principle, which guarantees that if the open circuit voltage and short-circuit currents are identical at the output of any two circuits, then the two circuits are completely equivalent electrical sources. The validity of test results obtained with this type or model therefore corresponds in part to the degree to which the ESD event being simulated is linear. In that regard, there are two potential sources of nonlinearity with respect to initial charge voltage to be considered: equivalent body electrical parameters and pre-breakdown corona and other effects in spark discharges. No solid evidence was found in the literature that there is any significant nonlinearity associated with the former, although there appeared to be a hint in one study of decreasing dynamic body resistance with increasing initial voltage.^[10] Most of the available data are too sparse and involve too many simultaneous variable changes to allow analysis for that particular effect. Complications with respect to reduction of peak current and rise rate due to corona effects^[11] are avoided altogether in the present model, since it is intended for direct connection to the test item prior to discharge.

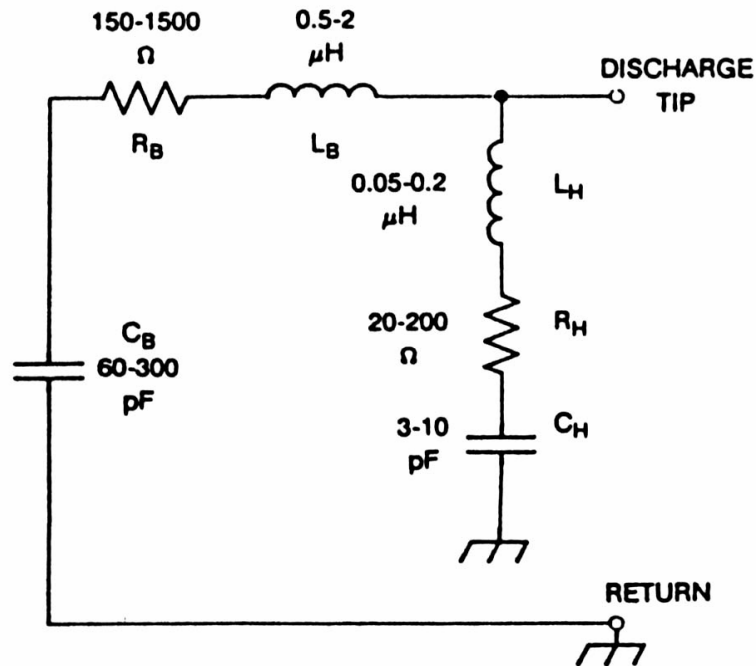


Figure 2. Dual-RLC equivalent human ESD circuit model due to Richman.^[9]

The basic form of Richman's 1985 model (Figure 2), shown by him to be capable of reproducing the important early spike,^[9] was adopted as the preferred baseline. Here, the components labeled C_H , R_H , and L_H are intended to correspond physically to the capacitance and other electrical parameters of the arm and hand as they reach out towards the victim. From this viewpoint, Figure 1 can be interpreted as a composite of a very fast and narrow initial pulse of limited energy content, corresponding to the rapid discharge of the hand capacitance, superimposed on the slower, broader discharge associated with the bulk body capacitance.

The present model (Figure 3) represents a slight modification of the form of Richman's circuit, in that the resistance and inductance associated with the hand and arm have been moved from a parallel branch into series with the discharge path to improve correspondence with physical reality. In the following, the database on equivalent body electrical parameters is reviewed, and the basis for selection of the specific element values reflected in Figure 3 is given.

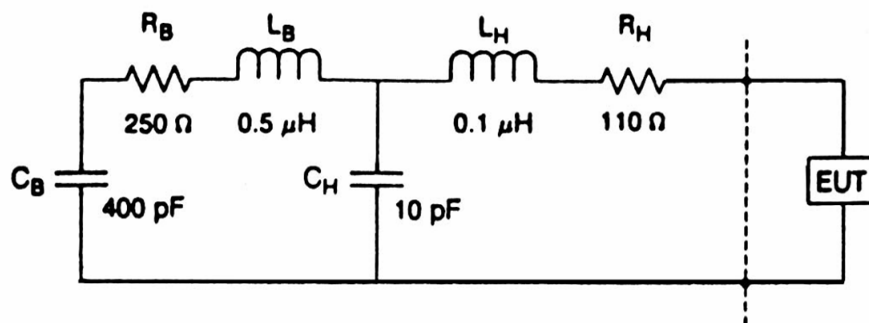


Figure 3. Modified human ESD source model for severe ESD simulation.

Electrical Parameters of the Human Body

Although values for body parameters are widely asserted in numerous ESD handbooks and papers, references in the literature actually describing either the data themselves or the methodology under which they were obtained are surprisingly meager. On the other hand, in the few better documented cases that were found, there is a rather comforting degree of agreement among data that were independently acquired using a considerable range of techniques.^[5,10,12-14] Among these were the direct use of commercial capacitance bridges and various schemes for extracting body R and C from recorded discharges from volunteers charged to controlled initial voltages. Capacitance data are reported for subjects of differing physical characteristics (height, weight, shoe size, etc.) and for various shoe sole and flooring material combinations. Table 1 summarizes these results. The extreme upper and lower values noted were 105 and 1100 pF, respectively, although several other authors alluded to body capacitances as low as a few tens of picofarads without description of the source of data. Sullivan and Underwood^[13] provide fitted normal distributions for their data (Figure 4). The low-end skirts of these

Table 1. Mean Measured Body Capacitance.

Investigator	Standing (pF)	Sitting (pF)
Tucker ^[5]	121	—
Tucker ^[12]	250	—
Cleves and Sumner ^[10]	~250	—
Sullivan and Underwood ^[13]	~120	280
Sperber and Blink ^[14]	130	300
Calvin et al. ^[15]	115	—
Mean/ σ	164/67	290

curves indicate values of this order, although nothing that low appeared explicitly in their tabulated results. Of more practical import, however, is the fact that, according to their distributions, nothing over 400 to 450 pF would be expected, even *in situ* in an automobile environment, which intuitively might be expected to yield the highest capacitance due to the increase in body surface area in close proximity to its surroundings.

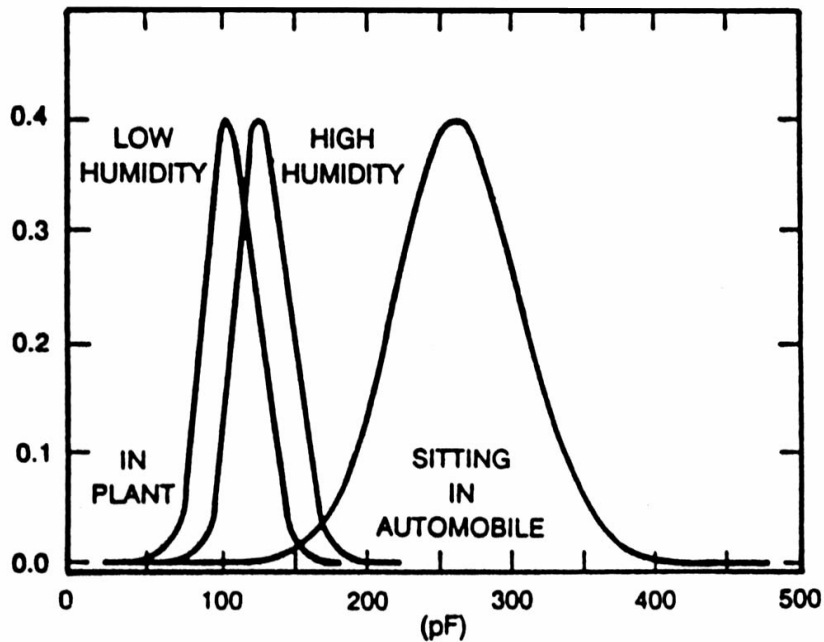


Figure 4. Measured body capacitance distributions for individuals under in-plant and automobile environments (After Sullivan and Underwood^[13]).

Body resistance apparently exhibits a much broader range of values, as is suggested by the data in Table 2. It is most dependent on skin moisture, the particular portion of the body involved in the discharge path, and the contact area and degree of pressure applied in grasping a metal object when some hand-held article is included. A distinction is made in Table 2 between the two main types of discharges from the hand, namely, those with and without the involvement of a metal object. Qualitatively, all of the data reviewed indicate that the latter case implies the highest effective resistance. Other values appearing in the literature without discussion of their origin range from 100 to 2500 ohms. The only values for body inductance found were between 0.1 and 2 μH . From this database, values for the various circuit elements were selected according to the following rationale.

Table 2. Measured Effective Human Body Resistance.

Investigator	Fingertip (ohms)	Metallic Object (ohms)
Tucker ^[5]	1330	357
Sullivan and Underwood ^[13]	1600	-700
Sperber and Blink ^[14]	2000	—
Calvin et al. ^[15]	1920	550
Mean/ σ	1713/308	535/172

First, in order to maximize the available discharge energy, the highest reasonable bulk body capacitance was selected. While the single highest value reported in any of the better documented studies reviewed was 1100 pF,^[14] this value was a factor of 3.5 higher than the next lower one (314 pF). Furthermore, from Figure 4, it is seen that a value of 400 pF represents something like the 4σ point of the Sullivan and Underwood data. Hence, in the spirit of a practical extreme, a value of 400 pF was selected for the main body capacitance C_B of the present model.

Total body resistance is the sum of that associated with the main trunk and that due to the arm and hand. In order to maximize both peak current and energy transfer to the victim, source resistance was minimized by selecting the lowest reasonable value of total body resistance found during the review. This is Tucker's 357 ohms (Table 2), which was rounded up to 360 ohms. This total was allocated between the main body (R_B) and the arm and hand (R_H), 250 ohms to the former and 110 to the latter.

Hand capacitance C_H was chosen to be the upper limit of Richman's range^[9] to maximize the amplitude and energy in the initial spike. Hand inductance L_H was then selected to be 0.1 μH to provide a 10–90% risetime for the initial peak of just under a nanosecond, corresponding to the faster risetimes evidenced in the data of King and Reynolds and Richman. Finally, a value of 0.5 μH for the less critical main body inductance L_B was adopted, also from the range of values reported by Richman.

It should be noted that both the severe waveshape definition and its equivalent model are based on actual short-circuit currents produced in configurations with very low return path inductance.^[3,6,7] Although other discharge scenarios could, in fact, involve substantial return path inductance, which would significantly affect the discharge current, this will not necessarily be the case. Hence, once again in the spirit of conservatism, no extraneous inductance is incorporated into the source model itself.

Initial Charge Voltage

Very few well-documented data were found regarding the ranges of electrostatic voltages acquirable by personnel under various environmental circumstances. In principle, the absolute upper limit on the voltage that can be sustained is set by the point at which charge leakage mechanisms, primarily corona, provide equilibrium with respect to further charge accumulation. This implies a practical upper limit on a person in normal proximity to his surroundings, variously stated to be in excess of 25 kV^[3,5] and 30 to 39 kV.^[16,17]

Table 3. Body Voltages and Capacitances after Exiting from an Automobile.^[14]

Capacitance	Voltage	Shoe Type	Vehicle
176	11.0	3/8-inch Plastic	Intermediate Size Station Wagon
176	10.8	3/8-inch Plastic	
172	7.2	3/8-inch Plastic	
174	11.5	3/8-inch Plastic	
176	15.0	3/8-inch Plastic	
172	17.5	3/8-inch Plastic	
314	4.0	Rubbers Over Shoes	
242	6.5	5/8-inch Rubber Sole	
1100	0.5	3/16-inch Leather Sole	
112	20.0	3/4-inch Plastic Sole	
112	21.5	3/4-inch Plastic Sole	
114	15.0	3/4-inch Plastic Sole	
109	17.0	3/4-inch Plastic Sole	

Sullivan and Underwood^[13] report measured data from a sample of subjects within laboratory and production plant environments. They give mean values of 5.8 kV and 1.4 kV (no standard deviations) for low and high humidity conditions, respectively, but point out that their data are skewed in the low direction due to limitations of their measuring equipment. Sullivan has privately reported measured personnel voltages in excess of 70 kV within an airplane environment.^[18] Sperber and Blink^[14] give measured data (Table 3) on a sample of people with varying heights and weights as they exited from automobiles. Their data contain the highest measured personnel voltages reported among

the better documented studies. Conspicuously absent from the database appear to be any measurements of personnel voltages acquired under outdoor conditions and activities. If levels of 20 kV or more can be developed under plant-type condition, one can readily envision significantly higher voltages in the case of, say, a soldier or airman operating outdoors in a dry wind. In view of these considerations, a reasonable upper bound for use in the present model was chosen to be 25 kV, although arguments could be entertained for an even higher value.

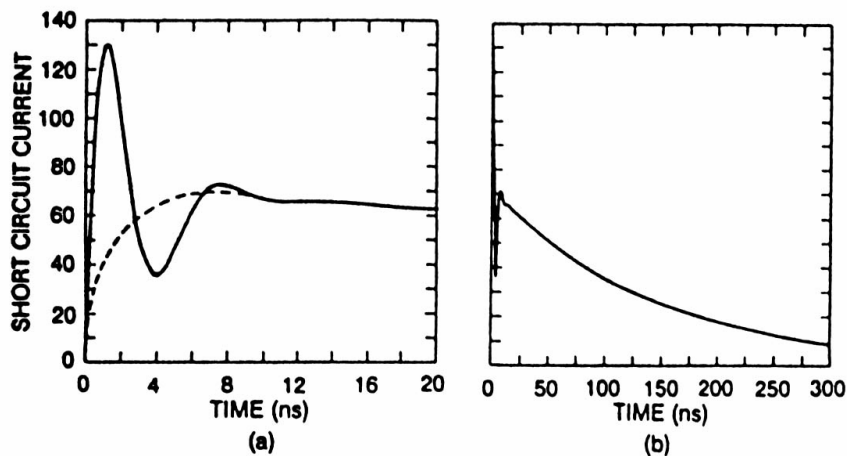


Figure 5. Output of the ESD model of Figure 3 computed for an initial charge voltage of 25 kV; (a) early and (b) longer time base.

Model Output

Figure 5 gives the short-circuit output current computed with the model shown in Figure 3 for an initial voltage of 25 kV. The waveshape compares favorably with the generic worst-case waveform represented in Figure 1. Although the model was specifically developed for use in system-level qualification testing at severe levels, it contains only linear elements; and its output amplitude therefore scales linearly with initial voltage. This allows it to be used at lower voltages while still preserving the desired waveform. The dashed early portion of Figure 5a represents the component or current due to the main body capacitance. Of the three main stress parameters, peak amplitude, rise rate, and total pulse energy, the initial peak accounts for the first two. The energy contained in the first peak, relative to that in the sustained current, is approximately the ratio of the capacitance of the hand to that of the body, which in this case is 0.025.

Conclusion

The ESD model presented herein provides a short-circuit output current corresponding to the acknowledged worst-case waveform evidenced in the available human ESD empirical database. Values of the constituent electrical components were chosen from the ranges of substantiated measurements of human body equivalent electrical parameters and acquired charge voltages reported in the literature. The severity of the resultant output is thought to replicate a reasonable worst-case ESD transient in terms of rise rate, peak amplitude, and total pulse energy available to the victim. The model was developed for specific application as a human ESD standard at Sandia National Laboratories for systems required to tolerate severe ESD. However, since its output is linear with initial voltage, the model can be used at more moderate levels as well.

References

- 1) B. Daout and H. Reyser "The Reproducibility of the Rising Slope in ESD Testing",

IEEE International Symposium on EMC, 1986.

- 2) G. Dash, "Standards and Regulations for Evaluating ESD Immunity at the Systems Level—an Update", *EOS/ESD Symposium*, 1988.
- 3) W. M. King, "Dynamic Waveform Characteristics of Personnel Electrostatic Discharge", *EOS/ESD Symposium*, 1979.
- 4) B. Daout and H. Reyser, "Fast Discharge Mode in ESD Testing", *Proc. Sixth EMC Symposium Zurich*, 1985.
- 5) T. J. Tucker, "Spark Initiation Requirements of a Secondary Explosive", *Annals of the New York Academy of Sciences*, Vol. 152, October 28, 1968.
- 6) W. M. King and D. Reynolds, "Personnel Electrostatic Discharge: Impulse Waveforms Resulting from ESD of Humans Directly Through Small Hand-Held Metallic Objects Intervening in the Discharge", *IEEE International Symposium on EMC*, 1981.
- 7) P. Richman, "Classification of ESD Hand/Metal Current Waves Versus Approach Speed, Voltage, Electrode Geometry and Humidity", *IEEE International Symposium on EMC*, 1986.
- 8) H. Hyatt, H. Calvin, and H. Mellberg, "A Closer Look at the Human ESD Event", *EOS/ESD Symposium*, 1980.
- 9) P. Richman, "Computer Modeling of the Effects of Oscilloscope Bandwidth on ESD Waveforms, Including Arc Oscillations", *IEEE International Symposium on EMC*, 1985.
- 10) A. C. Cleves and J. F. Sumner, *The Measurement of Human Capacitance and Resistance in Relation to Electrostatic Hazards with Primary Explosives*, Report No. 18/R/62, Atomic Weapons Research Establishment, Aldermaston, England, August 17, 1962.
- 11) H. Hyatt and H. Mellberg, "Bringing ESD Testing into the 20th Century", *IEEE International Symposium on EMC*, 1982.

- | | |
|---|---|
| <p>12) T. J. Tucker, "Electrostatic Discharges", Unpublished Internal Memo, Sandia National Laboratories, February 9, 1976.</p> <p>13) S. S. Sullivan and D. D. Underwood, "The Automobile Environment: Its Effect on the Human Body ESD Model", <i>EOS/ESD Symposium</i>, 1985.</p> <p>14) W. Sperber and R. P. Blink, "Characterization of Electrostatic Discharge Generated by an Occupant of an Automobile", <i>IEEE International Symposium on EMC</i>, 1987.</p> <p>15) H. Calvin, H. Hyatt, and H. Mellberg, "Measurement of Fast Transients and Ap-</p> | <p>plication to Human ESD", <i>EOS/ESD Symposium</i>, 1980.</p> <p>16) T. S. Speakman, "A Model for the Failure of Bipolar Silicon Integrated Circuits Subjected to Electrostatic Discharge", <i>IEEE International Symposium on EMC</i>, 1987.</p> <p>17) W. W. Byrne, "Development of and Electrostatic Model for Electronic Systems", <i>IEEE International Symposium on EMC</i>, 1982.</p> <p>18) Private Communication, March 3, 1988.</p> |
|---|---|

Events Calendar *(Continued from page 35)*

Explosives	Numerical Modeling of Explosives and Propellants
24th Annual Conference on Explosives and Blasting Technique	Detonation Physics
Feb. 8–11, 1998, New Orleans, LA USA	Introduction to Explosives
Contact: Int'l Society of Explosive Engineers	<u>Contact:</u> Computational Mechanics Associates
Phone: 440-349-4004	PO Box 11314
<u>Computational Mechanics Assoc. Courses:</u>	Baltimore, MD 21239-0314 USA
Material Behavior at High Strain Rates	Phone: 410-532-3260
April 28 – May 1, 1998, Monterey, CA, USA	FAX: 410-532-3261
Fundamentals of Shock Wave Propagation in Nonlinear Fluids and Solids	
April 20–24 1998, Austin, TX, USA	<i>Events are continued on Page 76</i>

Communications

Brief technical articles, comments on prior articles and book reviews

Consideration of Alternate Whistle Fuels

Rembert Amons
Veldheimlaan 23, 3702 TA Zeist,
The Netherlands
e-mail: rembie.amons@tip.nl

ABSTRACT

The following article aims to be a basic account of the use of phthalic acid salts in whistle compositions. The experiments I conducted with these compositions began when I came across the comments on modern Chinese whistle compositions in the new edition of Ronald Lancaster's Fireworks Principals and Practice. The writer reported problems with the use of these substances which stimulated me to investigate the matter in practice. The first part of this article deals with the properties of the basic materials, the second part is an experimental report and points at a few requirements for the successful use of these salts in whistle mixes. Finally some advantages of these salts over the more common materials are discussed.

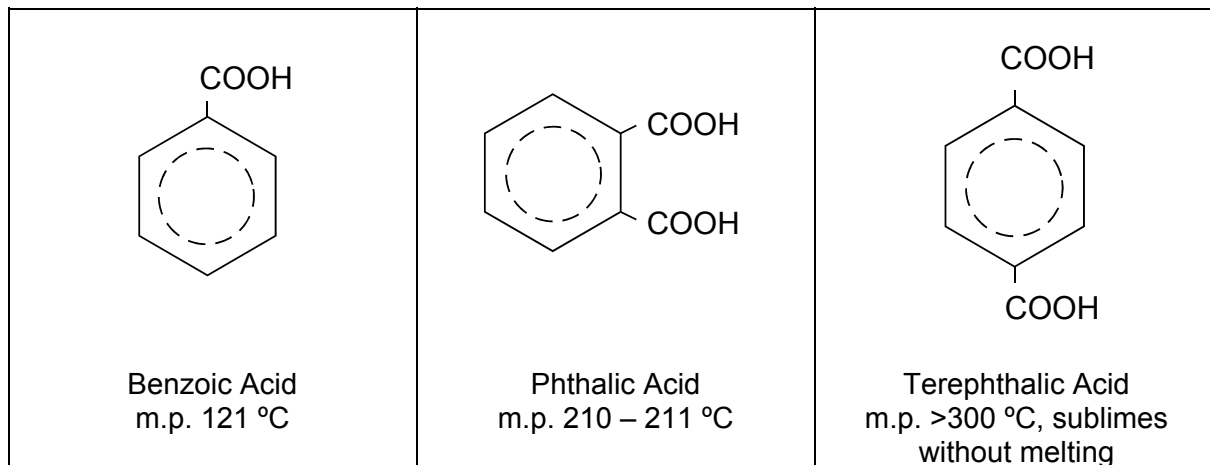
The Basic Materials

Modern whistle compositions typically contain a salt from an aromatic carboxylic acid as a fuel in combination with potassium chlorate or potassium perchlorate as the oxidizer. Salts like potassium benzoate and sodium salicylate have found extensive use and seem by far the most popular choice judged by their prominent presence in the literature. However, some reference works over the years have mentioned other substances which are used in fireworks from the East.^[1]

The alternatives mentioned are the salts from phthalic acid or benzene dicarboxylic acid. Basically the difference from benzoic acid, which may be used to produce potassium benzoate, is that phthalic acid is a polybasic benzene carboxylic acid. That is, it has two carboxylic acid groups instead of one. The situation with the phthalates is therefore a bit more complicated than with the benzoates.

First of all, phthalic acid or benzene dicarboxylic acid, comes in three different isomers which do not necessarily have the same properties. In fact in some respects they do have different properties, and so do their salts.

Secondly, phthalic acid forms salts in more than one way and either one or both acid groups may react with a base. The three different isomers are: 1,2 benzene dicarboxylic acid



(the ortho isomer; phthalic acid), 1,3 benzene dicarboxylic acid (the meta isomer; isophthalic acid) and 1,4 benzene dicarboxylic acid (the para isomer; terephthalic acid). The author has not experimented with the meta isomer yet, but the costs associated with this material might render any results of academic interest only. This leaves us with phthalic acid and terephthalic acid for the moment. Although these substances share the same formula, the molecule looks quite different. The para position of the carboxylic acid groups typically give a very low solubility in water, whereas the ortho position gives a good solubility. These properties must be reckoned with when producing the salts from the respective acids by neutralization with a base.

It is by no means be the only possibility, but the potassium salts seem the most likely candidates as whistle fuels. One of the salts that has been mentioned in the fireworks literature is potassium hydrogen phthalate. This is the salt whereby one acid group is neutralized. It is sometimes referred to as KHP, and it is readily soluble in water ($10^{25}\text{C}/33^{100}\text{C}$ grams in 100 cc). Because of the good solubility of phthalic acid, this salt can be comfortably produced with potassium carbonate. Potassium hydrogen terephthalate on the contrary is only sparingly soluble in hot water. It is said to be used extensively by the Chinese.^[2] In this case the acid/base neutralization is more difficult because of the low solubility of terephthalic acid and the reaction product. It can be done, but care must be taken that the reaction is complete. Both salts are suitable as a fuel in whistle mixes, but it must be noted that the salt from the para isomer is less likely to absorb moisture.

A salt of different properties will be formed by complete neutralization of the acid. In this case only the salt from the para isomer, dipotassium terephthalate, is usable. The salt from the ortho isomer is useless because it absorbs moisture strongly. But even with the salt of the para isomer, it is recommended to allow for a slight excess of acid to reduce moisture problems. The production of this salt is easier because the reaction product is readily soluble. This salt makes a good whistle fuel but has more affinity towards moisture than the *hydrogen* phthalates (about the same as sodium sali-

cyate). Small amounts of moisture will have a significant negative effect on performance.^[3]

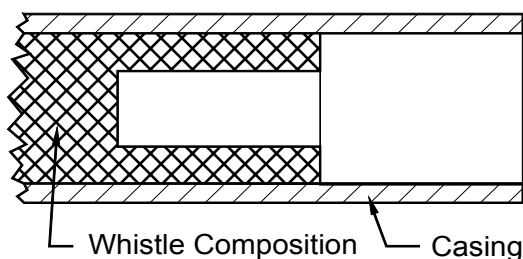
Whistles with Phthalic Acid Salts

As stated, both KHP and potassium hydrogen terephthalate will work in whistle compositions. They can be used in much the same way as potassium benzoate or sodium salicylate, though the performance can be somewhat less than with the former in terms of whistle power. Some, however, seem to be able to make their whistle rockets ascend to greater heights with the use of KHP.^[4]

To make these compositions perform close to the level of the benzoate based compositions a few important requirements have to be met. The first important point is the particle size. Normally materials passing #120 British Standard (BS) Sieve are recommended for whistle mixes. This will not suffice for the hydrogen phthalates if the average particle size is not way below that. Tubes (8, 10 mm ID) charged with potassium perchlorate and potassium hydrogen (tere)phthalate both passing a #120 BS sieve burned in a sputtering manner with short eruptions of whistle sound. This tendency seems to be strongest with whistle mixes with an oxidizer/fuel ratio around the stoichiometric point (for example, 2.3:1). Compositions with an excess of oxidizer (3:1) do not show this tendency as much, but the whistle sound seems somewhat softer. The irregular burning problem can be mitigated by the addition of at least 1% catalyst such as iron(III) oxide or copper(II) oxychloride (note: it is unwise to use this catalyst with potassium chlorate). It must be said that whistle mixes made with these salts benefit clearly from a catalyst. Further reduction of the particle size, if possible below #300 BS, also improves performance, but a catalyst might still be necessary for an optimum whistle sound.

A modification of the burning front such as a progressive burn taper will also help. In fact, superior whistles can be made this way. A 12 mm ID whistle rocket with about 15 mm of free space over the burning front and a cylindrical core of 6 mm ID and 15 mm in composition length will take a 20-gram load to an appropriate height using about 5 grams of whistle composition. The composition is a potassium

perchlorate/potassium hydrogen terephthalate mix in the ratio 2.3:1 with 1% additional catalyst [iron(III) oxide, Fe_2O_3]. The rocket is bottom lit (although it will not explode when core lit) and ascends with an aggressive howl that is quite distinct with this fuel. The dimensions of this whistle motor are adjusted to combine a high level of thrust and sound. Enlarging the burning surface through extended core length will increase the thrust, but not necessarily the sound effect. The pressure in the burning chamber of the whistle device should not be too high, or it will suppress the sound output. This phenomenon is known among whistle rocket builders, although the mechanism behind this seems not entirely clear.



The second important point is the loading pressure. Consolidation with hand pressure only, has proved to be unreliable and will reduce the whistle power of these mixes. In fact the loading pressure needs to be higher than with the mixtures based on potassium benzoate to obtain similar results.^[3] Frequently the whistle will burn without whistling right away if the composition is consolidated with insufficient pressure.

Possible Advantages of Phthalic Acid Salts

This is perhaps the most important question of this article: do these new materials have any advantage over the more common ones? The answer is both yes and no. Let's start with the drawback. The cost of these materials will probably be higher than the cost of the benzoates or salicylates, although everything depends on finding the right source (some suggested the plastics industry and this might indeed be a possibility).

The advantages are multiple. First of all, the low hygroscopicity of potassium hydrogen terephthalate will make this fuel an excellent choice in damp conditions. Potassium hydrogen terephthalate is also easy to reduce to a fine powder (potassium hydrogen phthalate is a bit more difficult in this respect). But more importantly, tests have shown the sensitivity to friction of the basic potassium perchlorate/potassium benzoate mix to be twice as high as with the potassium perchlorate/potassium hydrogen terephthalate mixture.^[3] Needless to say, an additional catalyst might increase the sensitivity.

Of course these matters should be investigated more extensively and with proper references. The information contained in this article is therefore to be regarded as only an indication. In practice, however the whistle mixes based on the phthalic acid salts perform well and have proven to be reliable. Hopefully this new material will give rise to interesting experiments.

Acknowledgments

I want to thank Arno Hahma and Mike Carter for willingly sharing their experiences with me.

References

- 1) J. Conkling, *Chemistry of Pyrotechnics*, 1985, p. 178; R. Lancaster, *Fireworks Principles and Practice*, 2nd ed., 1992, p 58, p 152.
- 2) R. Lancaster, *Fireworks Principles and Practice* 2nd ed. (1992) p 58, p152; Richard Dilg, *American Fireworks News*, No. 74, 1987, p 4.
- 3) Arno Hahma, personal communication.
- 4) Mike Carter, personal communication.

Frequency Stabilization of Large Diameter Strobe Flares

K. L. Kosanke

PyroLabs, Inc., Whitewater, CO 81527, USA

Pyrotechnic strobe devices burn to produce a series of approximately equal intensity light pulses at approximately equal time intervals, as illustrated in Figure 1. The typical pyrotechnic strobe process^[1] begins with a dark reaction during which a reactive slag is produced. Subsequently, hot spots develop within the slag, eventually triggering a flash reaction which consumes most of the slag to produce a bright flash of light. The process continues with the dark reaction again producing more reactive slag, which then eventually flashes. The process continues in this way to produce a series of short bright light flashes with relatively long periods of darkness in between. This pyrotechnic strobe process is illustrated in Figure 2.

There is interest using large diameter pyrotechnic strobe flares as signals and for potential military application.^[2] However, as the size of a strobe flare is increased, there is a tendency for the frequency of the flashes to increase and

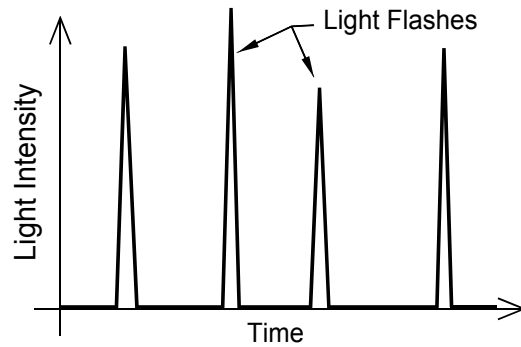


Figure 1. An illustration of the light output from a pyrotechnic strobe device.

become erratic in period and intensity. The result tends to more of a random flickering, or even continuous light output, than a true strobe effect with clearly defined dark periods between the flashes. This brief article has been prepared to suggest two potential methods to help control the burning of large diameter strobe devices, for which the author does not have time to investigate.

The idea for stabilizing the burning of large pyrotechnic strobes is analogous to a common method used to control analog electronic oscillators. It is often the case that a free running oscillator, with a natural frequency a little lower than desired, is controlled and stabilized by applying regular synchronization pulses, a

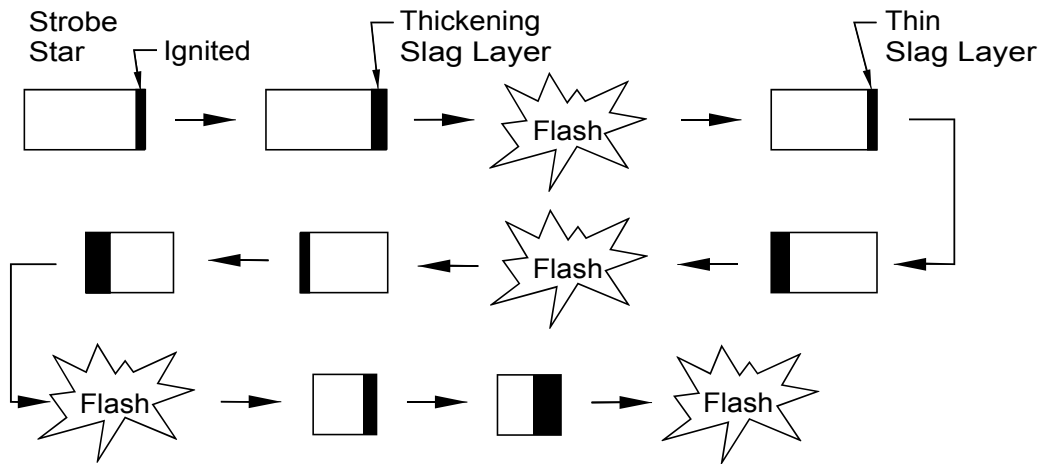


Figure 2. An illustration of the mechanism of pyrotechnic strobe burning.

little before each natural oscillator cycle is completed. In a somewhat similar process, it may be possible to control large strobe devices. If a strobe composition is formulated that has a low natural flash frequency, upon burning it will have prolonged periods of dark reaction during which slag is produced. (In fact, it might even be preferred to use a composition that produced the needed reactive slag, but, which never produced the hot spots needed to trigger the flash reaction.) Then, if at regular intervals the energy needed to trigger the flash reaction is supplied from another source, light flashes might be produced with the same regular intervals.

Two methods for providing the periodic energy for the flash reaction, have been considered. One method might be to incorporate a relatively small diameter core of normal strobe composition into the large diameter strobe device, such as illustrated in Figure 3. In that way, the energy regularly produced as the small strobe core flashes, might be used to trigger flash reactions of the slag across the surface of the large device.

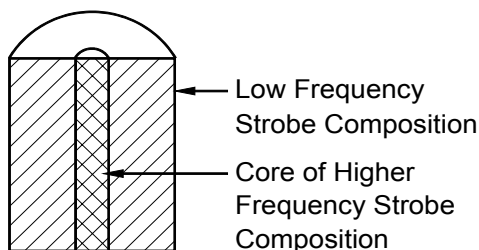


Figure 3. Illustration of a small core of strobe composition used to stabilize a larger strobe device.

In Figure 4, an alternative flash triggering energy source is suggested. If the large strobe device has a pair of electrical conductors incorporated into it, it might be possible to provide the triggering flash energy by causing a brief electric arc to occur between the tips of the two conductors. Of course it would be necessary that the ends of the conductors be consumed during the reaction such that the arcs occur within the slag layer. (This might be accomplished by using thin wires with low

melting points, or even using aluminized mylar.) The need for an electrical power supply and controlling circuit is definitely a drawback for this method. However, the ability to have nearly complete control of flash timing might be sufficient compensation. (Note that the intensity of the light flashes would be expected to be roughly proportional to the period between flashes, as this roughly corresponds to the amount of reactive slag produced for the next flash reaction.)

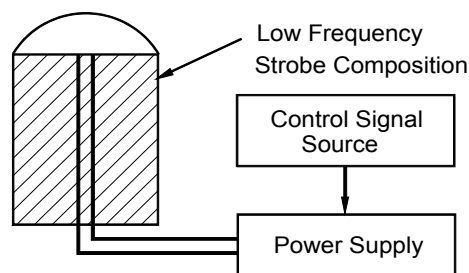


Figure 4. Illustration of electrically triggered strobe device.

The above approaches to controlling large diameter strobe devices may have no merit, and there are considerable technical difficulties to overcome in designing a reliable electrical device. However, since the author will not be able to investigate this, and because the idea may be of use, it was thought to be appropriate to share the idea with other researchers.

References

- 1) T. Shimizu, "Studies on Strobe Light Pyrotechnic Compositions", *Pyrotechnica* VIII, 1982.
- 2) Les Cox, private communication, 1997.

Estimating the Distribution of Molecular Energies

Wesley D. Smith

Department of Chemistry, Ricks College,
Rexburg, ID 83460-0500

For a reactant molecule to participate in a chemical change, it must possess, among other things, the requisite activation energy E_a . It may be useful^[1] to know approximately what fraction of all molecules in any collection (at a given temperature) has at least that much energy.

The differential fraction of molecules that has a particular energy ϵ is given by the Maxwell-Boltzmann distribution,^[2]

$$\frac{2\pi}{(\pi RT)^{3/2}} e^{-\epsilon/RT} \sqrt{\epsilon} d\epsilon$$

where R equals 8.314×10^{-3} kJ/mol·K, the gas constant, and T is the absolute temperature. So the fraction of molecules N that have an energy E_a or greater is the integral of this function from E_a to infinity. With the substitution $x = \epsilon/RT$, the integral becomes

$$N = \frac{2}{\sqrt{\pi}} \int_{x_a}^{\infty} e^{-x} \sqrt{x} dx$$

where $x_a = E_a/RT$.

To the best of my knowledge, the integral (for any bounds other than zero to infinity) can only be done numerically, but the calculation is straightforward. Having done several dozen integrals over a range of activation energies and temperatures and for a number of upper bounds (to approximate infinity), I find that the results fit the equation

$$\ln N = a - b \frac{E_a}{RT}$$

Linear regression gives $a = 0.9417$ and $b = 0.9672$. But a quick, order-of-magnitude estimation is generally all anyone needs. For that, $a=b=1$ suffices.

For example, suppose the activation energy of interest is 84 kJ/mol (about 20 kcal/mol) at room temperature (298 K), then

$$\ln N \approx 1 - 84/(8.314 \times 10^{-3} \times 298) = -33.90$$

and $N \approx 2 \times 10^{-15}$. That is, only about a quadrillionth of the molecules under these conditions have enough energy to react. If the temperature is increased to 623 K (350 °C), the fraction is $N \approx 2 \times 10^{-7}$. In other words, that rise in temperature produces one hundred million times as many molecules with the necessary energy.

References

- 1) K. L. and B. J. Kosanke, "Pyrotechnic Ignition and Propagation: A Review", *Journal of Pyrotechnics*, Issue No. 6, 1997, p 17-29.
- 2) For example, see Terrell L. Hill, *An Introduction to Statistical Thermodynamics*, Addison-Wesley, Reading MA, 1960, p 122.

Further Comment from Fred Ryan on:
Flash Powder Output Testing: Weak Confinement, Issue 4, Winter 1996, p 5-14. [For first comments, see pp 61-63, *Journal of Pyrotechnics*, No. 5, 1997.]

Thank you for the technical response to my comments on flash testing. It appears very clear now that the flash salutes that you were testing were still supersonic at 100 meters while the salutes that I was testing were sonic at 100 meters.

This raises an interesting point. Flash salutes produce sound waves that are initially supersonic but sooner or later will drop to sonic velocities, if not at 100 meters in your case, certainly at some distance probably not too much greater than 100 meters, since the energy in the wave will drop as about $1/r^3$. The perception of "noise" by the observer can be appreciably different if the observer is located within the supersonic zone or outside in the sonic zone. Thus an interesting study presents

itself. Determine the zone in which supersonic shock waves reach the observer, and the range at which the shock waves have reverted to sonic. Get some trained observers to judge the quality of the sound subjectively at those two zones. It would be of interest to see how the shape of the impulse affects their judgments!

Comment on:
Model Rocket Engines, Theory and Design, Issue No. 5, Summer 1997,
 p 1–7

I found this article extremely interesting. It was a pleasure to see the treatment of a cored endburner, which is a problem I've been reluctant to tackle. Now I can set up my spreadsheet with ease.

I have several comments regarding the article. First, the figures for Example 2, Table 3 are not totally correct. The nozzle diameter should be 1.70 mm and the cylindrical cavity height 0.37 mm, with other values changing as well.

In addition to the actual values of f_{max} and f_{min} , I would suggest that the ratio of these two should be chosen with care. For "poor" propellant the ratio f_{max}/f_{min} should be kept small, since the burn rate exponent is large for such propellant. When the motor operates well at f_{min} , there is danger of overpressurization at the large f_{max} . The ratio can never be smaller than approximately 2 for an endburner, because for a cylindrical core of zero height, A_{max} is virtually a hemisphere of area $2\pi r^2$, while A_{min} is a circle of area πr^2 ; $A_{max}/A_{min}=2$.

For the benefit of those using spreadsheets, here is an equation for the chamber pressure P_c derived from equations 12–15 from the article:

$$P_c = 10^{\frac{\log N}{1-\nu}}$$

$$\text{where } N = \frac{\pi d^2 U_o \cdot 0.00001 \cdot p \sqrt{RT_c}}{4bA_{noz}}$$

Note that neither burn time nor propellant mass need be known. Once the chamber pressure is

found, the burn rate U can be determined using equation 14. Finally, one fixes either propellant mass or burn time and calculates the other using equation 15. Constructing a spreadsheet for the calculations then becomes straightforward. "Playing around" with the spreadsheet will provide insight into what can and cannot be done with endburners.

The article has already helped in my construction of 24 mm endburners. My first three worked, in sharp contrast to my earlier trial-and-error efforts. Many thanks to Messrs. Clinger and Smith for their efforts.

Sincerely, Terry McCreary,
 Associate Professor, Chemistry

Authors' Reply to McCreary Comment:

Professor McCreary adds several useful insights to our article. We appreciate his comments.

A nozzle diameter of 1.70 mm and a cylindrical cavity height of 0.37 mm are correct in Example 2 if f_{min} is taken as 50. However, as we stated (rather obscurely) in the text, our results are for $f_{min} = 35$.

E. J. Klinger and Wesley D. Smith

Review of: Lecture Notes for Pyrotechnic Chemistry

Paul E. Smith

Director of Lecture Demonstrations, Purdue
University Department of Chemistry, 1393 Brown,
Box 177, West Lafayette, IN 47907-1393, USA

The recent output of books providing accurate scientific discourse on pyrotechnics has been almost nonexistent. While there are still copies of many good texts on this subject, new editions to this extant literature have been rare. The publication of the two-part syllabus of the course "Lecture Notes for Pyrotechnic Chemistry" is a welcome addition to the chemistry of pyrotechnics literature. (Note that earlier editions were called: "Chemistry of Fireworks" and "Chemistry of Pyrotechnics".) The layout of this publication exists somewhere between a course outline and a book and has many strong points.

Many great traditional pyrotechnic texts do not discuss or just briefly mention the topics of whistles and strobes. Their discussion in this publication is very strong and up to date. I especially found the description of their proposed burn mechanisms helpful. The text covers the fundamental principles necessary for a basic understanding of pyrotechnic chemistry. Readers with both a chemistry and non-chemistry background will find this text a valuable addition to their collection of pyrotechnic literature.

Hazard management, in the last section of the text, has good charts highlighting hazardous chemical combinations. This strong section could only be strengthened by providing information about proper disposal of residue and waste chemicals.

Because of the outline nature of the text, such things as references for some of the sources, page numbers, and an index did not appear in the earlier editions. However, edition 3.1 includes page numbers and a nine page index.

Discussion of major topics was well done, although I would like to see more on the effects of hygroscopicity. The presentation of oxidation states is very brief, and I would like to see this dealt with in more detail. Those without training in chemistry often find oxidation and reduction reactions a difficult subject.

This volume should be of real benefit to all those involved in pyrotechnics and a welcome new addition to my pyrotechnics library.

Review of Tom Perigrin's Introductory Practical Pyrotechnics

Tom Dimock

120 Maple Ave., Ithaca, NY 14850, USA
(e-mail: tad1@cornell.edu)

As a pyrotechnist who has a rather public persona on the Internet, I am often called upon to recommend a book on the craft of fireworks to beginning pyrotechnicians. This was always a problem because the available literature was either too advanced or too dated to be really suitable. This gap in the literature was filled with the publication in 1996 of *Introductory Practical Pyrotechnics* by Tom Perigrin.

In this small book of 200 information-filled pages, Mr. Perigrin more than lives up to the promise of the book's name. Although he is a Professor of Chemistry at a leading University, he makes no presumptions on the readers background—this book is readily accessible to anyone who can read. The book was designed to be the lab manual for a practical course in pyrotechnic chemistry and proceeds through a series of very specific projects beginning with making Black Powder by the "CIA method", then progressing through a series of progressively more challenging projects up to the level of small aerial shells.

As the reader works through these projects they will acquire not only the knowledge of how to make fireworks devices, but also how to build much of their own tooling, and perhaps most important, how to incorporate appropriate safety measures into every step of their work. Given the inherently dangerous nature of pyrotechnic compositions, this strong emphasis on safety is more than welcome in an introductory text.

If Mr. Perigrin had stopped with only the practical projects portion of the book, he would have produced an extraordinarily useful addition to the pyrotechnic literature. Instead, he went on to add sections on basic pyrotechnic chemistry, properties of common pyrotechnic chemicals, a bibliography (including an excellent anti-bibliography of dangerous fringe texts), and several useful appendices.

The section on pyrotechnic chemistry is very well presented and demonstrates Mr. Perigrin's talent for presenting complex material very clearly, without intimidating those with a weak chemistry background. References are provided to more rigorous texts, along with a strong recommendation that they be consulted before the reader proceeds into experimental formulations.

The appendices are the part of the book that I keep coming back to. The first appendix "For-

mulations" gives 49 pyrotechnic formulations selected from the pyrotechnic literature based upon their safety, efficacy, and reliability. The formulations are all given in a very clear presentation, along with references to their original publications.

Appendices 2 and 3 give a concise reference to chemical nomenclature and chemical names and abbreviations which is very useful to those of us with a less than stellar chemistry education. Appendix 4 digests some of the most relevant parts of the BATF Orange Book [*ATF-Explosives Law and Regulations*, Bureau of Alcohol, Tobacco, and Firearms, Department of the Treasury, ATF P 5400.7 (6/90)] into a concise reference. Appendix 5 is a table of screen sizes, something that can be infuriatingly hard to find when you need it. I would suggest to Mr. Perigrin that a table of Black Powder granulations for the sporting and blasting grades would make an excellent Appendix 6.

In summary, Mr. Perigrin has done the world of amateur pyrotechnics an immeasurable service by providing this excellent introductory text. It makes a great gift for the aspiring pyrotechnician and is filled with choice nuggets of information for the more experienced pyrotechnician. It is highly recommended.

Editorial Policy

Articles accepted for publication in the *Journal of Pyrotechnics* can be on any technical subject in pyrotechnics. However, a strong preference will be given to articles reporting on research (conducted by professionals or serious individual experimenters) and to review articles (either at an advanced or tutorial level). Both long and short articles will be gladly accepted. Also, responsible letters commenting on past Journal articles will be published, along with responses by the authors.

Journal Sponsors

Journal of Pyrotechnics wishes to thank the following Sponsors for their support.

Action Lighting , Inc.

Hugh Reid
P.O. Box 6428
Bozeman, MT 59715
Phone: 800-248-0076
FAX: 406-585-3078
e-mail: action_lighting@gomontana.com

Allied Specialty Insurance

Ed Schneider
10451 Gulf Blvd.
Treasure Island, FL 33706
Phone: 800-237-3355
FAX: 813-367-1407

American Fireworks News

Jack Drewes
HC 67 Box 30
Dingmans Ferry,
PA 18328-9506
Phone: 717-828-8417
FAX: 717-828-8695
e-mail: amerfwknws@aol.com
Web: www.barrettsweb.com/afn

Astro Pyrotechnics

Dan Hyman
2298 W. Stonehurst
Rialto, CA 92377
Phone: 909-822-6389
FAX: 909-822-6188
e-mail: astropyro@aol.com

Black Sky Research Assoc.

Scott Bartel
3179 Roosevelt Street
Carlsbad, CA 92008
Phone: 960-730-3702
FAX: 960-730-3704
e-mail: blacksky@earthlink.net

Ed Brown

P.O. Box 177
Rockvale, CO 81244
Phone: 719-784-4226

Canadian Expl. Res. Lab.

Ron Vandebek
CANMET, 555 Booth St.
Ottawa, ON K1A 0G1
Canada
Phone: 613-995-1275
FAX: 613-995-1230

Daveyfire, Inc.

Alan Broca
7311 Greenhaven Dr. - Ste 100
Sacramento, CA 95831
Phone: 916-391-2674
FAX: 916-391-2783

Delcor Industries Inc.

Sam Bases
19 Standish Ave.
Yonkers, NY 10710
Phone: 914-779-6425
FAX: 914-779-6463

Empire Specialty Products

Charles Hill
4533 Foster Valley Rd.
Endicott, NY 13760
Phone: 607-748-0667
FAX: 607-748-0899

Fire One

Dan Barker
863 Benner Pike
State College, PA 16801
Phone: 814-238-5334
FAX: 814-231-0950
e-mail: rjc@fireone.com
Web: www.fireone.com

Firefox Enterprises Inc.

Gary Purrington
11612 N. Nelson
Pocatello, ID 83202
Phone: 208-237-1976
FAX: 208-237-1976
e-mail: firefox@pcaxxess.net
Web: www.pcaxxess.net/~firefox

Fireworks

John Bennett
68 Ridgewood Gardens,
Bexhill-in-Sea
East Sussex, TN40 1TS
United Kingdom
Phone: +1424-733-050
FAX: +1424-733-050
e-mail: JFBen@netcomuk.co.uk
Web: fireworks.co.uk/fireworks-journal

Fireworks Business

Jack Drewes
HC 67 Box 30
Dingmans Ferry,
PA 18328-9506
Phone: 717-828-8417
FAX: 717-828-8695
e-mail: amerfwknws@aol.com
Web: www.barrettsweb.com/afn

Fireworks & Stage FX America

Kevin Brueckner
P.O. Box 488
Lakeside, CA 92040-0488
Phone: 619-596-2800
FAX: 619-596-2900
e-mail: go4pyro@aol.com
Web: www.fireworksamerica.com

Firework Professionals Ltd.

Anthony Lealand
PO Box 17-522
Christchurch, 8030
New Zealand
Phone: +64-3-384-4445
FAX: +64-3-384-4446
e-mail: firewxch@firework.co.nz

Fullam's Fireworks, Inc.

Rick Fullam
P.O. Box 1808 CVSR
Moab, UT 84532
Phone: 801-259-2666

Goex, Inc.

Mick Fahinger
PO Box 659
Doyline, LA 71023-0659
Phone: 318-382-9300
FAX: 318-382-3903
e-mail: BPMick@aol.com
Web: www.shooters.com/goex

High Power Rocketry

Bruce Kelley
PO Box 96
Orem, UT 84059
e-mail: 71161.2351@compuserve.com

Industrial Solid Propulsion Inc.

Gary Rosenfield
1955 S. Palm St. - Ste. 6
Las Vegas, NV 89104
Phone: 702-641-5307
FAX: 702-641-1883

Iowa Pyro Supply

Mark Mead
1000 130th St.
Stanwood, IA 52337
Phone: 319-945-6637

Island Fireworks Co. Inc.

Charles Gardas
N735 825th St.
Hager City, WI 54014
Phone: 715-792-2283
FAX: 715-792-2640

Kastner Pyro. & Fwks Mfg. Co

Jeri Kastner
Rt 3 , 938 Logtown Rd.
Mineral Point, WI 53565
Phone: 608-943-6287
FAX: 608-943-6287

Lantis Fireworks & Lasers

Ken Lantis
PO Box 491
Draper, UT 84020
Phone: 801-571-2444
FAX: 801-571-3516
e-mail: info@fireworks-lasers.com
Web: fireworks-lasers.com

Luna Tech, Inc.

Tom DeWille
148 Moon Drive
Owens Cross Roads, AL 35763
Phone: 205-725-4225
FAX: 205-725-4811
e-mail: PyropakUSA@aol.com

MP Associates Inc.

P.O. Box 546
Ione, CA 94640
Phone: 209-274-4715
FAX: 209-274-4843

Marutamaya Ogatsu Fwks Co. Ltd.

1-35-35 Oshitate Fuchu
Tokyo, 183
Japan
Phone: 81-423-63-6251
FAX: 81-423-63-6252
e-mail: moff@za2.so-net.or.jp

OXRAL, Inc.

Tom DeWille
P.O. Box 160
Owens Cross Roads, AL 35763
Phone: 205-725-4225
FAX: 205-725-4811
e-mail: Pyropak@juno.com

Precocious Pyrotechnics, Inc.

Garry Hanson
4420 278th Ave. N.W.
Belgrade, MN 56312-9616
Phone: 320-346-2201
FAX: 320-346-2403

Pyro Shows, Inc.

Lansden Hill
P.O. Box 1406
LaFollette, TN 37766
Phone: 800-662-1331
FAX: 423-562-9171

Pyrodigital Consultants

Ken Nixon
1074 Wranglers Trail
Pebble Beach, CA 93953
Phone: 408-375-9489
FAX: 408-375-5225
e-mail: pyrodig@aol.com

PyroLabs, Inc.

Ken Kosanke
1775 Blair Road
Whitewater, CO 81527
Phone: 970-245-0692
FAX: 970-245-0692
e-mail: kosankes@compuserve.com

RES Specialty Pyrotechnics

Steve Coman
4785 Dakota Street SE
Prior Lake, MN 55372
Phone: 612-447-7976
FAX: 612-447-0065
e-mail: respyro@minn.net

Service Chemical, Inc.

Marvin Schultz
 2651 Penn Avenue
 Hatfield, PA 19440
 Phone: 215-362-0411
 FAX: 215-362-2578

Skylighter, Inc.

Harry Gilliam
 PO Box 480
 Round Hill, VA 22141
 Phone: 703-554-2228
 FAX: 703-554-2849
 e-mail: custservice@skylighter.com

Special F/X Inc.

Ed Bartek
 P.O. Box 293
 South Bound Brook, NJ 08880
 Phone: 732-469-0519
 FAX: 732-469-1294
 e-mail: specfx@webspan.net

Stresau Laboratory Inc.

Mike Pesko
 N 8265 Medley Rd.
 Spooner, WI 54801
 Phone: 715-635-2777
 FAX: 715-635-7979
 e-mail: mpesko@syslan.net
 Web: <http://www.stresau.com>

Sunset Fireworks Ltd.

Gerald Walker
 10476 Sunset Drive
 Dittmer, MO 63023
 Phone: 314-274-1500
 FAX: 314-274-0883

Sunset Fireworks, Ltd. / Omaha

Jack Harvey
 2335 South 147th Street
 Omaha, NE 68144-2047
 Phone: 402-681-5822
 FAX: 402-333-9840

Theatre Effects Inc.

Nathan Kahn
 642 Frederick St.
 Hagerstown, MD 21740
 Phone: 301-791-7646
 FAX: 301-791-7719
 e-mail: nathan@theatrefx.com
 Web: <http://www.theatrefx.com>

Tri-Ess Sciences, Inc.

Ira Katz
 1020 W. Chestnut St.
 Burbank, CA 91506
 Phone: 818-848-7838
 FAX: 818-848-3521

Western Pyrotechnics, Inc.

Rudy Schaffner
 2796 Casey Road
 Holtville, CA 92250
 Phone: 619-356-5426
 FAX: 619-356-2051

Events Calendar *(Continued from page 64)*

Model Rocketry

NARAM-41

For further launch information visit the NAR web site at: <http://www.nar.org>

High Power Rocketry

LDRS XVII

August 6-9, 1998, Bonneville, UT

Contact: Neal Baker
 5352 West 6600 South
 West Jordan, UT 84084, USA

Phone: 801-359-5544

FAX: 801-359-5544

e-mail: nbaker@lgcy.com

Web Site: www.uroc.org/ldrs/indes.html